Alaska Department of Transportation & Public Facilities

Research & Technology Transfer

Experimental Study of Various Techniques to Protect Ice-Rich Cut Slopes

Prepared by:
Lin Li, M.S., Research Assistant
Department of Civil and Environmental Engineering
University of Alaska Fairbanks

Robert McHattie, P.E., Consultant
GZR Engineering
Fairbanks, Alaska

Xiong Zhang, Ph.D., P.E., Associate Professor
Department of Civil and Environmental Engineering
University of Alaska Fairbanks

Mingchu Zhang, Co-PI
School of Natural Resources and Agricultural Sciences
University of Alaska Fairbanks

Date:
August 2014

Prepared for:
Alaska Department of Transportation
Statewide Research Office
3132 Channel Drive
Juneau, AK 99801-7898

Publication Number: 4000(113)B

REPORT DOCUMENTATION PAGE

Form approved OMB No.

Public reporting for this collection of information is estimated to average 1 hour per response, including the time for reviewing instructions, searching existing data sources, gathering and maintaining the data needed, and completing and reviewing the collection of information. Send comments regarding this burden estimate or any other aspect of this collection of information, including suggestion for reducing this burden to Washington Headquarters Services, Directorate for Information Operations and Reports, 1215 Jefferson Davis Highway, Suite 1204, Arlington, VA 22202-4302, and to the Office of Management and Budget, Paperwork Reduction Project (0704-1833), Washington, DC 20503

1. AGENCY USE ONLY (LEAVE BLANK)	2. REPORT DATE	3. REPORT TYPE AND DATES COVERED
4000(113)B	August 2014	Final Report: July 2011 – August 2014

4. TITLE AND SUBTITLE

Experimental Study of Various Techniques to Protect Ice-Rich Cut Slopes

5. FUNDING NUMBERS

Alaska DOT&PF: 4000(133)B
AUTC: 510010

6. AUTHOR(S)

Lin Li, M.S., Research Assistant UAF
Robert mcHattie, P.E., Consultant, GZR Engineering
Xiong Zhang, Ph.D., P.E., Associate Professor, UAF
Mingchu Zhang, Co-PI, UAF

7. PERFORMING ORGANIZATION NAME(S) AND ADDRESS(ES)

Alaska University Transportation Center
University of Alaska Fairbanks
Duckering Building Room 245
P.O. Box 755900
Fairbanks, AK 99775-5900

8. PERFORMING ORGANIZATION REPORT NUMBER

INE/AUTC 15.08

9. SPONSORING/MONITORING AGENCY NAME(S) AND ADDRESS(ES)

State of Alaska, Alaska Dept. of Transportation and Public Facilities
Research and Technology Transfer
2301 Peger Rd
Fairbanks, AK 99709-5399

10. SPONSORING/MONITORING AGENCY REPORT NUMBER

4000(113)B

11. SUPPLENMENTARY NOTES

12a. DISTRIBUTION / AVAILABILITY STATEMENT

No restrictions

12b. DISTRIBUTION CODE

13. ABSTRACT (Maximum 200 words)

Cut slopes are usually required to achieve roadway design grades in the ice-rich permafrost areas in Alaska. However, excavation and exposure of a cut slope destroy the existing thermal balance and result in degradation of ice-rich permafrost. Environmentally acceptable, legal, and economically viable solutions for ice-rich slope protection are still rare. Three potential thermal-erosion mitigation techniques were investigated. Four test sections (Section A: 1 ft wood chips, Section B: coconut blanket, Section C: coconut blanket + Tecco-mesh, and Section D: 1 ft crushed rock as a control section) were constructed at the Dalton Highway 9 Mile Hill during the period of April 17 through April 27, 2013. Temperature and moisture sensors were installed to monitor four test sections and evaluate the effectiveness of the different mitigation techniques. Also, a weather station was built to record climatic information at the test site by April 30, 2013. The filed monitoring period ended on November 11, 2014. No obvious erosion was observed in Sections A and B due to less ice content when compared with Sections C and D which failed one and a half months after construction. The performance of four techniques was discussed in detail.

14- KEYWORDS :

Permafrost (Rbespfp), Ice (Rbdbf), Embankments (Pdxe), Erosion control (Jngse), and Photogrammetry (Esmsfj)

15. NUMBER OF PAGES

16. PRICE CODE

N/A

17. SECURITY CLASSIFICATION OF REPORT	18. SECURITY CLASSIFICATION OF THIS PAGE	19. SECURITY CLASSIFICATION OF ABSTRACT	20. LIMITATION OF ABSTRACT
Unclassified	Unclassified	Unclassified	N/A

Notice

This document is disseminated under the sponsorship of the U.S. Department of Transportation in the interest of information exchange. The U.S. Government assumes no liability for the use of the information contained in this document. The U.S. Government does not endorse products or manufacturers. Trademarks or manufacturers' names appear in this report only because they are considered essential to the objective of the document.

Quality Assurance Statement

The Federal Highway Administration (FHWA) provides high-quality information to serve Government, industry, and the public in a manner that promotes public understanding. Standards and policies are used to ensure and maximize the quality, objectivity, utility, and integrity of its information. FHWA periodically reviews quality issues and adjusts its programs and processes to ensure continuous quality improvement.

Author's Disclaimer

Opinions and conclusions expressed or implied in the report are those of the author. They are not necessarily those of the Alaska DOT&PF or funding agencies.

METRIC (SI*) CONVERSION FACTORS

APPROXIMATE CONVERSIONS TO SI UNITS

Symbol	When You Know	Multiply By	To Find	Symbol
		LENGTH		
in	inches	25.4		mm
ft	feet	0.3048		m
yd	yards	0.914		m
mi	Miles (statute)	1.61		km
		AREA		
in^2	square inches	645.2	millimeters squared	cm^2
ft^2	square feet	0.0929	meters squared	m^2
yd^2	square yards	0.836	meters squared	m^2
mi^2	square miles	2.59	kilometers squared	km^2
ac	acres	0.4046	hectares	ha
		MASS (weight)		
oz	Ounces (avdp)	28.35	grams	g
lb	Pounds (avdp)	0.454	kilograms	kg
T	Short tons (2000 lb)	0.907	megagrams	mg
		VOLUME		
fl oz	fluid ounces (US)	29.57	milliliters	mL
gal	Gallons (liq)	3.785	liters	liters
ft^3	cubic feet	0.0283	meters cubed	m^3
yd^3	cubic yards	0.765	meters cubed	m^3

Note: Volumes greater than 1000 L shall be shown in m^3

		TEMPERATURE (exact)		
ºF	Fahrenheit temperature	5/9 (ºF-32)	Celsius temperature	ºC
		ILLUMINATION		
fc	Foot-candles	10.76	lux	lx
fl	foot-lamberts	3.426	candela/m^2	cd/cm^2
		FORCE and PRESSURE or STRESS		
lbf	pound-force	4.45	newtons	N
psi	pound-force per square inch	6.89	kilopascals	kPa

These factors conform to the requirement of FHWA Order 5190.1A *SI is the symbol for the International System of Measurements

APPROXIMATE CONVERSIONS FROM SI UNITS

Symbol	When You Know	Multiply By	To Find	Symbol
		LENGTH		
mm	millimeters	0.039	inches	in
m	meters	3.28	feet	ft
m	meters	1.09	yards	yd
km	kilometers	0.621	Miles (statute)	mi
		AREA		
mm^2	millimeters squared	0.0016	square inches	in^2
m^2	meters squared	10.764	square feet	ft^2
km^2	kilometers squared	0.39	square miles	mi^2
ha	hectares (10,000 m^2)	2.471	acres	ac
		MASS (weight)		
g	grams	0.0353	Ounces (avdp)	oz
kg	kilograms	2.205	Pounds (avdp)	lb
mg	megagrams (1000 kg)	1.103	short tons	T
		VOLUME		
mL	milliliters	0.034	fluid ounces (US)	fl oz
liters	liters	0.264	Gallons (liq)	gal
m^3	meters cubed	35.315	cubic feet	ft^3
m^3	meters cubed	1.308	cubic yards	yd^3

		TEMPERATURE (exact)		
ºC	Celsius temperature	9/5 ºC+32	Fahrenheit temperature	ºF
		ILLUMINATION		
lx	lux	0.0929	foot-candles	fc
cd/cm^2	candela/m^2	0.2919	foot-lamberts	fl
		FORCE and PRESSURE or STRESS		
N	newtons	0.225	pound-force	lbf
kPa	kilopascals	0.145	pound-force per square inch	psi

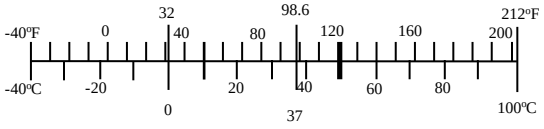

ACKNOWLEDGMENTS

The authors wholeheartedly thank those people who helped with this research project. The Alaska University Transportation Center, Alaska Department of Transportation and Public Facilities (ADOT&PF), and TransCanada Gas Pipeline Corporation jointly provided funding for this study. Geobrugg North America, LLC donated the Tecco-mesh used in one of the test sections. Polar Supply Company provided the erosion control blankets for two of the test sections. Alaska Foundation Technology Inc. provided special services for drilling and installing the grouted anchors and duckbills. Great Northwest Inc. was the contractor responsible for general construction of the test sections. The ADOT&PF Construction Section coordinated and monitored work on the project. Special thanks are extended to the following people: Billy Connor, Jeff Curry, James Sweeney, Jack Beattie, Jim Oswell, Steve Hickman, Tim Shevlin, Errol Master, Justin Morgan, and John Chamberlain. The authors would also like to thank Joel Bailey, Chuang Lin, and Peng Li for their contributions to the fieldwork.

EXECUTIVE SUMMARY

Permafrost underlies most areas of Alaska. Cut slopes are usually required to achieve roadway design grades in these ice-rich permafrost areas. However, excavation and exposure of a cut slope destroy the existing thermal balance and result in degradation of ice-rich permafrost. Uncontrolled erosion and runoff as well as slope failure of cut slopes result from thawing ice-rich permafrost and cause environmental distress, project delays, change orders, and claims. The problem has been documented for more than fifty years, and it still exists. Solutions that are environmentally acceptable, legal, and economically viable are still rare, while new and strict environmental laws make long-accepted Alaska Department of Transportation and Public Facilities (ADOT&PF) methods for dealing with ice-rich permafrost either undesirable or completely unacceptable.

This research project involves the study of three potential thermal-erosion mitigation techniques (1 ft wood chips, coconut blanket, and coconut blanket + Tecco-mesh) that address the regulatory concerns raised by current practices and effectively control erosion from a cut slope in the first thaw season. Four test sections (Section A: 1 ft wood chips, Section B: coconut blanket, Section C: coconut blanket + Tecco-mesh, and Section D: 1 ft crushed rock) were constructed at the Dalton Highway 9 Mile Hill. Temperature and moisture sensors were installed to monitor the four test sections and for evaluating the effectiveness of the different mitigation techniques. Also, a weather station was built to record climatic information at the Experimental Feature (the study) site.

During the first thaw season, it was found that the performance of the slope protection method was highly dependent on the ice content of the slope. The same coconut blanket was used to cover the slope surface of Sections B and C. About one and a half months after construction, the performance of the slope protection was drastically different. No erosion was found at Section B; however, Section C failed due to thermal erosion. This difference in performance was considered mainly due to massive ground ice present in Section C.

In Section A, which was protected by 1 ft of wood chips, no significant erosion was identified until August 2014. Also, it was found that the temperature in this section was lower than the

temperatures in Sections B and C, which indicated that wood chips worked better than the coconut blanket.

The Tecco-mesh did not protect the ice-rich slope that contained massive ice inclusions. Once the ice-rich permafrost in the slope thawed, a large quantity of the fully saturated silty soil behaved like mud, flowing out from under the robust and intact tent of strongly suspended Tecco-mesh. The Tecco-mesh itself did not fail, but it did nothing to hold the saturated silty soil in place. It is stressed here that there were absolutely no problems with the Tecco-mesh material itself. This experimental application of Tecco-mesh was simply a use for which it was not suited. Also, the anchored Tecco-mesh survived intact during the soil thawing process that occurred beneath it.

Crushed rock was used to protect Section D. Due to the presence of massive ground ice, detected during construction. Obvious thermal erosion was found in this section, even though 1 ft of crushed rock was used to cover the slope. However, temperatures in this section were generally lower than in Section C. Also, erosion in Section D was less compared with Section C and was not problematic—even though Section D contained massive ice. The crushed rock treatment was more effective at erosion control than the Section C treatment (coconut blanket + Tecco-mesh).

A photogrammetric method was adopted to monitor the changing topography of the ice-rich cut slope. This method proved reliable and cost-effective. To apply this photogrammetric method for such a purpose, stable control points were required to build the coordinate system. By comparing the exact locations of the slope surface at different times within a given period, the total volume of the erosion or surface accumulation during that period could be measured. Also, erosion measurement results from this study were consistent with previous research-related observations.

TABLE OF CONTENTS

ACKNOWLEDGMENTS i
EXECUTIVE SUMMARY ii
LIST OF FIGURES v
LIST OF TABLES x
CHAPTER 1. INTRODUCTION 1
General 1
General Research Objectives and Research Approach 5
CHAPTER 2. LITERATURE REVIEW 7
General 7
Ice-rich Cut Slope Protection 7
Slope Protection 12
CHAPTER 3. DESIGN OF EXPERIMENTAL FEATURE 14
General 14
Test Section A 15
Test Section B 16
Test Section C 19
Test Section D 22
CHAPTER 4. CONSTRUCTION OF EXPERIMENTAL SECTIONS 25
CHAPTER 5. CONSTRUCTION OF DATA ACQUISITION STATION 43
CHAPTER 6. PERFORMANCE PROBLEMS SOON AFTER CONSTRUCTION 51
CHAPTER 7. RESULTS AND ANALYSIS 59
Site Climatic Conditions 59
Temperature Changes in the Test Section 64
Moisture Changes in the Test Section 80
Photogrammetric Erosion Monitoring 83
CHAPTER 8. CONCLUSIONS AND RECOMMENDATIONS 100
Conclusions Specific to the Experimental Feature 100
Some Generalized Thoughts and Conclusions Pertinent to the Experimental Feature 102
REFERENCES 105
APPENDICES 106
Appendix A. Photogrammetric Method for Erosion Monitoring 106
Appendix B. Alaska DOT&PF Construction Observations and Comments 116

LIST OF FIGURES

Figure 1.1 Idealized development of stability in ice-rich cut (after Berg and Smith, 1976) 2
Figure 1.2 Dalton Highway 3
Figure 1.3 Location of ice-rich cut slope (from Google Maps®) 4
Figure 1.4 Ice-rich cut slope site prior to construction (looking north) 4
Figure 2.1 Ice-rich cut slope (Mageau and Rooney, 1984) 8
Figure 2.2 Four test sections and control section at Hess Creek, Alaska (after APSC, 1974) 10
Figure 2.3 Dalton Highway cut in ice-rich permafrost (Vinson and McHattie, 2009) 11
Figure 2.4 Erosion control blanket (from http://www.thelandstewards.com/blankets.htm) 13
Figure 2.5 Tecco-mesh field examples (Tecco slope stabilization system product manual, 2010) 13
Figure 3.1 Experimental Feature layout with three experimental and one control section 15
Figure 3.2 Profile of Section A 16
Figure 3.3 Profile view showing temperature sensor locations in Section A 16
Figure 3.4 Profile of Section B 17
Figure 3.5 Layout of Section B 18
Figure 3.6 Enlargements of duckbill earth anchor and pins 18
Figure 3.7 Profile for Section C 19
Figure 3.8 Section C, anchor and sensor locations 20
Figure 3.9 Detail of Section C anchor 20
Figure 3.10 Nail and anchor detail with boundary rope 21
Figure 3.11 Plan view – connection of mesh sheets in Section C 21
Figure 3.12 Connection details 22
Figure 3.13 Profile of Section D 23
Figure 3.14 Layout for temperature sensor locations 23
Figure 3.15 Layout for temperature sensor locations 24
Figure 4.1 Cut slope at Dalton Highway 9 Mile Hill construction project location 25
Figure 4.2 Layout on the cut slope 26
Figure 4.3 Drilling on the cut slope 27

Figure 4.4 Drilling at the upper part of the slope 27
Figure 4.5 Installation for sensor housing 28
Figure 4.6 Instrumentation hole with sensor housing installed 28
Figure 4.7 Cut slope erosion during construction 29
Figure 4.8 Ice in the cut slope 30
Figure 4.9 Ice exposed in the cut slope 30
Figure 4.10 Cut slope protected from erosion during drilling 31
Figure 4.11 Cable end of installed duckbill earth anchor 32
Figure 4.12 Installation of hollow rebar anchor 32
Figure 4.13 Re-smoothing the cut slope surface 33
Figure 4.14 Seeded cut slope 34
Figure 4.15 Placement of the coconut erosion control matting 35
Figure 4.16 Placement of coconut erosion control matting 35
Figure 4.17 Section B showing duckbill anchor plates after construction 36
Figure 4.18 Enlargement of a circle wire top pin 37
Figure 4.19 Placement of Tecco-mesh 38
Figure 4.20 Cutting away excess Tecco-mesh 38
Figure 4.21 Connecting adjacent Tecco-mesh strips 39
Figure 4.22 Section C appearance after construction 39
Figure 4.23 Close-up view of Tecco-mesh at an anchoring point 40
Figure 4.24 Construction of Section D 41
Figure 4.25 Spreading wood chips along top portion of cut slope 41
Figure 4.26 Appearance of Experimental Feature soon after completion 42
Figure 5.1 Backfilling with sand after insertion of temperature sensor string 43
Figure 5.2 Installation of moisture sensor at top of temperature sensor string 44
Figure 5.3 Temperature and moisture sensor location 44
Figure 5.4 Data collection station 46
Figure 5.5 Data collection station after completion 47
Figure 5.6 CR1000 data logger and AM16/32B multiplexing equipment 47
Figure 5.7 Air Temp/Relative Humidity sensor 48
Figure 5.8 Wind sensor 48
Figure 5.9 Radiation sensor 49
Figure 5.10 Precipitation sensor 49

Figure 5.11 Two cameras installed for slope monitoring 50
Figure 6.1 Panorama view of Experimental Feature showing failure in Tecco-mesh section 52
Figure 6.2 Close view of failure within the Tecco-mesh section.....52
Figure 6.3 Close views showing exposure of soil anchor grout (left) and portion of massive ice feature under Tecco-mesh (right) 53
Figure 6.4 Surface protection matting in area showing no grass growth is not in direct contact with ground surface.....54
Figure 6.5 Section C without Tecco-mesh and coconut blanket.....56
Figure 6.6 Massive ice in Section C 56
Figure 6.7 Covering Section C with crushed rock.....57
Figure 6.8 Cut slope after construction on Section C 57
Figure 6.9 Start of thaw related damage at top of Experimental Feature cut slope 58
Figure 7.1 Air temperatures at the Experimental Feature site 60
Figure 7.2 Temperature variations for four different days.....60
Figure 7.3 Precipitation at the Experimental Feature site.....61
Figure 7.4 Relative humidity at the Experimental Feature site.....61
Figure 7.5 Wind direction frequencies at the Experimental Feature site.....62
Figure 7.6 Wind speed at the Experimental Feature site 63
Figure 7.7 Incident solar radiation received at the Experimental Feature site.....63
Figure 7.8 Incident solar radiation at the Experimental Feature site on three different days 64
Figure 7.9 Battery output voltage at the Experimental Feature site.....64
Figure 7.10 Temperature variations in Section A 66
Figure 7.11 Temperature variations in Section B 68
Figure 7.12 Temperature variations in Section C 70
Figure 7.13 Temperature variations in Section D 72
Figure 7.14 Temperature contours at different times in Section A.....74
Figure 7.15 Temperature contours at different times in Section B.....76
Figure 7.16 Temperature contours at different times in Section C.....77
Figure 7.17 Temperature contours at different times in Section D.....78
Figure 7.18 Temperature contours at different times in Section D.....80
Figure 7.19 Volumetric moisture content variations in Section A 82
Figure 7.20 Volumetric moisture content variations in Section B.....82

Figure 7.21 Volumetric moisture content variations in Section C.....83
Figure 7.22 Volumetric moisture content variations in Section D 83
Figure 7.23 Surface volume change on Section A.....85
Figure 7.24 Section A after construction on April 26, 2013.....85
Figure 7.25 Section A with more wood chips on April 30, 2013 86
Figure 7.26 Section A with more wood chips on September 27, 2013.....86
Figure 7.27 Section A with more wood chips on August 8, 2014 87
Figure 7.28 Surface volume change on Section B 88
Figure 7.29 Section B on June 17, 2013 88
Figure 7.30 Section B on July 15, 2013.....89
Figure 7.31 Section B on August 8, 2013.....89
Figure 7.32 Section B on September 27, 2013 90
Figure 7.33 Section B on August 8, 2014.....90
Figure 7.34 Surface volume change on Section C 92
Figure 7.35 Section C on April 30, 2013 92
Figure 7.36 Section C on June 13, 2013 93
Figure 7.37 Section C on June 17, 2013 93
Figure 7.38 Section C on September 27, 2013 94
Figure 7.39 Section C on May 20, 2014 94
Figure 7.40 Section C on August 8, 2014.....95
Figure 7.41 Surface volume change on Section D.....96
Figure 7.42 Section D on April 30, 2013.....96
Figure 7.43 Section D on June 13, 2013.....97
Figure 7.44 Section D on June 17, 2013.....97
Figure 7.45 Section D on September 27, 2013 98
Figure 7.46 Section D on May 20, 2014 98
Figure 7.47 Section D on August 8, 2014.....99
Figure A.1 Camera and lens.....106
Figure A.2 Principle of photogrammetry.....107
Figure A.3 Typical image captured for erosion monitoring 108
Figure A.4 Coordinate system for erosion measurement.....110
Figure A.5 Camera stations at different view angles 111
Figure A.6 Point cloud for erosion monitoring.....112

Figure A.7 Mesh generated for Section A for volume calculation 112
Figure A.8 Mesh generated for Section B.....113
Figure A.9 Mesh generated for Section C.....113
Figure A.10 Mesh generated for Section D 114
Figure A.11 Volume calculation for a single mesh cell.....115

LIST OF TABLES

Table A.1 Camera calibration parameters.....108

CHAPTER 1. INTRODUCTION

General

The Alaska Department of Transportation and Public Facilities (ADOT&PF) and other users (such as pipeline companies) need to make construction cuts in ice-rich permafrost. In general, the technique used in the past was to make, for example, an over-wide ditch and cut the ice-rich permafrost vertically at the back of the ditch. Over a period of years, the vertical, ice-rich permafrost face thaws. The thaw progresses rapidly into the vertical face mainly because the thermally protective natural vegetation has been removed, causing the bank to collapse and the vegetation mat to slump on top of the thawing soil/ice mass (see Figure 1.1). Eventually the cut becomes an undulating slope, covered with relatively stable vegetation. In the interim, meltwater carrying soil and organics from within the slumped mass flows onto the bench and potentially into protected areas such as wetlands, streams, and lakes. Over the last several decades, regulatory agencies have refined and developed stringent environmental regulations that prohibit such discharges. At present, thermal-erosion mitigation techniques that are both environmentally acceptable and economically viable require much in the way of development and testing. Consequently, there is a significant need for research in this direction, which justifies the work documented in this report.

The first thaw season after construction of the soil cut represents a critical period, as thawing and soil erosion will be most active at this time. Long-term, natural processes such as revegetation reduce the volume of eroded soil. Hence, mitigation techniques that are effective in the first thaw season are of primary importance. This research involves the study of three potential thermal-erosion mitigation techniques that have been designed to address the concerns raised by current practices and to be effective at controlling erosion from a cut slope in the first thaw season.

The design and construction of the Experimental Feature (the cut slope at the study site) are described in this report, as well as the initial performance results based on data collected during the first thawing season after construction.

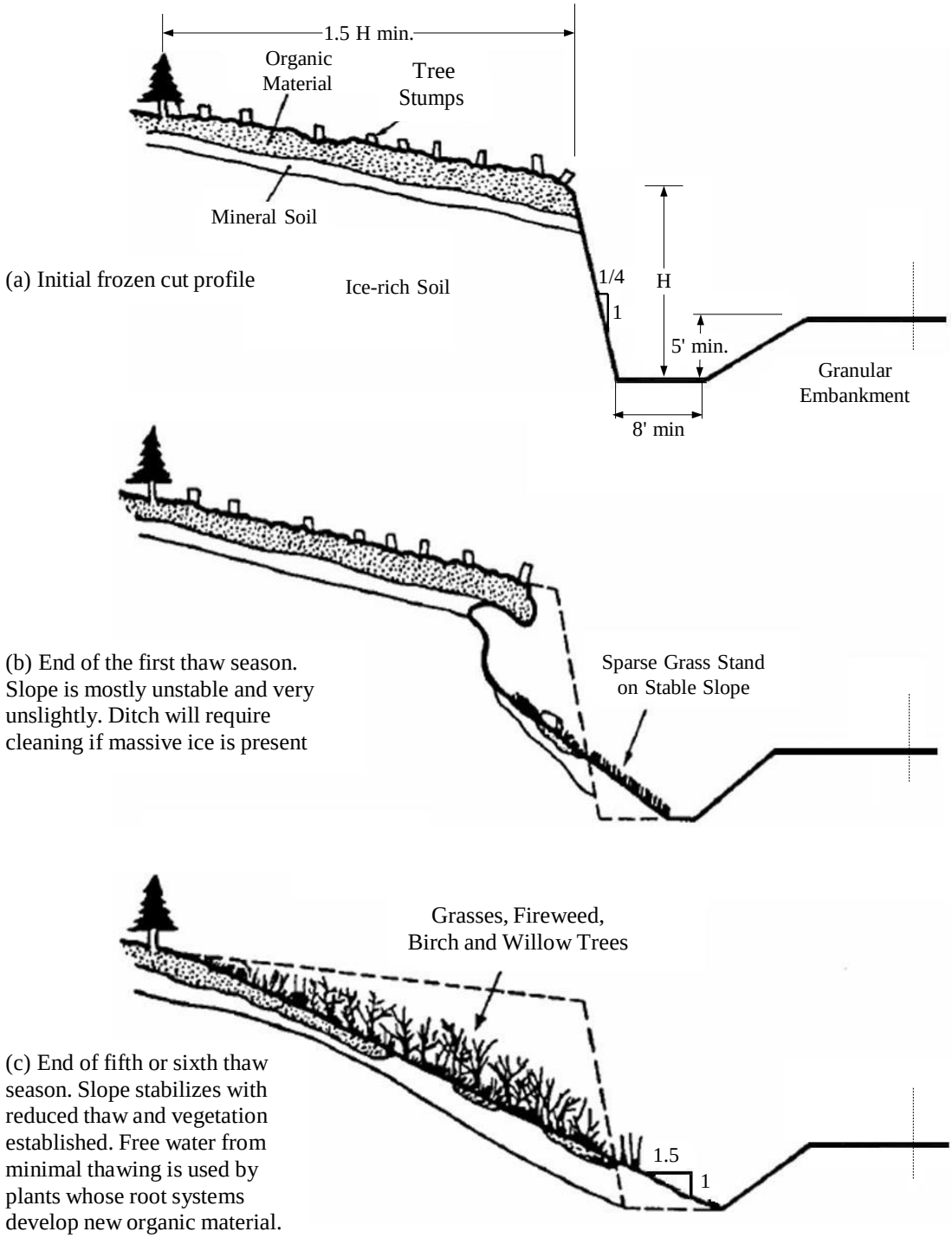

Figure 1.1 Idealized development of stability in ice-rich cut (after Berg and Smith, 1976)

The following map (Figure 1.2) shows the Dalton Highway location of the Experimental Feature. The location of the Experimental Feature (see Figure 1.3) can be seen using Google Maps®. The Experimental Feature area, shown in Figure 1.4, is located at approximately latitude 65.553584°N and longitude 148.905602°W (near Milepost 10 of the Dalton Highway).

Figure 1.2 Dalton Highway

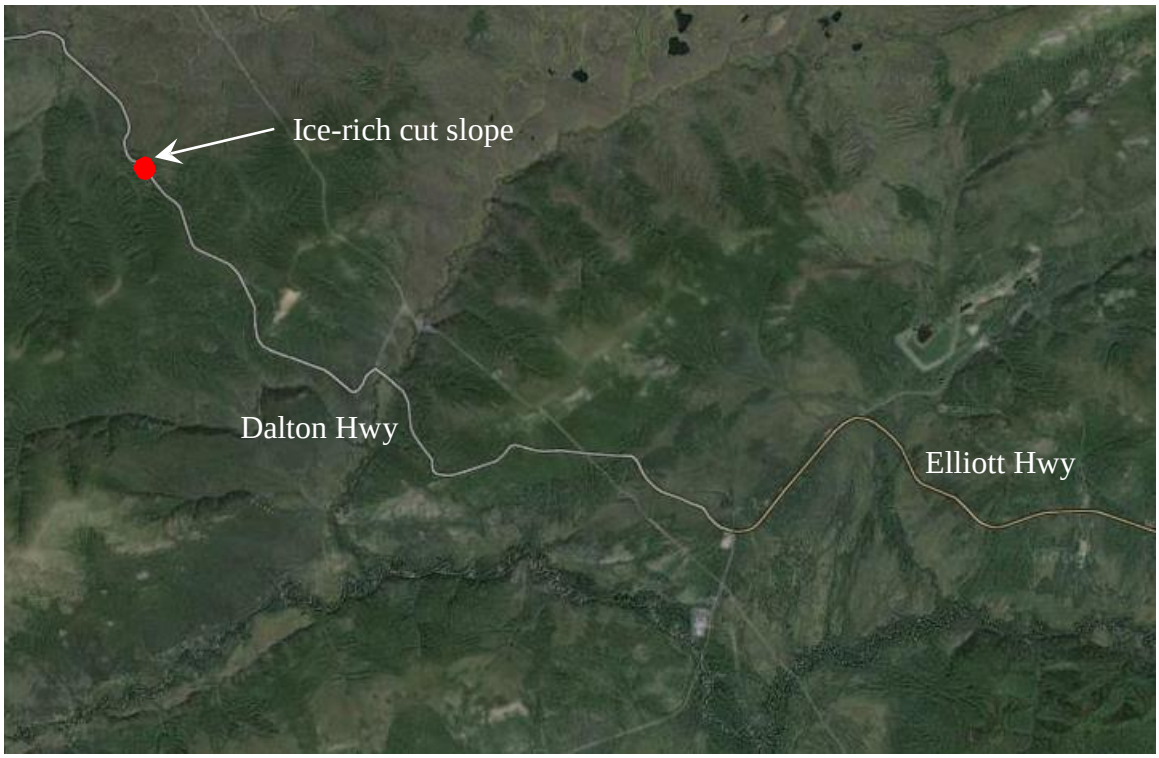

Figure 1.3 Location of ice-rich cut slope (from Google Maps®)

Figure 1.4 Ice-rich cut slope site prior to construction (looking north)

The test sections incorporated the following design techniques:

• Biodegradable Erosion Control Blanket with Hydro-seeding: This mitigation technique involved hydro-seeding the cut slope, then applying a well-anchored erosion control blanket. The purpose of hydro-seeding is to establish vegetation that, with time, provides necessary erosion control on the slope. The erosion control blanket that is placed over the slope functions as a short-term erosion control measure while the vegetation is becoming established. The biodegradable erosion control blanket eventually decomposes to mulch or compost consistency as the surface vegetation is established.

• Anchored Tecco-mesh with Biodegradable Erosion Control Blanket and Hydro-seeding: This mitigation technique is a heavy-duty version of the above-mentioned biodegradable erosion control blanket with hydro-seeding. A well-anchored, non-biodegradable layer of steel Tecco-mesh is applied over a layer of biodegradable erosion control blanket that is placed on an ice-rich cut slope that has been hydro-seeded. This treatment, which is thought to improve slope stability during thawing, will be compared with the previous technique to determine if the more robust slope-stabilization measure is necessary.

• Wood Chip Slope Treatment: For this mitigation technique, a relatively thin layer of wood chip material is placed on the cut slope face. The wood chip layer is approximately 1 ft thick. Past experience with the use of wood chips for both thermal and erosion control has been well documented. Wood chips have proved extremely effective in reducing the velocity of the water (released from thawing ice-rich soils as well as from precipitation) that percolates through them. An additional attractive feature of this surface treatment is that, as the subgrade deforms in response to the thawing underlying material, the wood chips tend to conform to the deforming ground surface. This property of wood chips ensures that they remain in contact with the mineral soil, thus protecting it by preventing piping and direct erosion along the surface of the thawing ground.

General Research Objectives and Research Approach

The objective of this experimental research is to investigate the feasibility of using three promising erosion mitigation techniques to protect slope cuts in ice-rich permafrost. Four test sections were constructed at the Dalton Highway 9 Mile Hill: (1) a control section; (2) a wood chip layer (1 ft thick) section; (3) a biodegradable erosion control blanket with hydro-seeding

section; and (4) an anchored Tecco-mesh with biodegradable erosion control blanket and hydro-seeding section. Assessment of the experimental sections began during spring 2013, and monitoring continued to August 2014. Observations from this initial stage are presented in this report. As data collection and analyses progress, additional recommendations and guidelines for design, construction, and maintenance will be provided. Continued monitoring ensures appropriate application of the tested mitigation methods on future construction projects that require cuts in ice-rich permafrost. Construction problems, contractor personnel requirements, special equipment needs, and initial results are discussed in this report.

To meet the general objectives of this study, the following major tasks were completed:

- Task 1: Literature survey
- Task 2: Identification of an ice-rich permafrost site and obtaining of permits for construction and agreement, soil sampling, and laboratory testing
- Task 3: Construction of test sections with implementation of various mitigation techniques
- Task 4: Field monitoring of the performance of test sections
- Task 5: Draft of final report and recommendations

CHAPTER 2. LITERATURE REVIEW

General

In this chapter, a literature review was performed on protection methods for ice-rich soils in cold regions. For ice-rich cut slopes, the protection usually involves erosion control and protection from slope failure. Generally, the majority of erosion on ice-rich cut slopes comes from running water due to melting ice and snow. This kind of erosion is commonly referred to as *thermal erosion*. Thermal erosion occurs in two stages: when snow melts and when ground ice melts. When air (ambient) temperature rises above the freezing point, snow begins to melt. During this first stage of thermal erosion, the runoff from melting snow can cause significant slope erosion. During the second stage, when the air temperature is high enough to melt ice wedges and other forms of ground ice, significant thaw-settlement and runoff erosion often occur. Runoff from individual precipitation events is not a significant source of thermal erosion. Thus, erosion due to precipitation is not discussed in this study.

Ice-rich Cut Slope Protection

In Alaska, problems associated with excavation of cut slopes in ice-rich permafrost were reported as early as the 1920s during development of the Fairbanks mining district and in the early 1940s during military construction of the Alaska Highway. Unfortunately, there was very limited technical documentation of ground conditions and slope performance. In general, the technique used in the past was to make a wide, relatively level "bench" area and cut the ice-rich permafrost vertically some distance from the bench. Over a period of years, the ice-rich permafrost thaws where the vegetation has been removed. The bank collapses and the vegetation mat slumps on top of the thawing soil/ice mass. Eventually the cut becomes an undulating slope covered with vegetation that becomes relatively stable. Due to the difficulties associated with thermal degradation of ice-rich soils, subsequent emphasis has been given to minimize cuts in ice-rich frozen soil. Evaluation and documentation of frozen soil cut slope performance in Alaska has been limited (Mageau and Rooney, 1984). In 1969, major near-vertical cuts were made in ice-rich silts on the initial 56-mile segment of the Dalton Highway from Livengood to the Yukon River. Performance of these near-vertical cut slopes was monitored by Alyeska Pipeline Service Company (APSC). The overall natural restabilization and revegetation of the thermally degraded slopes were considered satisfactory at a time when worries about

environmental impacts were attuned to localized observable consequences. Of course, this view has become obsolete with the present reality of far-reaching, comprehensive, and rigorously enforced state and federal regulations. Figure 2.1 shows two pictures of a near-vertical ice-rich cut slope, indicating the condition immediately after the slope was cut (top photo) and after a new thermal equilibrium was established (bottom photo).

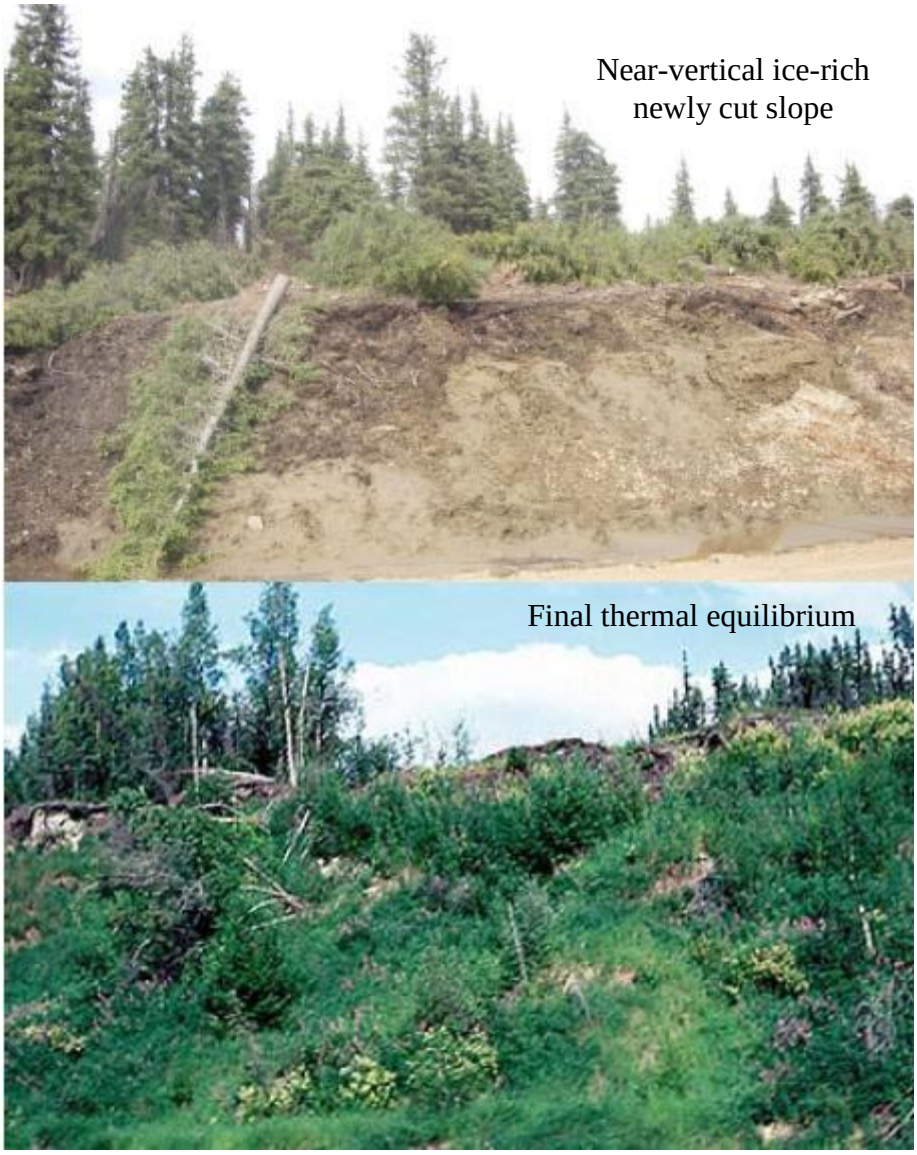

Figure 2.1 Ice-rich cut slope (Mageau and Rooney, 1984)

In 1973, a test site was constructed by APSC near Hess Creek on the Dalton Highway to evaluate the effect of four different surface treatments for reducing thermal erosion on slopes cut at about

1.5:l (horizontal to vertical) into ice-rich silt (APSC, 1974, 1975). The test sections, originally monitored during the 1973 and 1974 summer seasons, are shown in Figure 2.2. The findings were summarized in Vinson and McHattie (2009). All test sections were sprayed with the same grass seed mixture after construction. For Test Section I, during the second summer, large thaw-induced depressions developed under the insulation and large downslope movements of the thawed soil occurred. The slope movements destroyed 70% of the insulation. Thaw depths averaged 0.7 m (2.3 ft) in 1974. Test Section II experienced failure during the first summer, especially near the toe, with much of the failed material flowing into the ditch. By the end of the second summer, 50% of the slope was covered with the excelsior blanket, a vertical scarp had formed at the top of the slope, and the overall appearance was similar to Test Section I. Thaw depths averaged 0.8 m (2.6 ft) in 1974.

Test Section III, which was originally burlap (East) or nylon (West) coated with high-reflectivity titanium dioxide paint, became soaked and distorted with mudflows during construction. Two layers of excelsior blanket were placed over this material. Test Section III failed repeatedly in 1973. Mass movements in this test section were greater than in the other four sections during 1973. Thaw depths in 1974 were 0.9 m (3 ft) at the toe and greater than 1.5 m (5 ft) at the top of the slope. The insulation layer in Test Section IV was treated with straw mulch and seed to stimulate vegetation growth. It was intended that the sand filter layer would intercept meltwater and reduce excess pore water during periods of rapid thawing. Very little evidence of soil movement, sloughing, or meltwater release was observed in this section through 1974. Thaw depths were 0.6 to 0.9 m (2 to 3 ft) in 1974. Test Section V (control) experienced considerable caving and sloughing in 1973. The material was not transported far from the slope, as was the case for Test Sections I and II. By the end of the summer (1973), a vertical scarp developed at the top of the slope. No caving, sloughing, or erosion was observed in 1974, and sparse vegetation appeared on the slope surface. Thaw depths were 0.9 to 1.2 m (3 to 4 ft) in 1974.

Longer-term performance of the test sections was evaluated during two field investigations conducted in the 1983 summer season. The investigators noted that all the slopes were stable. However, significant slope deterioration caused by large-volume reduction and downslope movement occurred on the majority of the test sections. Revegetation was well established on

slopes that had experienced significant displacement and consequent flattening. Revegetation on steeper, less deformed slopes was not well established or was non-existent.

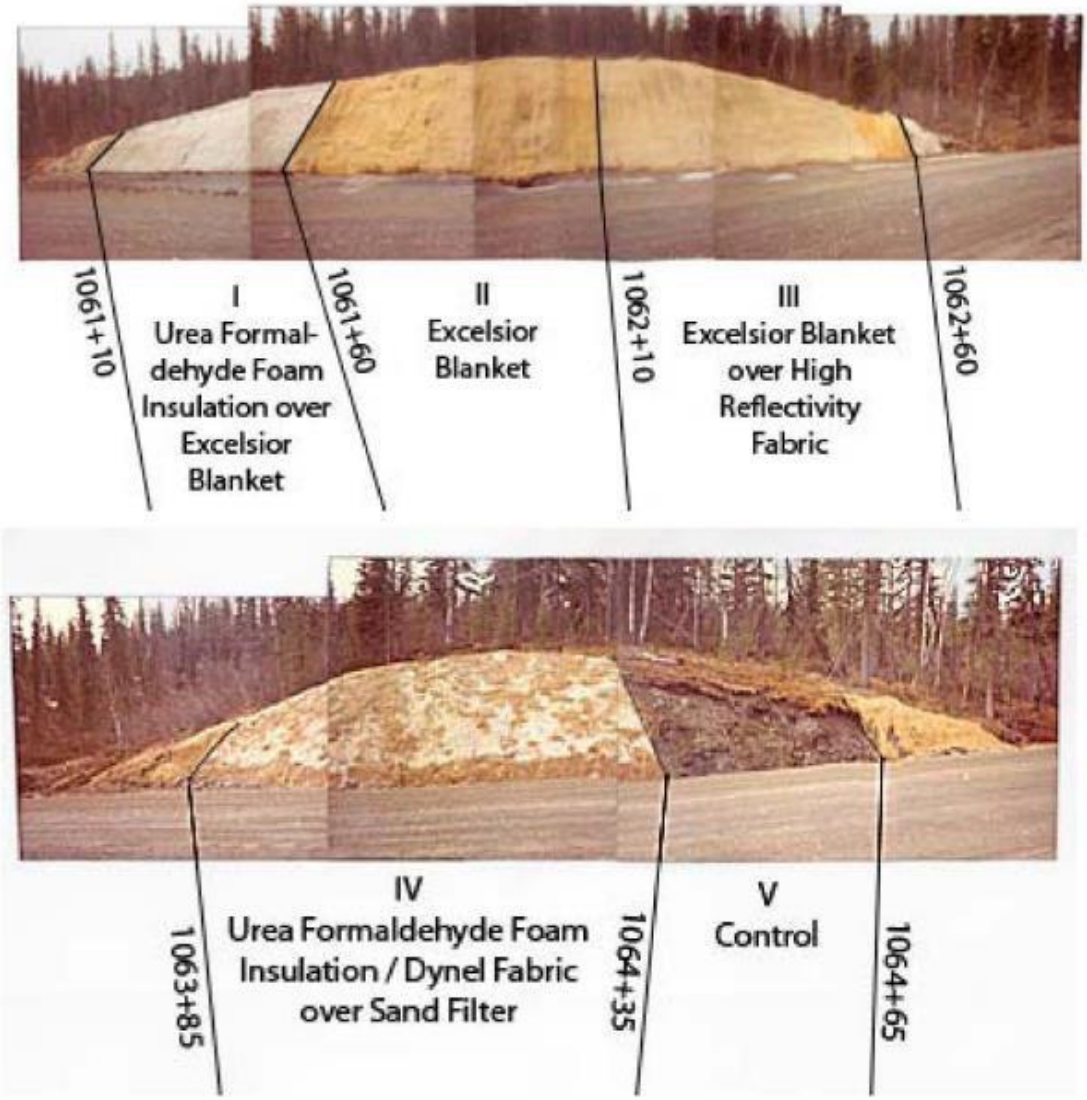

Figure 2.2 Four test sections and control section at Hess Creek, Alaska (after APSC, 1974)

A recent example (Vinson and McHattie, 2009) related to thermal erosion of cut slopes in ice-rich permafrost is located along the Dalton Highway, Milepost 37 to 49 (see Figure 2.3). The cut volume, originally considered bedrock and weathered bedrock, was actually highly weathered ice-rich bedrock. The cut design, though appropriate for weathered bedrock, was inappropriate for the unexpected ice-rich mineral soils. Uncontrolled erosion, thawed slurry runoff, and slope failure resulted in significant environmental concern.

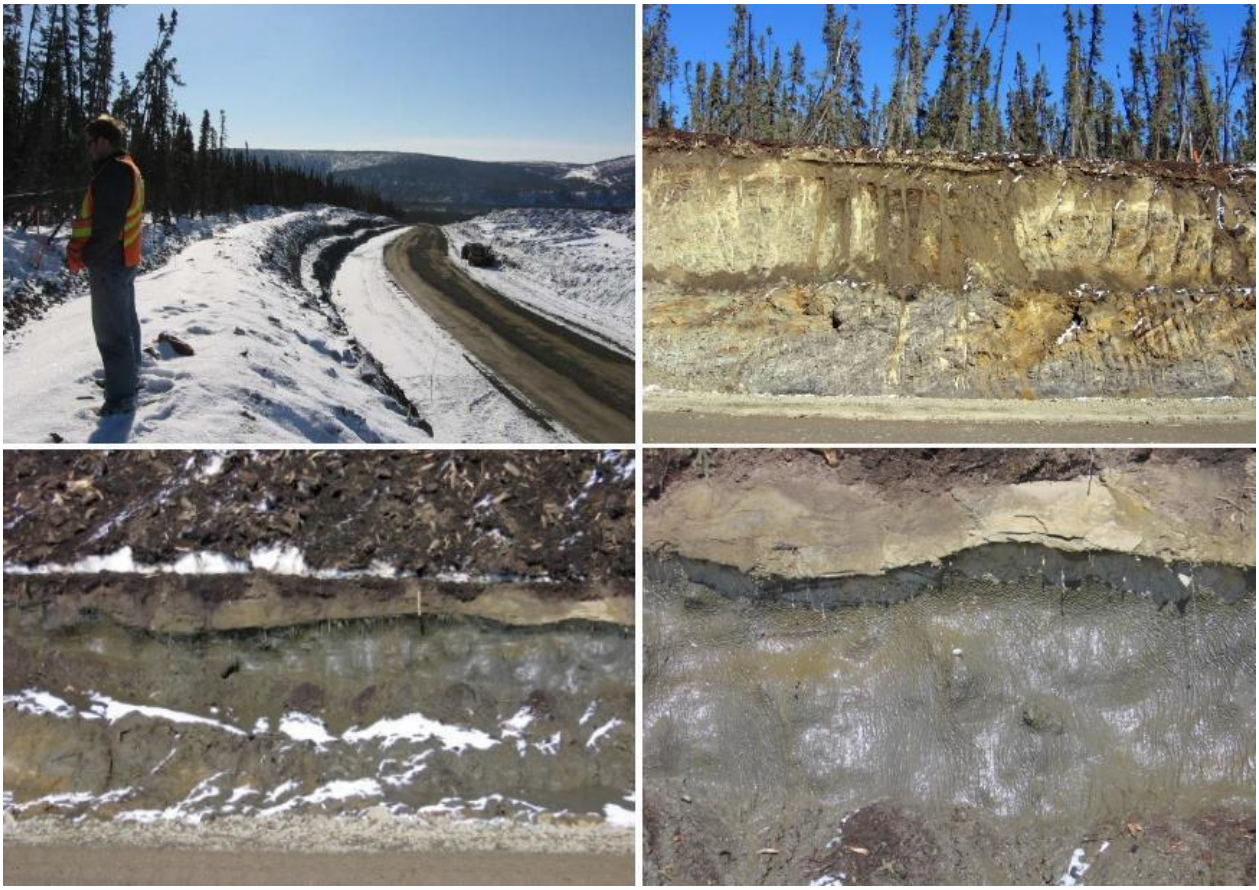

Figure 2.3 Dalton Highway cut in ice-rich permafrost (Vinson and McHattie, 2009)

McHattie and Vinson (2008) and Vinson and McHattie (2009) summarized the best management practices for ice-rich permafrost exposed during construction operations. They concluded that solutions that are environmentally acceptable and economically viable must be developed and evaluated, because new and strict environmental laws and regulations make the historical ADOT&PF methods for dealing with ice-rich permafrost either undesirable or unacceptable. In addition to the near-vertical cut method presented before, another ADOT&PF technique has included cutting the ice-rich permafrost slope at about 1.5H:1V and placing a free-draining gravel blanket on the slope surface. The horizontal width of one successful gravel blanket was about 8 ft—the width being an expedient to allow rapid construction using a belly-dump truck. The 1.5H:1V blanket side slope matched the cut slope.

The gravel blanket performs several functions; it serves as insulation, as a filter, and as a retaining structure, all of which reduce thermal erosion of the soil and runoff. In addition, the blanket can accommodate large thaw settlement and deformation by conforming to the changing

shape of the underlying cut slope surface as thawing progresses. The disadvantage of this option is that the gravel surface limits growth of vegetation, and at locations where gravel is not readily available, the cost for constructing such a blanket can be prohibitively high. The use of wood chips as a thermal mitigation technique to reduce the rate of permafrost thawing on selected slopes along the Norman Wells pipeline is well documented (Naviq Consulting Inc. and AMEC Earth & Environmental, 2007). Less well documented is the secondary benefit of the erosion control aspects of wood chips.

While the problem of environmentally acceptable and economic erosion mitigation remains unsolved, it is expected that the need for such mitigation will recur in the future, as during the construction of the proposed natural gas pipelines. It is hoped that techniques evaluated during this research project will provide some of the needed cost-effective and environmentally friendly solutions to the problem.

Slope Protection

The major factors affecting soil erosion are soil characteristics, climate, runoff intensity and duration, vegetation or other surface cover, and topography. Also, the quantity and size of the soil particles that are loosened and removed increased with the velocity of the runoff. Soil erosion is evident in many situations, and the environmental impact can be significant. In China, crushed stone has been used as shade and insulation to prevent ground ice in cut slopes from melting.

To prevent soil erosion from non-frozen slopes, commonly available erosion control materials are easy to use and quite affordable. Erosion control blankets are generally a machine-produced mat of organic, biodegradable mulch such as straw, curled wood fiber (excelsior), coconut fiber, or a combination thereof, evenly distributed on or between photodegradable polypropylene or biodegradable natural fiber netting. Erosion control blankets can provide immediate soil surface stabilization, as shown in Figure 2.4. Even if herbaceous vegetation does not grow, the blankets will provide excellent protection for at least one season. After the vegetation grows, the erosion control blanket degrades over time until only the vegetation is left in place. The vegetation, once established, provides permanent erosion control. Erosion control blankets also protect seeds from predators and reduce desiccation and evaporation by insulating the soil and seed environment.

Figure 2.4 Erosion control blanket (from http://www.thelandstewards.com/blankets.htm)

Tecco-mesh, one of the materials evaluated during this research project, represents an extremely heavy-duty version of a slope protection blanket. Tecco-mesh is a high-tensile mesh slope-stabilization system, usually considered appropriate for stabilizing steep soil, sediment, and rock slopes. Tecco-mesh can be pre-tensioned on the slope at a defined force, using soil or rock nails and spike plates (see Figure 2.5). Generally, no maintenance is required provided the slope stabilization system is correctly installed, fastened, and pre-tensioned, and has not been damaged by external influences.

Figure 2.5 Tecco-mesh field examples (Tecco slope stabilization system product manual, 2010)

CHAPTER 3. DESIGN OF EXPERIMENTAL FEATURE

General

This chapter describes the design of the test section treatments and the sensor instrumentation. In October 2012, the slope at the site was cut at a gradient of 1.5H:1V. In order to evaluate different methods of permanently protecting the stability of cut slopes in ice-rich permafrost soils, the cut slope was divided into four sections (Sections A, B, C, and D), and a different treatment method was used on each section. These treatments included three protection designs: wood chips, a coconut erosion control blanket, and a coconut erosion control blanket plus Tecco-mesh. The fourth treatment method, which involved using a blanket of crushed rock, provided a control section for the Experimental Feature. The crushed rock blanket was the ADOT&PF designer's standard treatment, used throughout the project for protecting ice-rich cut slopes. For all sections, hydroseeding was performed before any treatment on the ice-rich cut slope. Construction of the different slope protection methods was performed from April 17 through April 27, 2013, and instrumentation installation was completed April 30, 2013.

Designs for the different protection methods used on the cut slope are summarized in Figure 3.1. Section A, which is at the left side, as well as the upper part of the slope was covered with wood chips. Section B was protected by one layer of coconut erosion control blanket. Section C was protected by one layer of coconut erosion control blanket as well as Tecco-mesh. Section D—the control section, located at the right side of the slope, was protected by two ft of crushed rock.

Detailed designs for these sections, as well as information about the design and installation of the instrumentation, are presented on the following pages. Various types of sensors such as for recording soil temperature, moisture, precipitation, radiation, wind speed, and air temperature were used to monitor locations above, on, and under the Experimental Feature's cut slope face.

Figure 3.1 Experimental Feature layout with three experimental and one control section

Test Section A

Test Section A was protected by 1 ft of wood chips. The profile for this section is shown in Figure 3.2. This section, which is 30 ft (slope length) by 35 ft (centerline length), extends from station 520 + 10 to 520 + 45. Three holes (2 inches in diameter) at station 520 + 30, located near the top, middle, and bottom of the treated slope, were drilled for placement of temperature sensors, as shown in Figure 3.3. The top and bottom sensor holes are 10 ft deep, and the middle hole is 20 ft deep. The diameter and depth of these holes and sensor placement locations are the same for the other three sections. Holes for the sensors were drilled perpendicular to the surface of the cut slope. Temperature sensors were installed at various depths in the holes, according to Figure 3.3. Also, some moisture measurement sensors were installed at the surface of the slope with the surface temperature sensors.

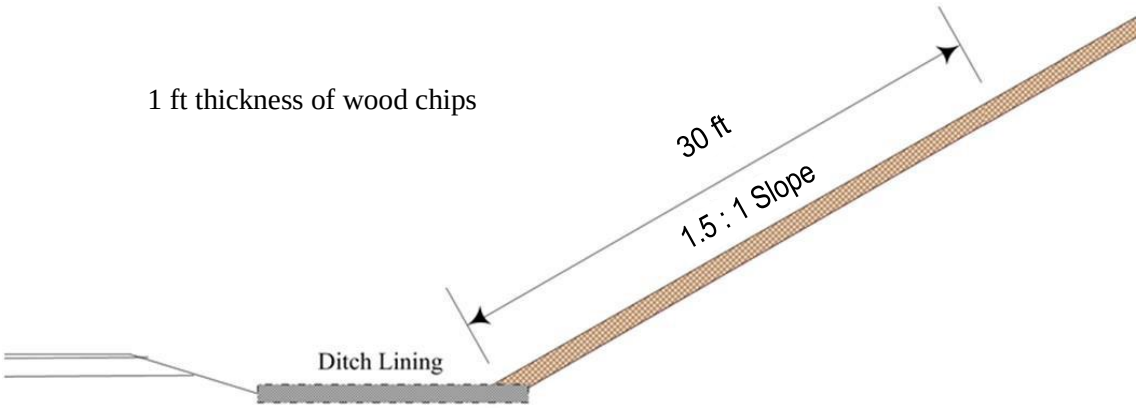

Figure 3.2 Profile of Section A

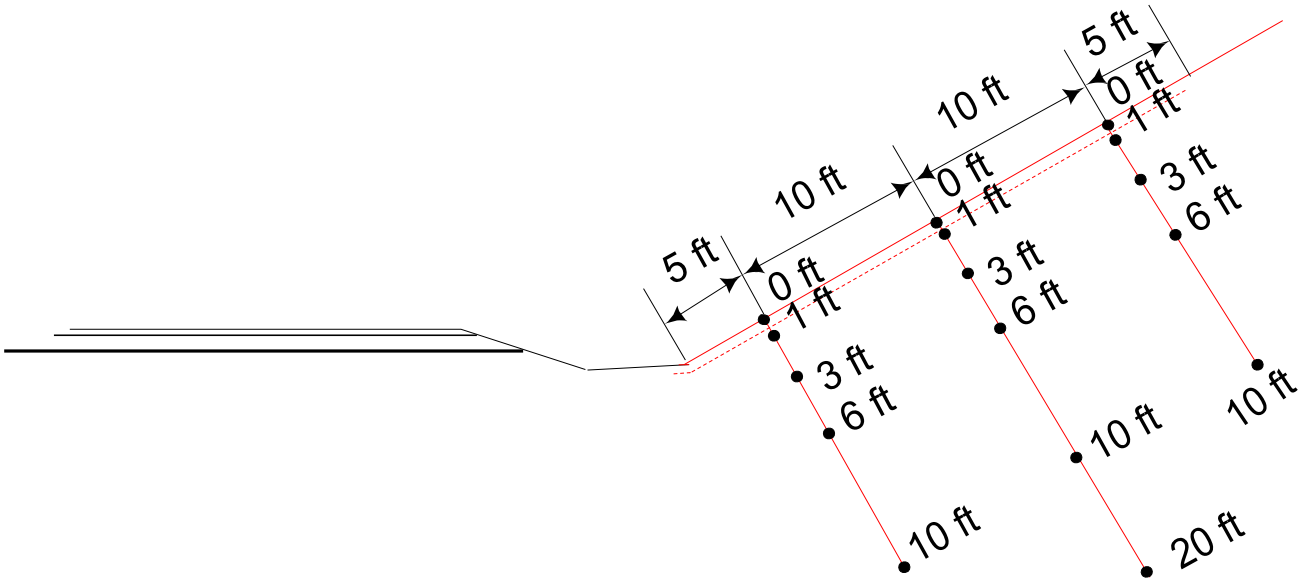

Figure 3.3 Profile view showing temperature sensor locations in Section A

Test Section B

Test Section B was protected by one layer of coconut erosion control blanket. The profile for this section is shown in Figure 3.4. This 30-ft by 50 ft section extends between stations 519 + 60 and 520 + 10, as shown in Figure 3.4. Similar to Section A, three holes at station 519 + 85, located at the top, middle, and bottom, were drilled for placement of temperature sensors. Also, three moisture measurement sensors were installed at the surface of the slope, along with the surface temperature sensors. In addition to the coconut matting, a heavy application of mulch seeding

was included as part of the design. To hold the coconut mat in place, 32 holes (each with a diameter of 2 in. and a depth of 8 ft) were drilled to allow placement of modified duckbill earth anchors. The duckbill anchors were modified in such a way that it is possible to easily readjust tension on them after construction to ensure that good contact between the coconut matting and the ground surface is maintained.

The duckbill anchors were installed along the cut slope and spaced 7.5 ft and 6 ft in the vertical and horizontal directions, respectively, as shown in Figure 3.6. Also, circle top wire pins were installed with a spacing of 1.5 ft and 1.2 ft in the vertical and horizontal directions, respectively, as shown in Figure 3.7. The wire pins were added to the design in an attempt to ensure initial maximum contact between the coconut matting and the cut slope surface. This additional anchoring measure was intended to promote vegetation growth as soon as possible after construction.

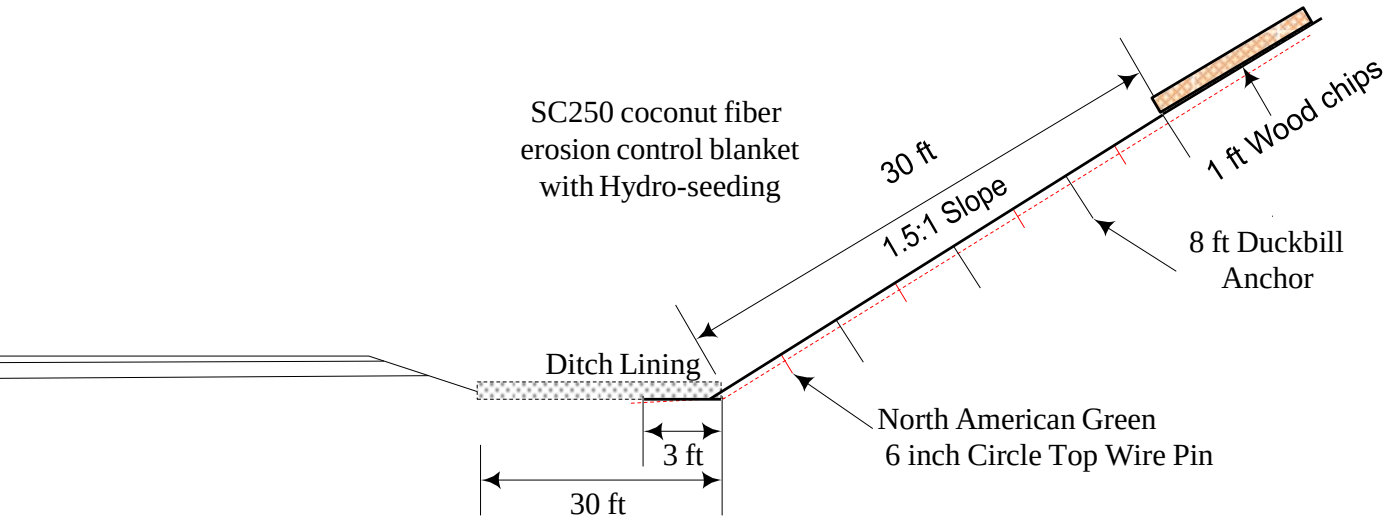

Figure 3.4 Profile of Section B

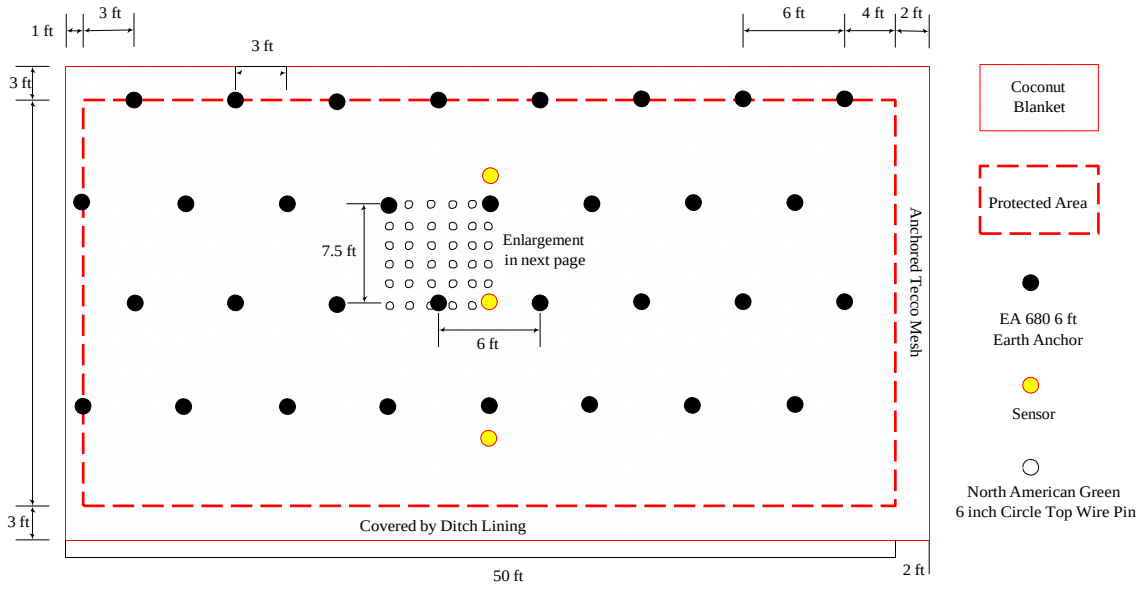

Figure 3.5 Layout of Section B

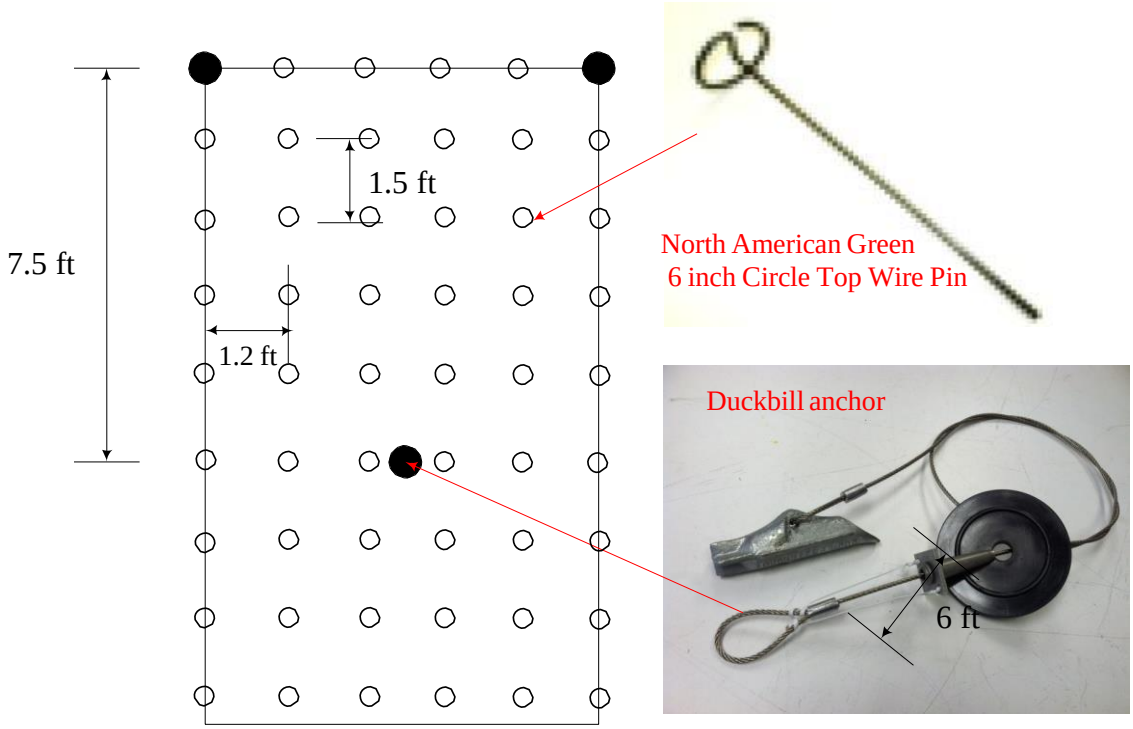

Figure 3.6 Enlargements of duckbill earth anchor and pins

Test Section C

Test Section C was protected by one layer of coconut erosion control blanket as well as Tecco-mesh. The profile for this section is shown in Figure 3.7. This section is identical in size to Section B (30 ft by 50 ft) and extends from station 519 + 10 to 519 + 60, as shown in Figure 3.8. Similar to Section A, three holes at station 519 + 35, located at the top, middle, and bottom, were drilled for temperature sensors. Three moisture measurement sensors were installed at the surface of the slope with the temperature sensors. As with Section B, mulch seeding was done in this section. Larger earth anchors were used to hold the Tecco-mesh in place instead of the smaller duckbill type used to anchor the coconut matting in Section B. The Tecco-mesh was affixed to the cut slope using hollow-core steel rebar anchors. Thirty-two 3-inch-diameter holes were drilled for anchor installation on the slope, with spacing of 7.5 ft and 6 ft in the vertical and horizontal directions (see Figure 3.8). The holes for the anchors are 9 ft deep. Details of the Tecco-mesh installation can be found in Figures 3.9 through 3.12.

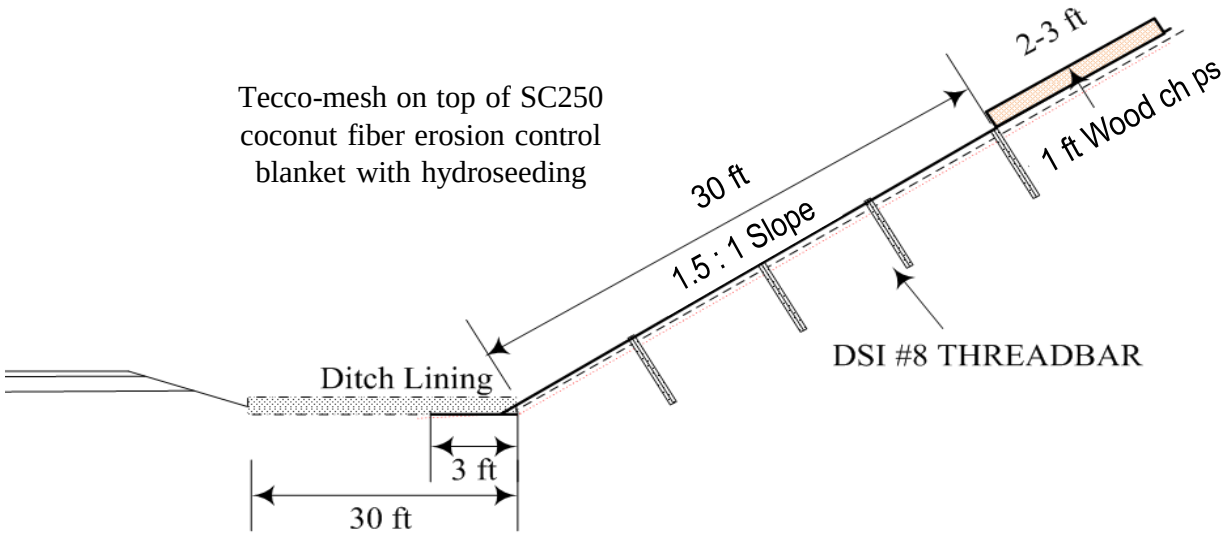

Figure 3.7 Profile for Section C

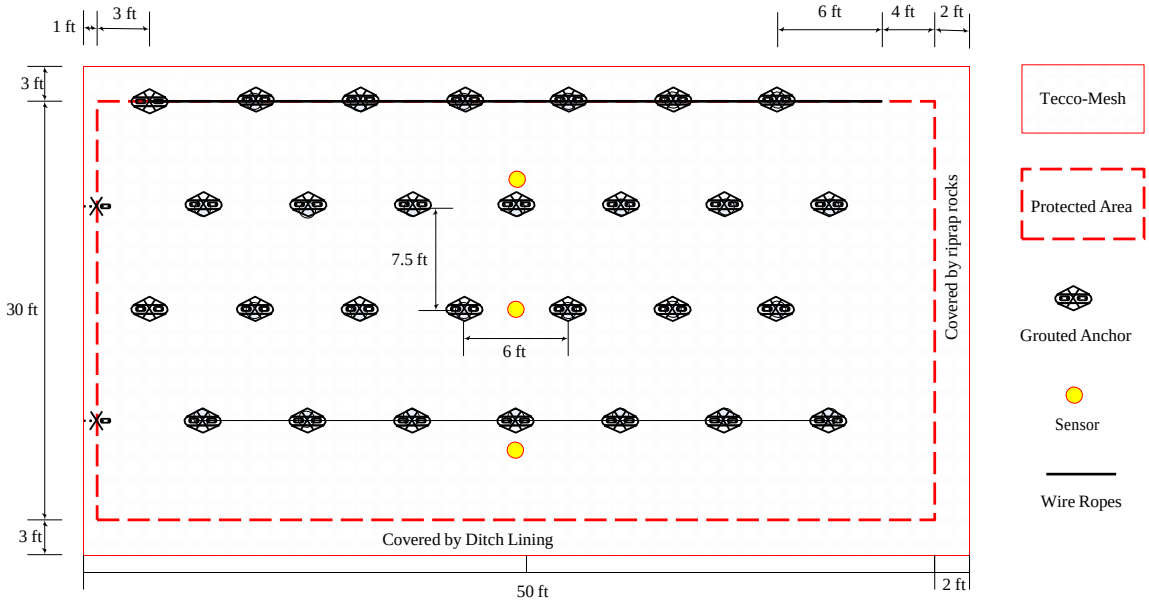

Figure 3.8 Section C, anchor and sensor locations

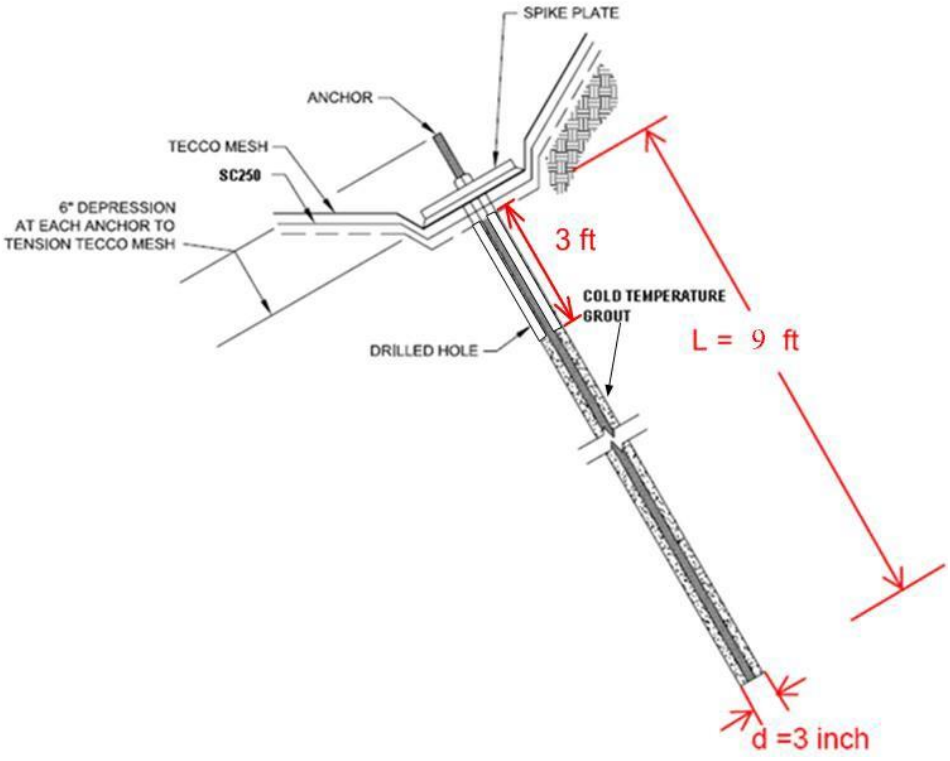

Figure 3.9 Detail of Section C anchor

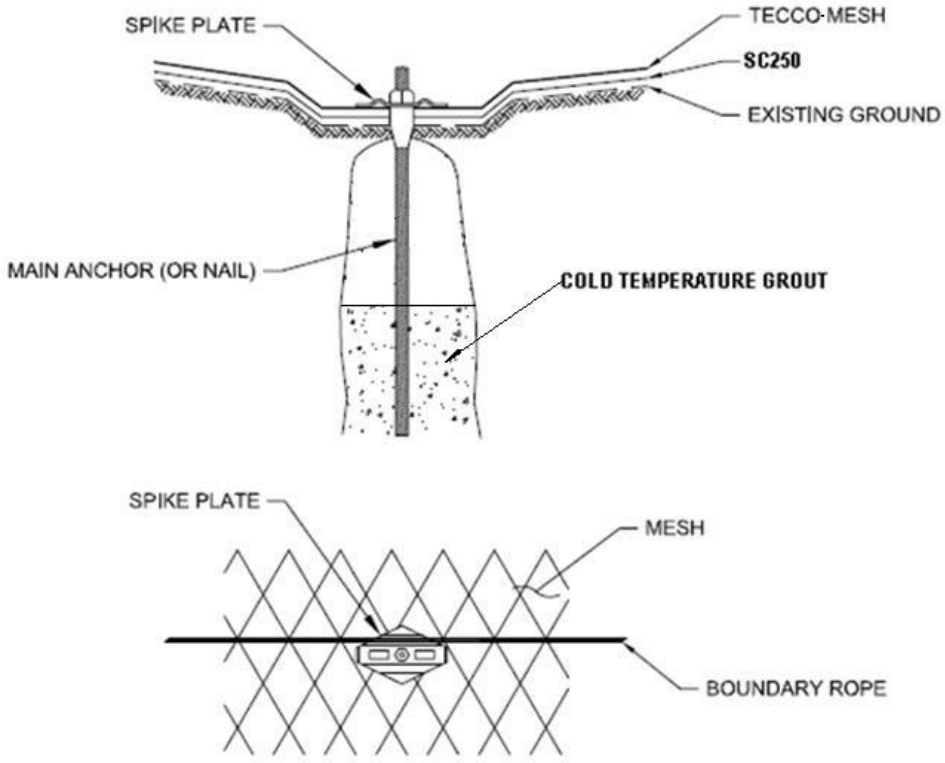

Figure 3.10 Nail and anchor detail with boundary rope

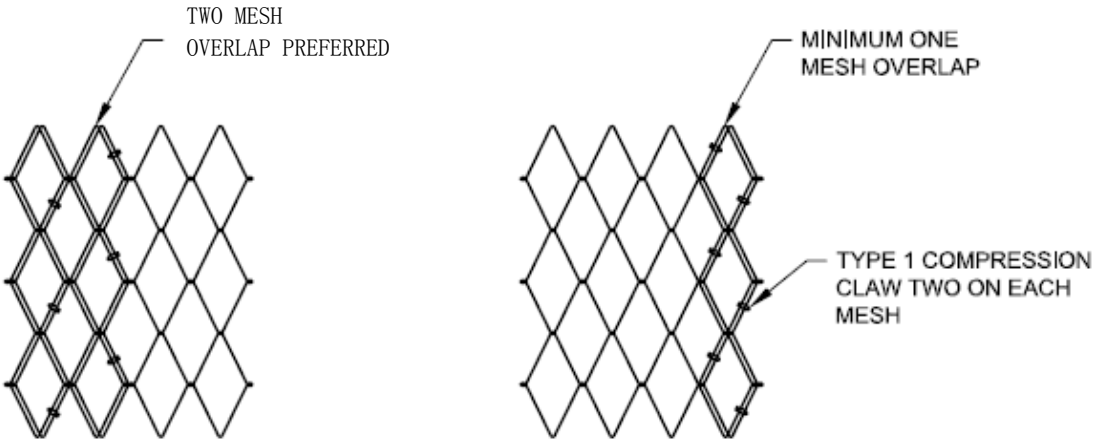

Figure 3.11 Plan view – connection of mesh sheets in Section C

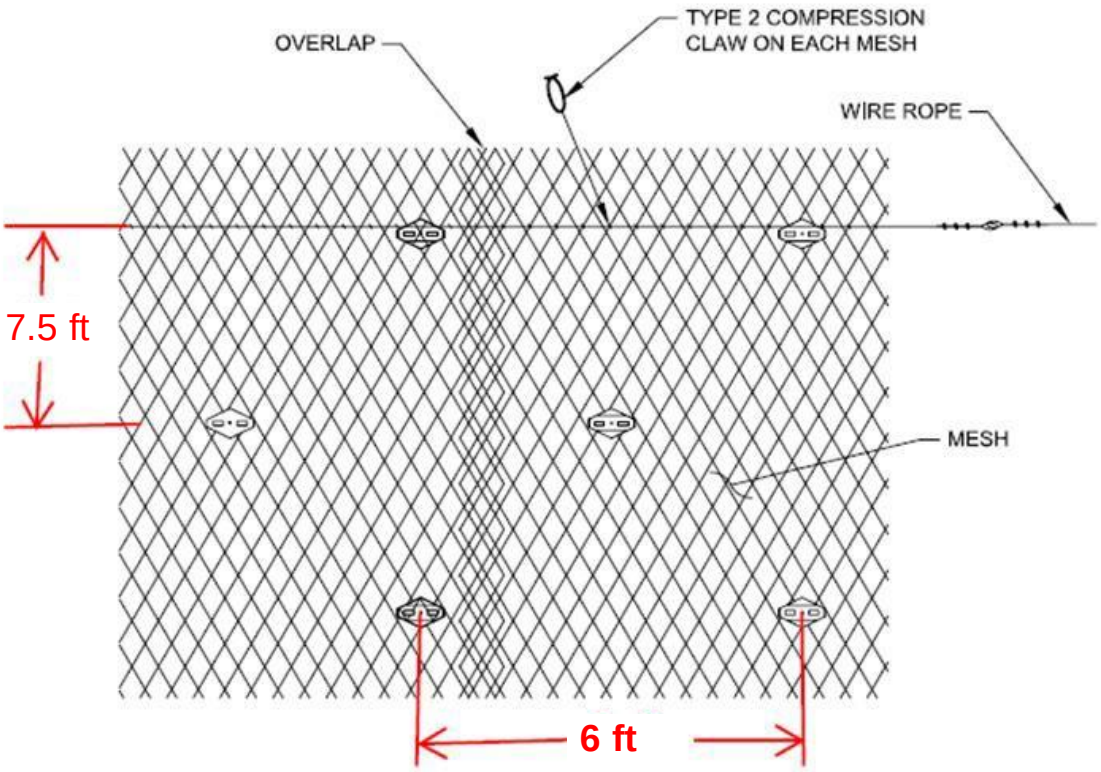

Figure 3.12 Connection details

Test Section D

Test Section D is the control section. This section was protected by the standard project-design crushed rock blanket intended to protect ice-rich soil cut slopes. The standard-design crushed rock blanket is 2 ft thick. The profile for the control section's standard rock blanket is shown in Figure 3.13. This section, identical in size to Section A, is 30 ft by 35 ft, and extends between stations 518 + 75 and 519 + 10. Three holes at station 518 + 90, located at the top, middle, and bottom, were drilled for temperature sensors (see Figures 3.14 and 3.15). As for the other subsurface sensors, the holes were drilled perpendicular to the surface of the cut slope. Temperature sensors were installed at the depths indicated in Figure 3.3. Moisture measurement sensors were installed at the surface of the slope with the temperature sensors.

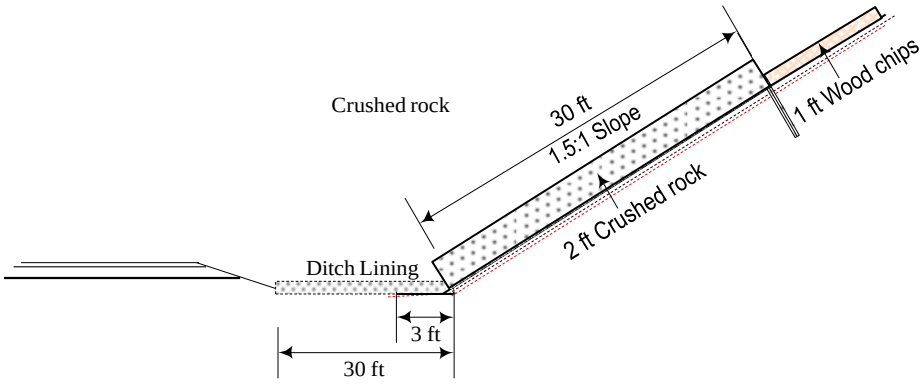

Figure 3.13 Profile of Section D

The layout for the temperature sensors for four sections is presented in Figures 3.14 and 3.15. The data collection station was installed at the top of Section D, which is the control section. Other sensors were installed at the data collection station and at the top of the cut slope. These sensors will be discussed later in this report.

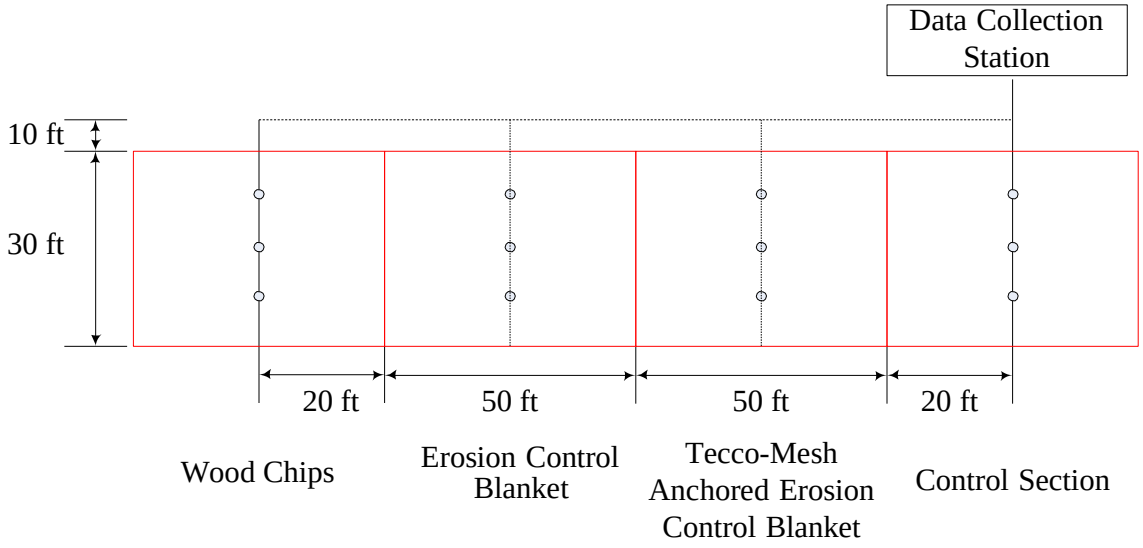

Figure 3.14 Layout for temperature sensor locations

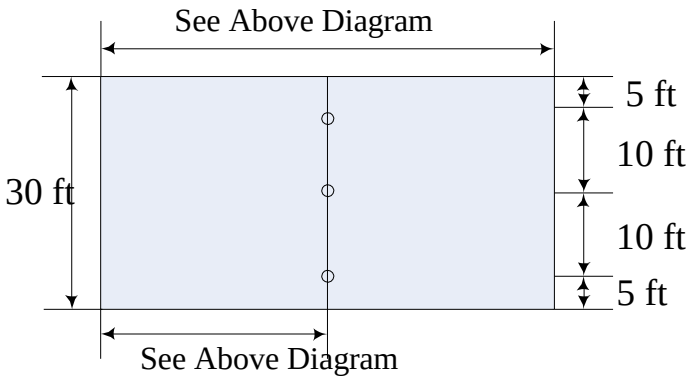

Figure 3.15 Layout for temperature sensor locations

CHAPTER 4. CONSTRUCTION OF EXPERIMENTAL SECTIONS

This chapter describes the construction process for the experimental cut slope treatments and instrumentation. Construction of all experimental sections within the Experimental Feature was performed during the period April 17 through April 27, 2013. Instrumentation was completed by April 30, 2013.

On April 17, 2013, the snow on the cut slope at the Experimental Feature site was removed. Figure 4.1 shows the cut slope before placement of the various surface treatments. Sensors for obtaining data on soil temperature, moisture, precipitation, radiation, wind speed, and air temperature were installed as part of the construction process. These sensors are now being used to monitor environmental conditions at the Experimental Feature site.

Figure 4.1 Cut slope at Dalton Highway 9 Mile Hill construction project location

Before placing the individual surface treatments on the cut slope on April 17, 2013, a layout of each section was drawn on the slope (see Figure 4.2) according to the designs indicated in Chapter 3. Holes for anchors and temperature sensors were marked with different colors. After this step, drilling on the slope was performed. Holes were drilled with diameters of either 2

inches or 3 inches depending on purpose and location (2 in. for duckbill holes and 3 in. for rebar anchor holes). Figure 4.3 shows a close-up of drilling activity on the slope. During construction, the slope was initially exposed to the air without any insulating protection. The afternoon temperatures rose to above freezing, and the slope began to thaw and become wet, as shown in portions of Figure 4.2. The slope was a rather steep workplace and, especially in the afternoon, became slippery. Therefore, it was sometimes necessary to tie the drilling machine to an excavator at the top of the cut slope (Figure 4.4).

Figure 4.2 Layout on the cut slope

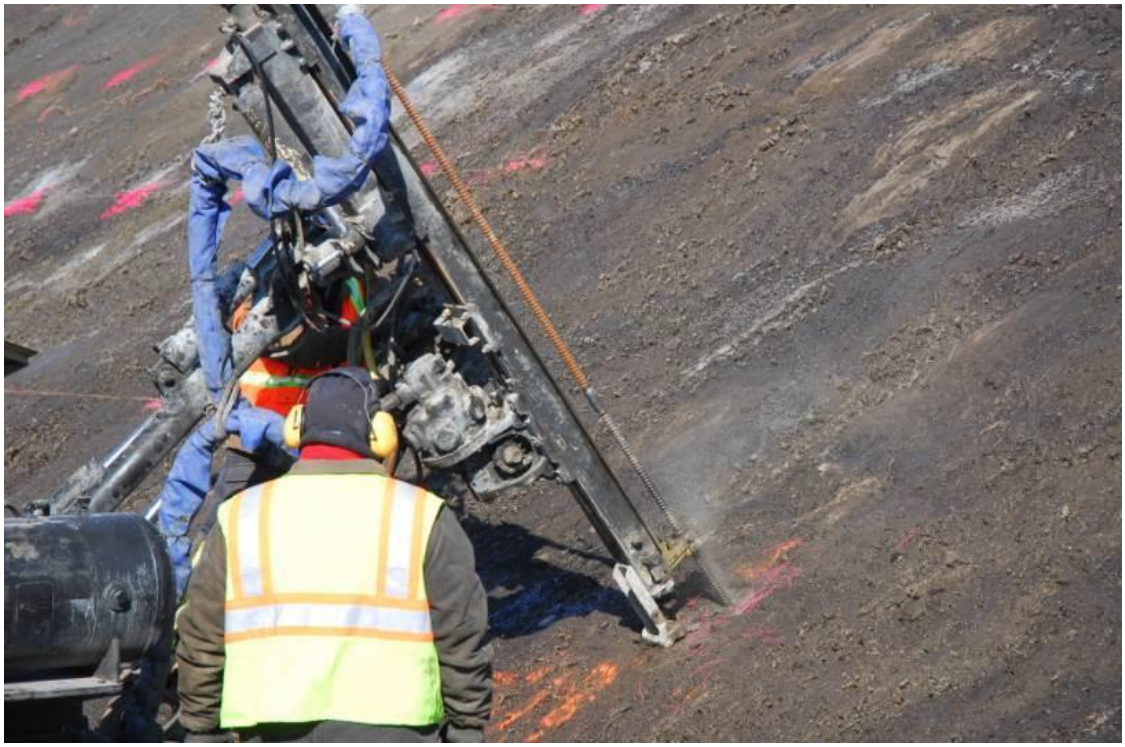

Figure 4.3 Drilling on the cut slope

Figure 4.4 Drilling at the upper part of the slope

For temperature sensor installations, PVC pipe was placed into the holes to protect them from intrusion of thawed material from the cut slope (Figure 4.5). Figure 4.6 shows an instrumentation hole after the PVC pipe was installed. It was obvious that mud released from the surrounding cut slope face would have filled the instrumentation holes if the PVC housings had not been used.

Figure 4.5 Installation for sensor housing

Figure 4.6 Instrumentation hole with sensor housing installed

Due to high afternoon temperatures, thawing at the cut slope surface created obvious areas of erosion. Compared with the slope before construction (see Figure 4.1), significant erosion can be seen on the slope shown in Figure 4.7, especially within Sections C and D. Close-ups of this erosion are shown in Figures 4.8 and 4.9. To protect the slope from erosion during construction, insulating tarps (normally used to aid concrete curing during cold weather) were used to cover the entire cut slope, as shown in Figure 4.10. Nails were used to affix the tarp sections to the cut slope surface.

Figure 4.7 Cut slope erosion during construction

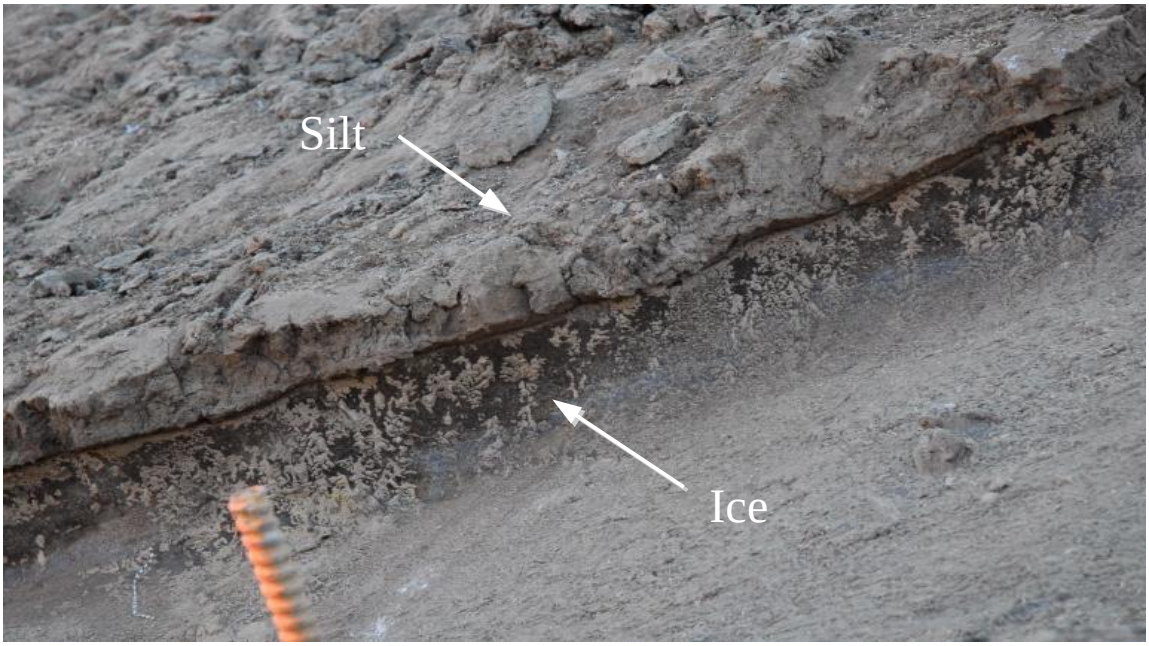

Figure 4.8 Ice in the cut slope

Figure 4.9 Ice exposed in the cut slope

Figure 4.10 Cut slope protected from erosion during drilling

After the holes were drilled, the duckbill earth anchors and the large hollow steel rebar anchors were installed in the holes. Figure 4.11 shows the cable end of a duckbill earth anchor (with its adjustable cinch mechanism) after the anchor had been placed in the slope. After the hollow rebar anchors were placed in the holes, each was grouted in place. A close-up photo of one of the grouted anchors is shown in Figure 4.12.

Figure 4.11 Cable end of installed duckbill earth anchor

Figure 4.12 Installation of hollow rebar anchor

As mentioned previously (and shown in Figure 4.7), significant erosion was observed after the drilling process on the slope. The eroded, uneven slope surface quickly became unsuitable for placement of the coconut erosion control matting and the Tecco-mesh. It was necessary that both of these treatments be placed on a smooth ground surface to prevent air circulation between the treatment matting and the cut slope surface. Such air circulation would reduce the thermally protective effects of both treatment types. Therefore, prior to placement of the coconut matting (Section B) and Tecco-mesh (Section C) slope coverings, the bucket of a large backhoe excavator was used to smooth the uneven surface of the cut slope. This operation is shown in Figure 4.13. Then Sections B and C were seeded. Figure 4.14 shows a small area of the cut slope after seeding.

Figure 4.13 Re-smoothing the cut slope surface

Figure 4.14 Seeded cut slope

The coconut erosion control blankets were placed after seeding. Coconut matting rolls were hauled to the top of Sections B and C, and then unrolled down the cut slope (see Figures 4.15 and 4.16). The overlap for adjacent mat strips was about 1 ft. All soil anchors used on the cut slope penetrated the coconut matting.

Figure 4.15 Placement of the coconut erosion control matting

Figure 4.16 Placement of coconut erosion control matting

After placement of the coconut erosion control blankets in Sections B and C, the duckbill earth anchors were locked into place in Section B by pulling upward on each anchor's cable. Because of the duckbill anchor design, an upward pull on the anchor's cable (after the anchor has been placed in its hole) causes the anchor head to rotate and then dig into the undisturbed soil at the anchor head location. After the duckbill anchors were set, the round plates, located high on the anchor cable (the special cinching mechanisms), were pushed firmly downward, thus cinching the anchor cables to the ground surface to tightly hold the coconut blankets in place (see Figure 4.17). After the duckbill anchor plates had been cinched in place within Section B, circle top wire pins were inserted through the Section B coconut matting and into the cut slope surface. Due to the initially hard-frozen nature of the slope surface, these pins could not simply be hammered into the soil. A portable drill was used to create a pilot hole for each pin, facilitating the pin's placement. Figure 4.18 shows a pin that has been placed into the slope.

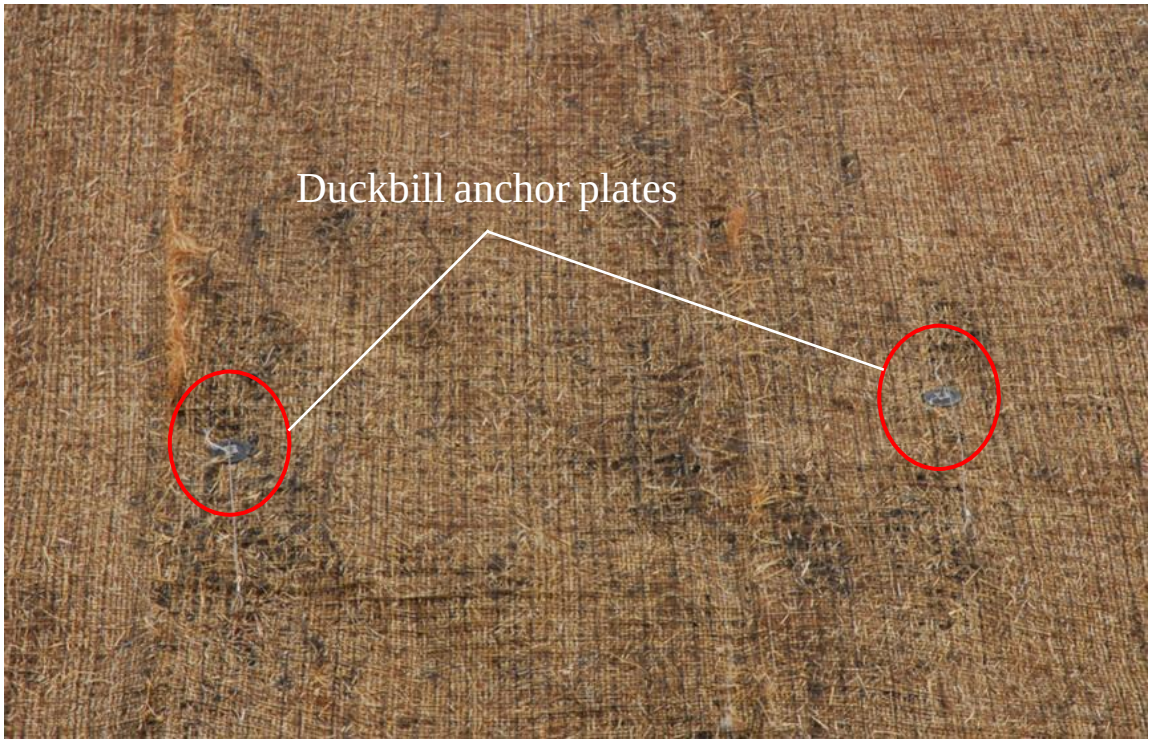

Figure 4.17 Section B showing duckbill anchor plates after construction

Figure 4.18 Enlargement of a circle wire top pin

For Section C, after the placement of the coconut blanket, Tecco-mesh was installed as a second layer. Similar to the installation of the coconut mat, Tecco-mesh was hoisted to the top of Section C and then unrolled down the cut slope (see Figure 4.19). Extra Tecco-mesh was trimmed off at the bottom of the slope (Figure 4.20). Adjacent Tecco-mesh strips were connected along their adjoining lengths using connection clips (Figure 4.21). A Tecco-mesh connection clip is shown in the upper right corner of Figure 4.21. After the Tecco-mesh had been installed in Section C, spike plates were put in place to hold the Tecco-mesh tightly to the cut slope surface. The plates were held in place, across the cut slope surface, with hex nuts as shown in Figure 4.22. A close-up view of the anchor plate and nut is shown in Figure 4.23.

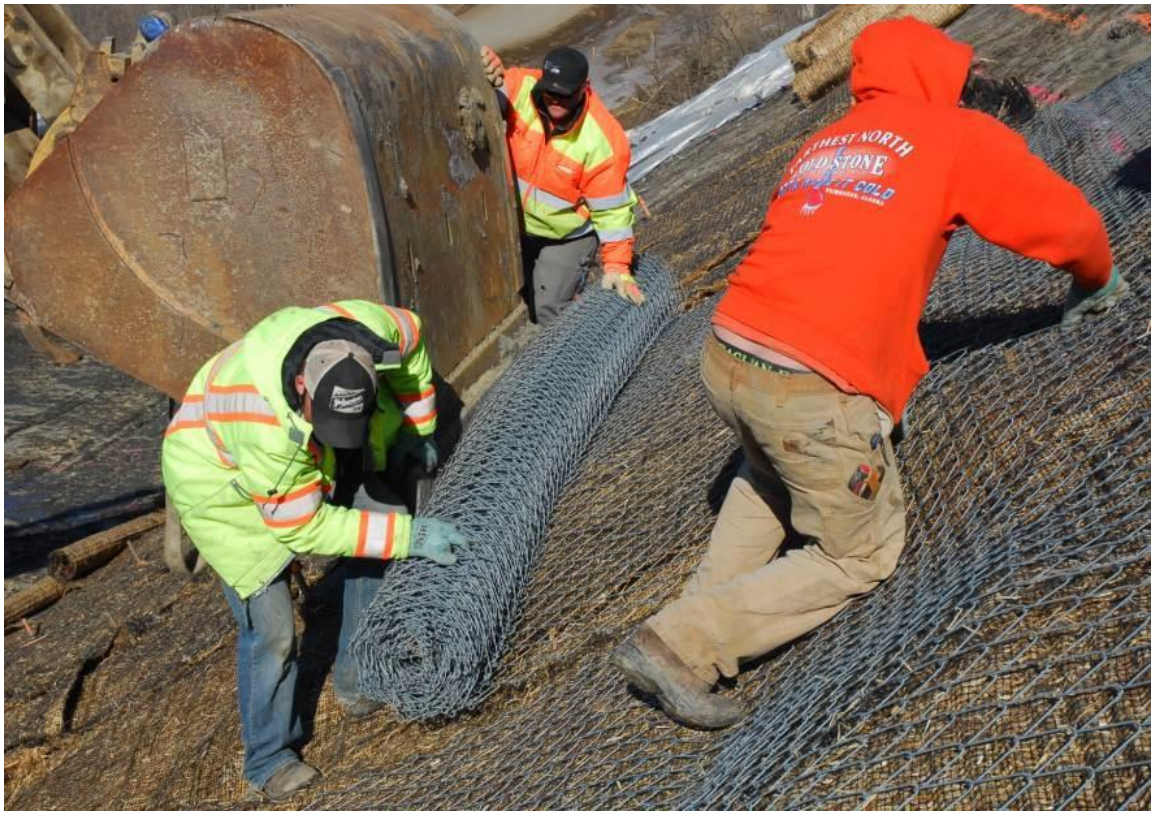

Figure 4.19 Placement of Tecco-mesh

Figure 4.20 Cutting away excess Tecco-mesh

Figure 4.21 Connecting adjacent Tecco-mesh strips

Figure 4.22 Section C appearance after construction

Figure 4.23 Close-up view of Tecco-mesh at an anchoring point

After construction of Test Sections B and C, crushed rock was hauled to the test site. A backhoe excavator was used to cover Section D with two ft of crushed rock, as shown in Figure 4.24.

Finally, wood chips were hauled to the top of the slope and spread along the upper part of the cut slope and on Section A (see Figure 4.25). An enlargement in the upper right corner of Figure 4.25 shows the wood chips used at the experimental site. Figure 4.26 is a panorama of the cut slope Experimental Feature shortly after construction.

Figure 4.24 Construction of Section D

Figure 4.25 Spreading wood chips along top portion of cut slope

Figure 4.26 Appearance of Experimental Feature soon after completion

CHAPTER 5. CONSTRUCTION OF DATA ACQUISITION STATION

On April 24, 2013, temperature sensors were installed at the Experimental Feature. In Sections A and D, the PVC tubes were frozen in the ground; thus, it was necessary to leave those tubes in place. It was possible, however, to remove the PVC tubes from the middle two test sections (B and C) before the sensors were installed. Dry sand was used to fill the holes after sensor installation (see Figure 5.1). A moisture sensor was installed at the ground surface at the top of each string of temperature sensors (see Figures 5.2 and 5.3). After installation, cables for these sensors were bundled, and the cable bundles were extended across the cut slope to their termination location at the data collection station.

Figure 5.1 Backfilling with sand after insertion of temperature sensor string

Figure 5.2 Installation of moisture sensor at top of temperature sensor string

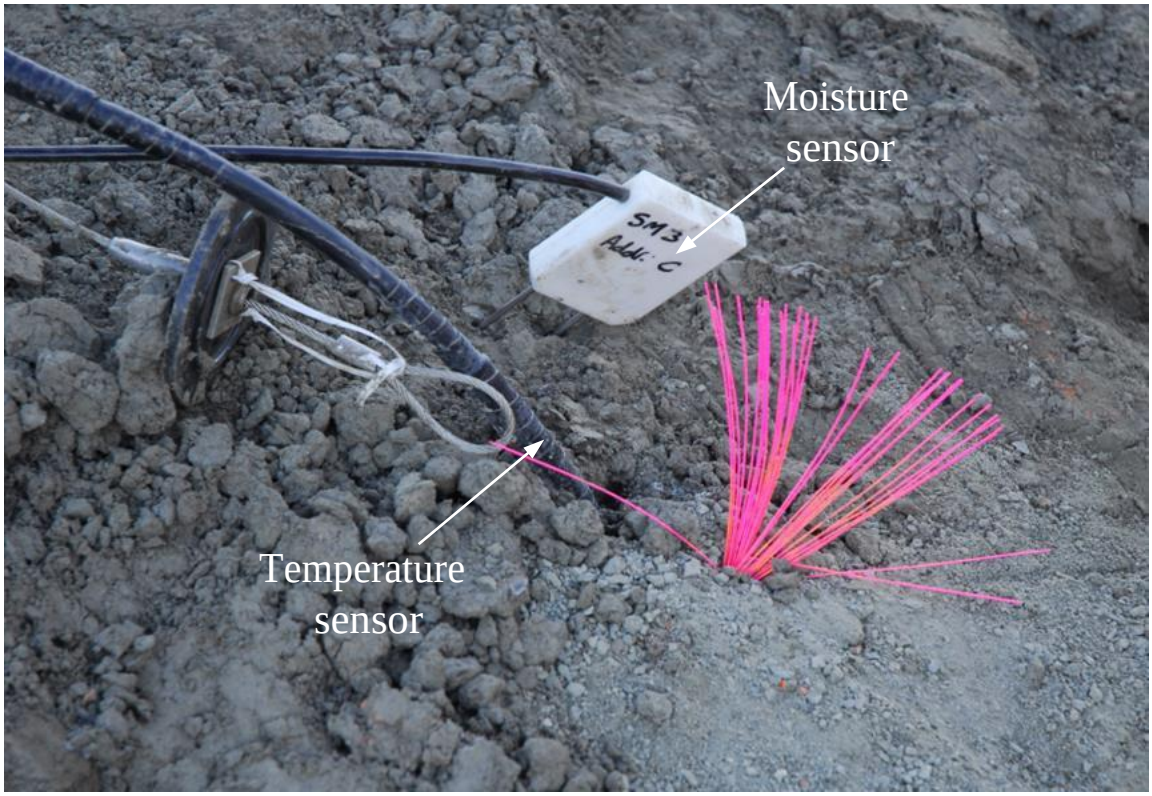

Figure 5.3 Temperature and moisture sensor location

Aluminum conduits were used to protect the cable running along the surface of the ground from damage. The aluminum conduits were grouped together and routed to the data collection station located above Section D. The data station is shown in Figure 5.4. Figure 5.5 is a picture of the data station after completion. The Campbell Scientific data collection box was mounted on a tripod as shown in Figure 5.4. The sensor cables were attached to a Campbell Scientific CR1000 data logger through two AM16/32B relay multiplexers. The data logger was set to record temperatures and moisture contents from all sensors at 15-minute intervals. Figure 5.6 shows the interior of the data logger box after the data logger and multiplexer attachments were made. In addition to the individual temperature and moisture sensors located at discrete points on or under the cut slope face, an HMP45C Air Temp/Relative Humidity sensor was installed (above the data logger box) to monitor air temperature and air relative humidity generally representative of the Experimental Feature area. The HMP45C sensor is shown in Figure 5.7. Radiation, wind, and precipitation sensors were also installed near the data logger box to collect other environmental data generally representative of the Experimental Feature site. These sensors are shown in Figures 5.8 to 5.10.

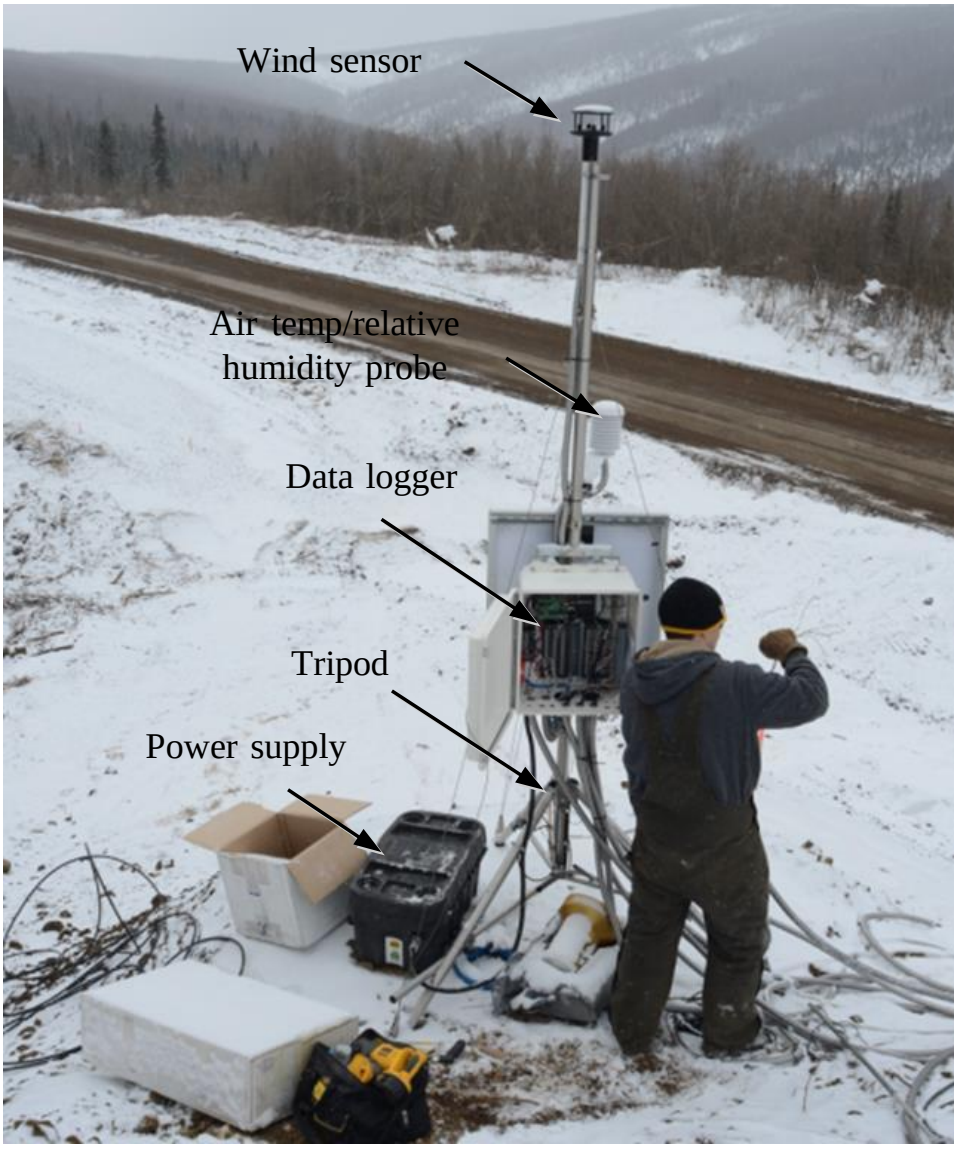

Figure 5.4 Data collection station

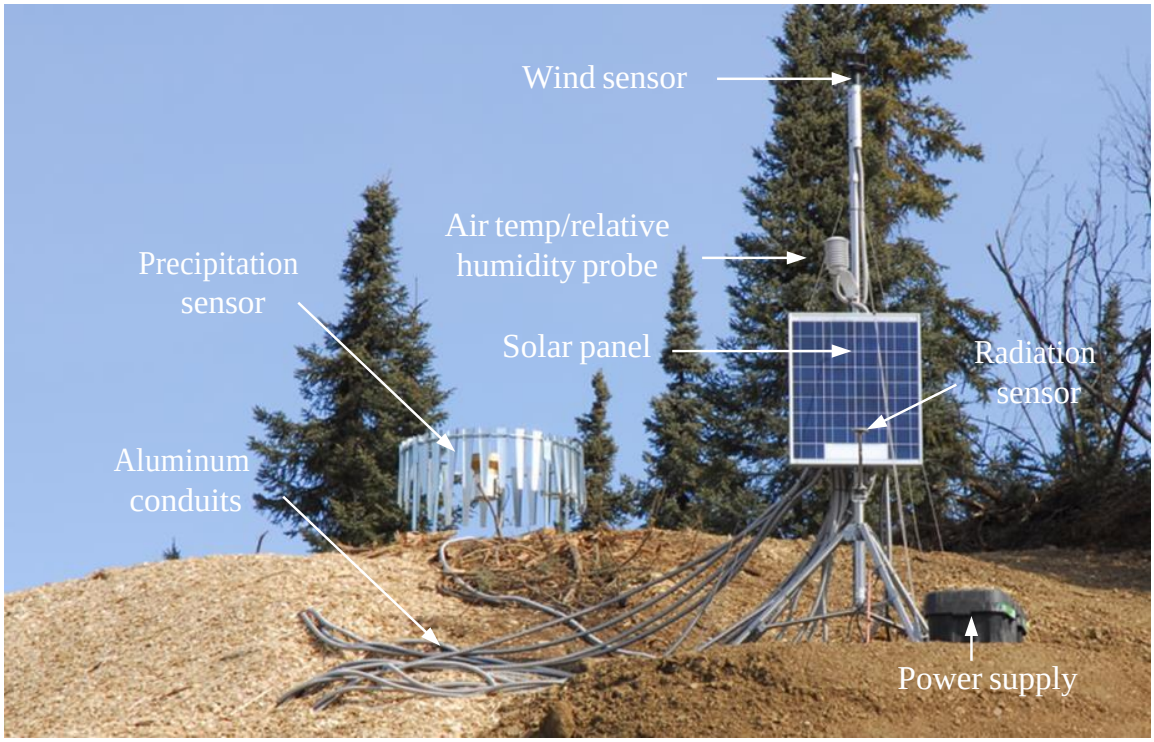

Figure 5.5 Data collection station after completion

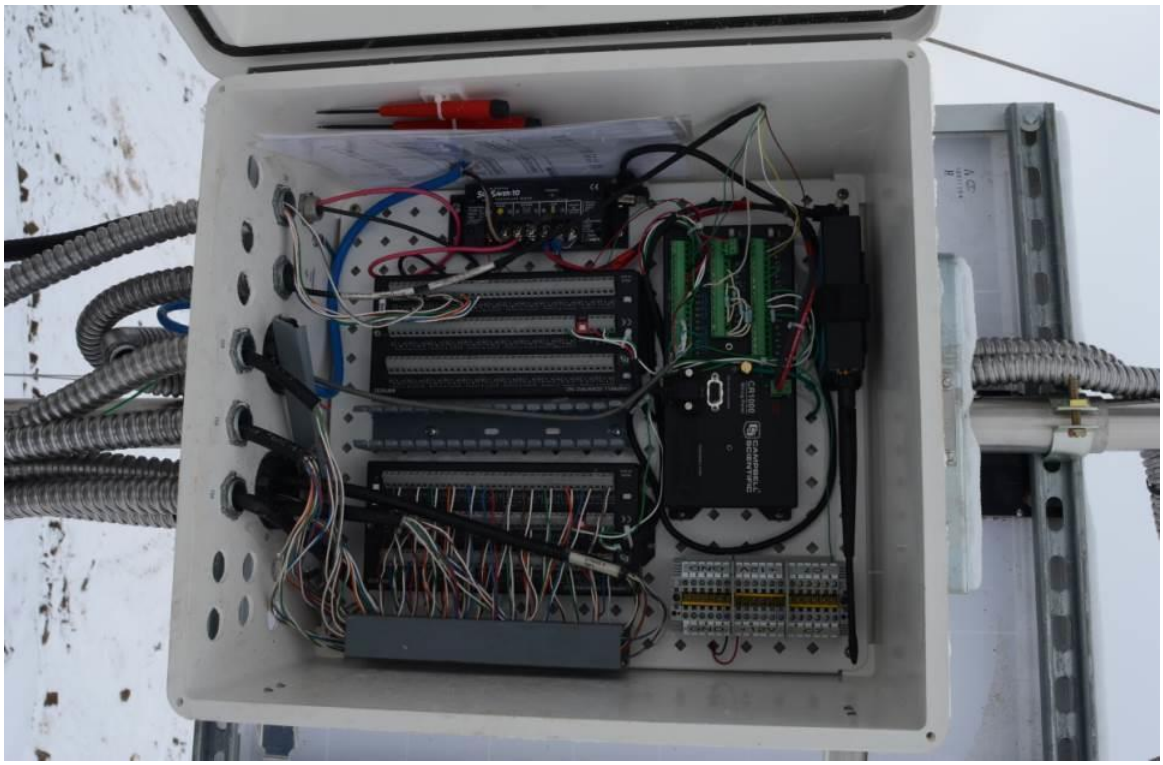

Figure 5.6 CR1000 data logger and AM16/32B multiplexing equipment

Figure 5.7 Air Temp/Relative Humidity sensor

Figure 5.8 Wind sensor

Figure 5.9 Radiation sensor

Figure 5.10 Precipitation sensor

Besides these sensors, on September 27, 2013, two cameras mounted on a tripod (see Figure 5.11) were installed at the other side of the road to monitor changes over time in the ice-rich slope. Each camera covered about half of the slope. The two cameras were set to capture two pictures of the slope per day.

Figure 5.11 Two cameras installed for slope monitoring

CHAPTER 6. PERFORMANCE PROBLEMS SOON AFTER CONSTRUCTION

By the first week of June 2013, researchers discovered substantial problems within the Tecco-mesh section of the Experimental Feature. Based on problems that were obvious in photos and in observations by L. Li (project team member) on Friday, June 7, R. McHattie (project team member) visited the site on Sunday, June 9, 2013. During this visit, Li's observations were confirmed, and more photos of observations were obtained. After discussions that resulted from the observations and photos, the project team and personnel with ADOT&PF Construction concurred that remedial action was necessary to prevent the rapid occurrence of further damage at the Experimental Feature site.

The panorama photo labeled Figure 6.1 shows the entire face of the Experimental Feature and the circled failure areas within the Tecco-mesh section. Observation at the site revealed an obvious loss in volume of original cut slope soil from the slope face. This loss of volume could be seen easily through the Tecco-mesh—an observation that was confirmed by probing and peering through the Tecco-mesh at many locations along the mesh surface.

The obvious loss of volume from the cut slope can be seen through the Tecco-mesh in Figure 6.2, especially where massive ice is exposed near the upper right corner of the photo. What had initially been exposed during construction as a planar area of ice-rich material on the surface of the cut slope prior to Tecco-mesh placement eventually was recognizable (after thawing) as an irregular *massive ice feature,* which unfortunately extended across much of the Tecco-mesh section. By June 9, the massive ice feature was easily recognizable through the Tecco-mesh at a number of locations (labeled and clearly visible in Figure 6.3).

Considerable surface volume had been lost beneath the Tecco-mesh due to thaw and runoff. This condition extended beneath the roll of coconut matting (in Section B) closest to the Tecco-mesh section, but less soil volume had been lost there. By far, the worst soil volume loss was within the central portion of the Tecco-mesh section itself. It appeared that most of the volume loss occurred from runoff of silt and water into the ditch, with little if any loss due to thaw consolidation. As of June 9, the soil/ice material visible across much of the Tecco-mesh section existed as an irregular thawing surface with an intact Tecco-mesh covering (a sort of tent)

suspended one to several ft above the present soil/ice surface. At that time, none of the Tecco-mesh and only small areas of the coconut matting within Section C had failed.

Figure 6.1 Panorama view of Experimental Feature showing failure in Tecco-mesh section

Figure 6.2 Close view of failure within the Tecco-mesh section

The significant loss of material from the original cut slope is evident in the left side of Figure 6.3, where the anchor grout is exposed. The depth from cut slope face to top-of-grout was 3 ft. The lighter gray material labeled in the right side of Figure 6.3 is some of the massive ground ice that caused serious problems with the Tecco-mesh experimental section.

Figure 6.3 Close views showing exposure of soil anchor grout (left) and portion of massive ice feature under Tecco-mesh (right)

In Figure 6.4, the areas where the ground surface is *not* in contact with the Tecco-mesh or the adjoining coconut matting are those areas where no grass had yet appeared. As Figure 6.4 shows by the appearance of grass, only the very top portion of the Tecco-mesh section still has soil/Tecco-mesh contact.

Figure 6.4 Surface protection matting in area showing no grass growth is not in direct contact with ground surface

Based on the June 7 and the June 9 appearance of the test section, the Tecco-mesh, although intact, did not appear to serve any useful function relevant to retarding thaw or preventing further loss of cut slope material to the ditch. It may have been possible to perform some adjustments on the Tecco-mesh anchors to bring the mesh closer to the existing cut slope surface. However, it was apparent that such adjustments would not have offered much improvement given the large volume of cut slope material that had already been lost. Obvious evidence of the foregoing and a realization that continued deterioration/runoff would almost certainly produce a noticeable environmental issue required a substantial change in the Experimental Feature plan. The following recommendations were agreed upon by the research team, the ADOT&PF, and the contractor—and were executed by the contractor:

June 2013 Recommendations to Modify the Design of the Experimental Feature:

- Detach the Tecco-mesh and underlying coconut matting from its anchors within the Tecco-mesh section, and remove the mesh and matting from the slope surface.
- Extend the rock blanket material (control section material) across that section. During this process, leave as many of the Tecco-mesh anchors in place as possible. It was thought that thaw-related problems would initially continue given the very high ice content of some of the cut slope material, and that the rock blanket would conform to the slope surface as the slope receded. The rock blanket would provide some degree of insulation and serve as a filter to keep silt from running into the ditch. Initial failure of the project's standard design thickness of blanket material, due to loss of massive ice volume, would require placement of additional blanket material.
- Cinch down all duckbill anchors in the coconut matting test section. This was particularly necessary in the portion of that section closest to the Tecco-mesh section.

According to the recommendations listed above, on June 17, 2013, Tecco-mesh and the coconut erosion control blankets at Section C were removed (shown in Figure 6.5). The great loss of volume in cut slope soil at Section C can be seen in Figure 6.6, especially where massive ice is exposed. Crushed rock was hauled to the test site, and an excavator was used to cover Section C with crushed rock (see Figure 6.7). The hollow rebar anchors were left intact during these repairs to serve as survey and photogrammetric reference points. Figure 6.8 shows the cut slope after completion of repairs on June 17, 2013.

Figure 6.5 Section C without Tecco-mesh and coconut blanket

Figure 6.6 Massive ice in Section C

Figure 6.7 Covering Section C with crushed rock

Figure 6.8 Cut slope after construction on Section C

Dr. Zhang (Mingchu Zhang, project Co-P.I.) visited the Experimental Feature site on Friday, June 21. During his inspection of the site, he noticed that an area of significant size, along the top of the Experimental Feature cut slope, had been cleared of natural vegetation. Figure 6.9 presents a close-up (left) and total view (right) of the cleared area on the date of his visit.

Dr. Zhang was concerned that thermal degradation might progress downward from the surface of the cleared area and eventually influence the thermal regime of soils behind the experimental cut slope face. He recommended (1) that the wood chips first be removed from the surface of the cleared area; (2) that the entire area be graded to drain; (3) that the entire area then be covered with an erosion control blanket, using remnants of the Experimental Feature's coconut matting or functionally similar erosion control matting; and finally (4), that the mat-covered area be heavily seeded to encourage a quick, lush growth of vegetation. This recommended treatment will eliminate water ponding along the top of the cut slope. Even more importantly, the natural cooling system (via evapotranspiration and shading) provided by a thick growth of vegetation will significantly reduce the thermal degradation of underlying soils.

This work remains to be done at the time of this report's preparation (August 2014).

Figure 6.9 Start of thaw related damage at top of Experimental Feature cut slope

CHAPTER 7. RESULTS AND ANALYSIS

As reported in the previous chapter, a weather station was built at the test site. Air temperature, wind speed, wind direction, precipitation, solar radiation, and humidity information was recorded throughout the measurement period (from April 30, 2013 to November 11, 2014). In addition, moisture and temperature information on and beneath the slope face were monitored by the installed TDR and temperature sensors. Field monitoring data for the time period between July 15, 2013 and September 27, 2013 was missing due to the malfunctioning of the data collection station. The recorded weather information as well as the moisture and temperature information is presented in this chapter. The analysis regarding these recorded results is also presented. Erosion volume estimates for each section were obtained using a special survey method based on sophisticated analyses of sets of photographs of the slope surface.

Site Climatic Conditions

Figure 7.1 shows air temperatures, based on hourly data, at the Dalton Highway 9 Mile Hill Experimental Feature after the sensor's installation. In the first year, before the middle of May, 2013, there was also a period with temperatures above 0 ^{o}C. The air temperature climbed to above 0 ^{o}C at the middle of May, 2013 and remained at above 0 ^{o}C until October, 2013. The air temperature generally varied between 5 °C and 30 ^{o}C. The air temperature dropped to subfreezing temperatures with fluctuations in October. The lowest air temperature at the Experimental Feature was identified to be at the end of December. Then, the temperature started to rise up to nonfreezing temperatures in May. The maximum temperature in 2014 was found at the end of June. Then, air temperature continuously decreased with fluctuations as shown in Figure 7.1. Diurnal temperature variations, based on hourly data, for four selected dates are presented in Figure 7.2. It was found that hourly temperatures varied with different magnitudes over a 24-hour period. The maximum and minimum of these diurnal temperatures were also found to different between the different days. On January 1, 2014, the air temperature continuously increased over the 24-hour period. On April 1, 2014, the highest and lowest temperatures occurred at 7:00 p.m. and 9:00 a.m., respectively. On July 1, 2014, the air temperature did not varied very much over the 24-hour period. Precipitation information presented in Figure 7.3, based on hourly data, shows that rainfall occurred on days with low average air temperatures (refer to Figure 7.1). Relative humidity information during the field

data collection period is presented in Figure 7.4. Relative humidity, based on hourly data, varied from 15% to 95%. There were periods when, on some days, the relative humidity was higher than 90%. These periods were considered rainfall events at the test section.

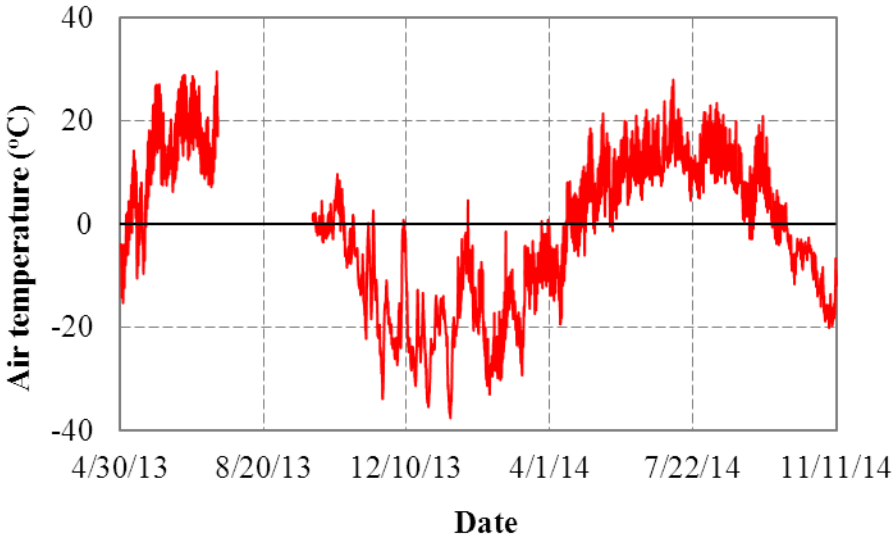

Figure 7.1 Air temperatures at the Experimental Feature site

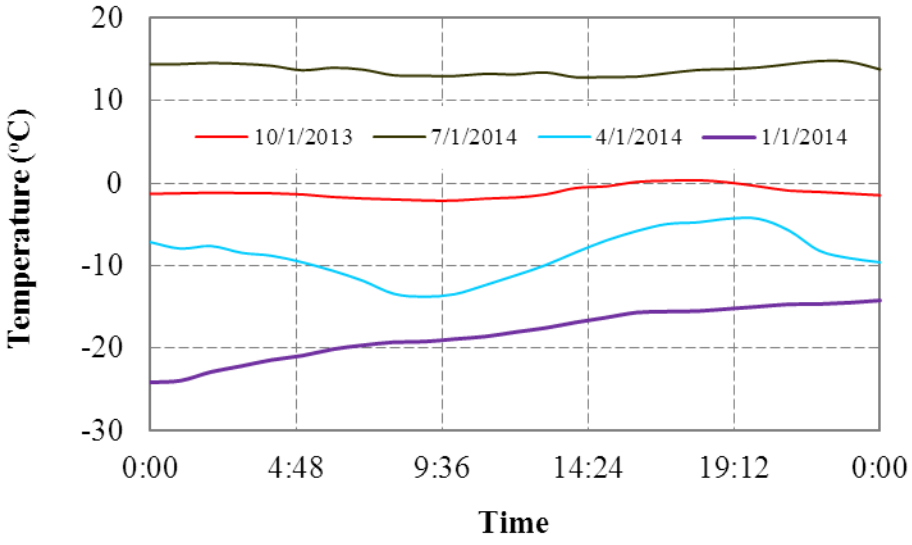

Figure 7.2 Temperature variations for four different days

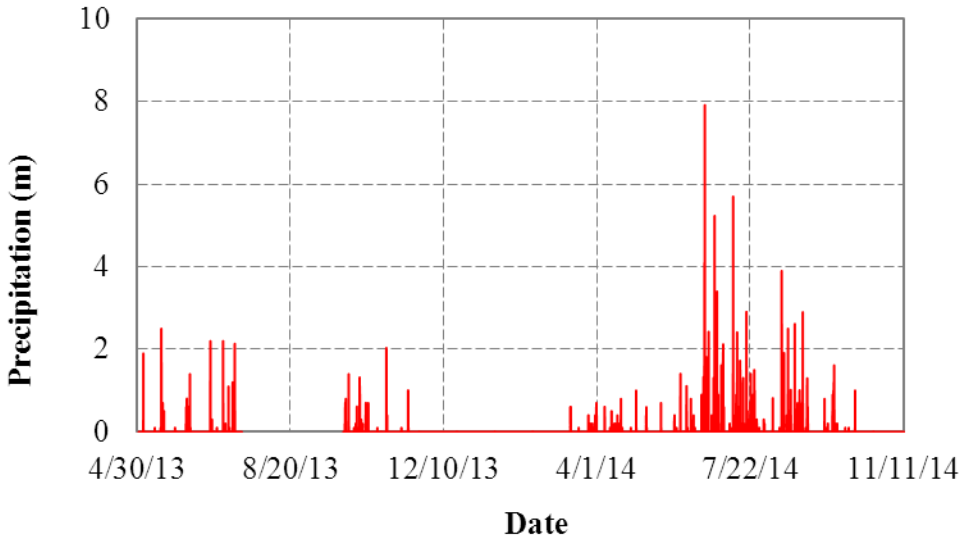

Figure 7.3 Precipitation at the Experimental Feature site

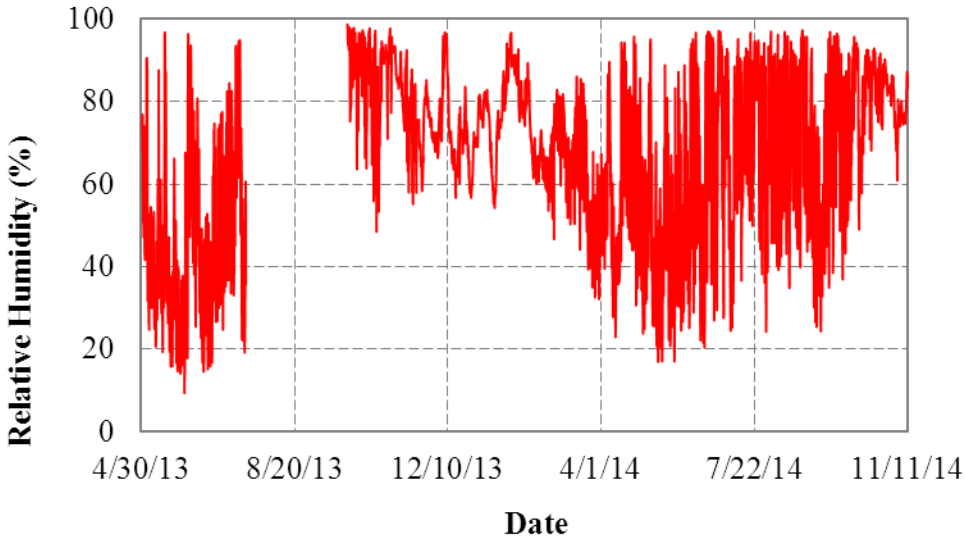

Figure 7.4 Relative humidity at the Experimental Feature site

Besides air temperature, relative humidity, and precipitation monitoring at the Experimental Feature, wind speed, wind direction, and solar radiation at the test site were recorded by the installed weather station. Wind direction frequency distribution at the test site during the recorded period is presented in Figure 7.5. About 30% of the time, the wind blew from the northwest direction. Wind distribution from the other directions varied from approximately 5% to 15%. Wind speed throughout the recorded period significantly varied, with an average of about 2.5 m/s, as seen in Figure 7.6. On some days, the wind speed was higher than 6 m/s

especially from mid-October to March. Incident solar radiation at the test site was also monitored and recorded on an hourly basis, as presented in Figure 7.7. In summer, due to the presence of rainfall on some of the days, the solar radiation detected was much lower than days without rainfall, as shown in Figure 7.7. However, for non-rainy days, the variation in solar radiation at the test site was very low. The highest radiation was found to be at the end of June which is consistent with that the highest temperature occurred at the end of June. In winter, due to short of day light, the solar radiation detected was much lower than that in summer, as shown in Figure 7.7. In Figure 7.8, the variation in 24-hour solar radiation for four selected days is presented. The highest incident radiation was recorded at around 3:00 pm on October 1, 2013, April 1, 2014, and July 1, 2014. The voltage of the power supply battery for the sensors during the recording period is presented in Figure 7.9. The voltage output, based on hourly data, was stable and well above the required 12 volts in the summer with an average about 13.5 V. In winter time, the voltage output dropped to 12.5 volts which indicating that in terms of voltage requirements, the sensor readings should be reliable.

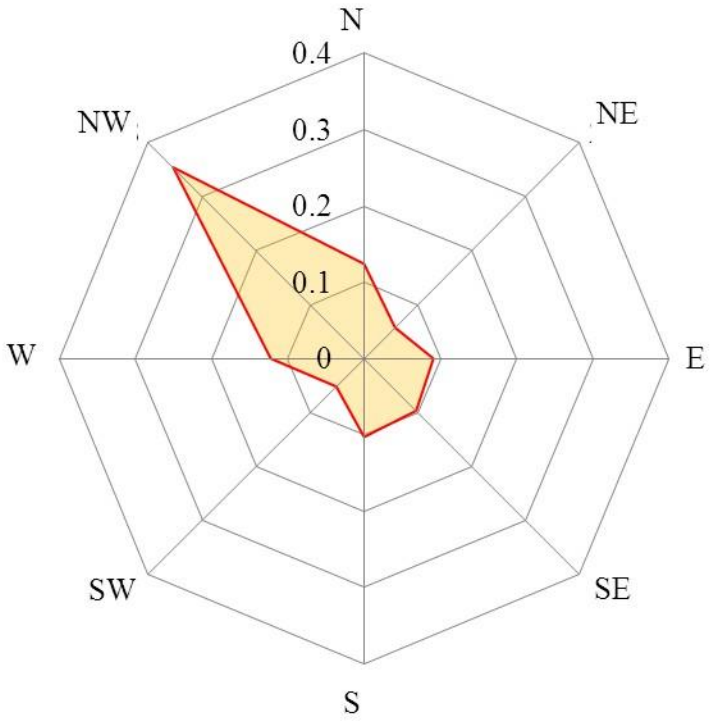

Figure 7.5 Wind direction frequencies at the Experimental Feature site

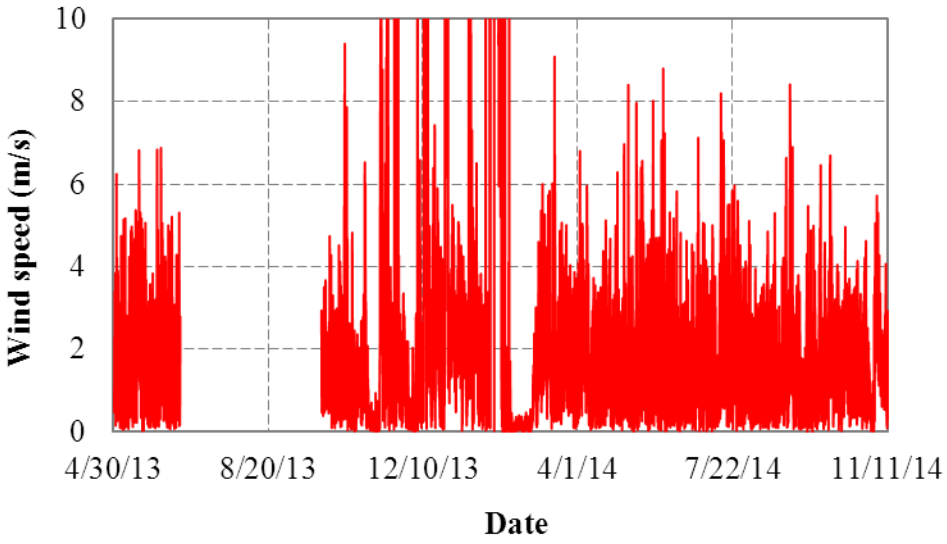

Figure 7.6 Wind speed at the Experimental Feature site

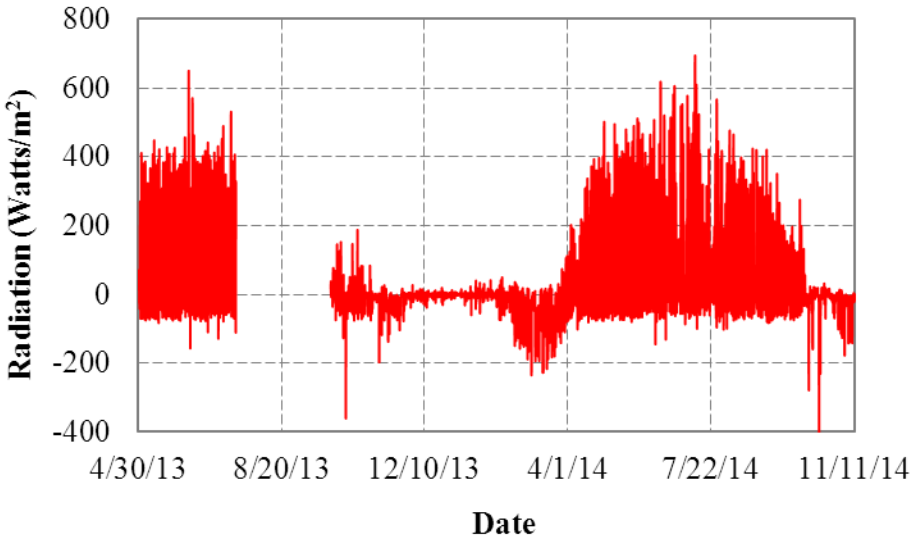

Figure 7.7 Incident solar radiation received at the Experimental Feature site

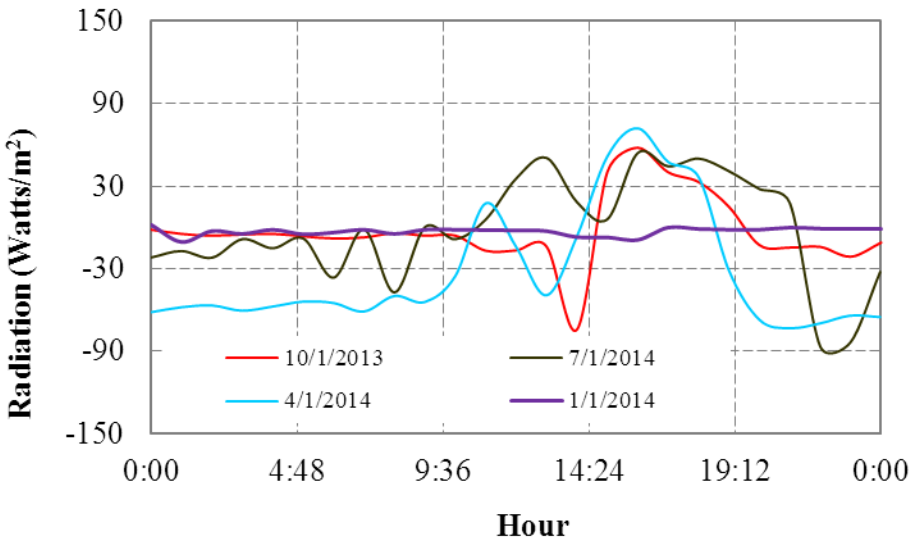

Figure 7.8 Incident solar radiation at the Experimental Feature site on three different days

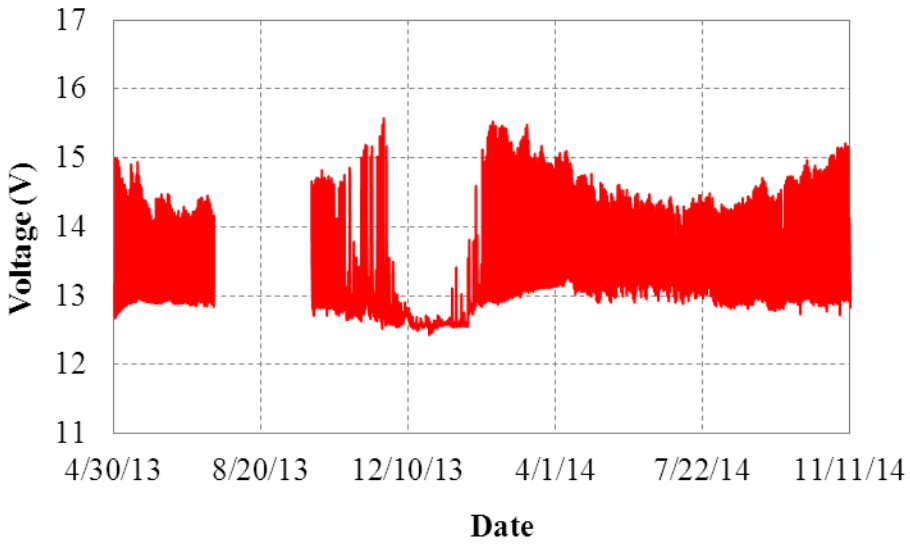

Figure 7.9 Battery output voltage at the Experimental Feature site

Temperature Changes in the Test Section

Figure 7.10 shows the temperature changes at the bottom, middle, and top of the Section A slope (wood chips) at different depths (0, 1, 3, 6, 10, and 20 ft). Temperature variations at different depths are presented in different colors. As indicated in Chapter 3, the maximum sensor depth, perpendicular to the slope face, is 10 ft for the sensor strings at the top and bottom of the slope face for all four sections. The maximum depth for the sensor string at the middle of the slope for

all sections is 20 ft. At the middle of Section A, no temperature data were obtained from sensors at depths of 1 and 6 ft due to malfunctioning.

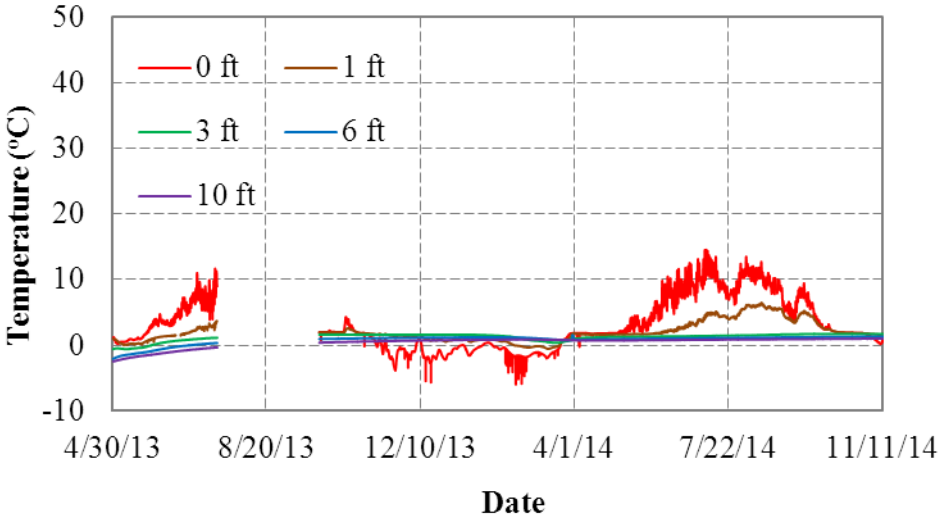

(a) Bottom

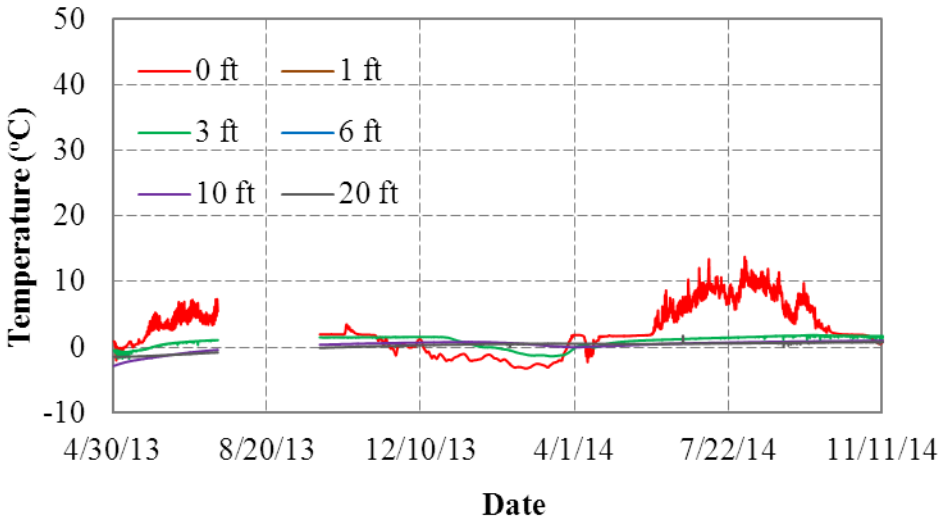

(b) Middle

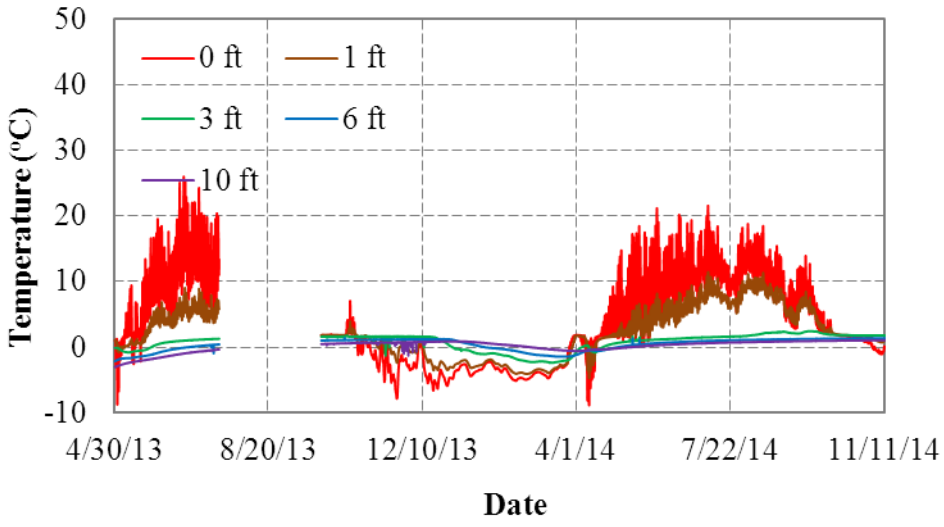

(c) Top

Figure 7.10 Temperature variations in Section A

Figure 7.10 indicates that temperatures increased at all depths within Section A during the time period between April 30 and July 15, 2013 and decreased during the time period between November and December 2013. Then, in March, soil temperature at 0 ft started to rise up with fluctuations till the end of June and then continuously decreased. However, the soil temperature at depths below 0 ft continuously decreased from January to April and then rose up till August and then decreased. Close to the slope face, temperature variations were controlled by daily air temperature variations, even though one ft of wood chips covered the slope surface. Soil temperatures at deeper locations were lower and varied less with time in the summer when compared with the soil temperatures at lower depths. However, in winter, soil temperatures at deeper locations were higher and slightly varied with time. Temperatures at various depths, according to the sensor string at the upper part of the slope, were slightly higher than temperatures measured by the strings further down the slope. This difference is because the wood chips were not evenly distributed on this section. The lower part of the slope (Figure 7.10a) was covered with more wood chips than that at the top (Figure 7.10c), and the wood chips worked as insulation, which protected the slope from air temperature changes. At the start of the monitoring period (the first week after construction), temperatures close to the ground surface decreased slightly because the new cut slope surface was exposed to low ambient air

temperatures early on. Air temperatures warmed by the season soon produced warming soil temperatures on and under the slope surface.

Figure 7.11 shows temperature changes at the bottom, middle, and top of Section B (coconut blanket) at different depths (0, 1, 3, 6, 10, and 20 ft). For Section A, temperature variations at different depths are presented in different colors.

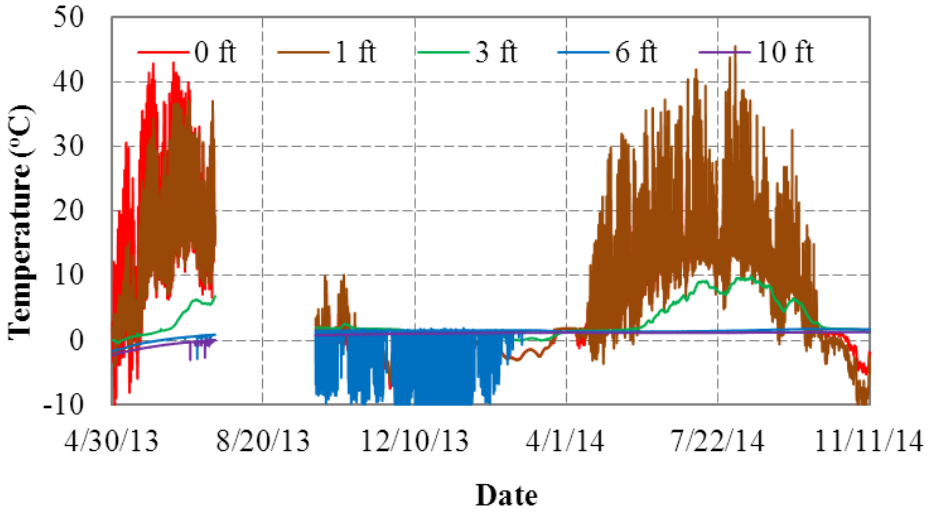

(a) bottom

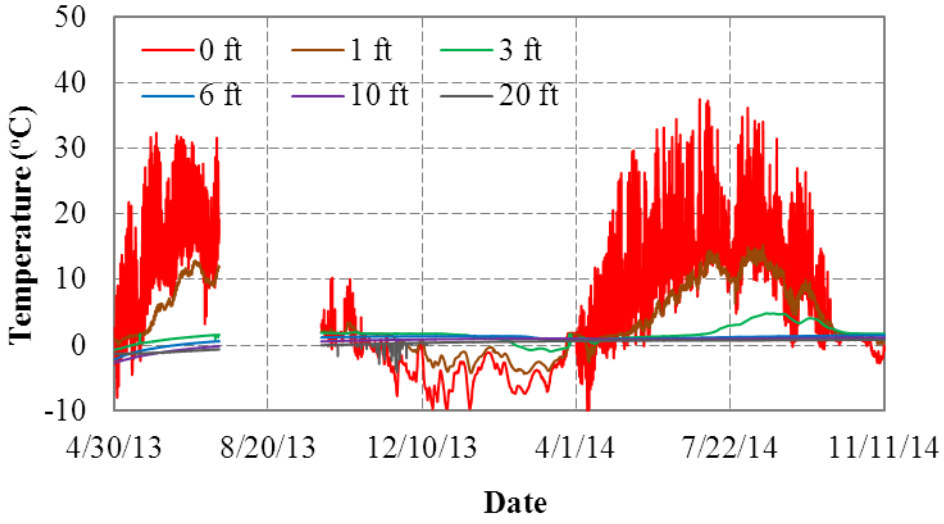

(b) middle

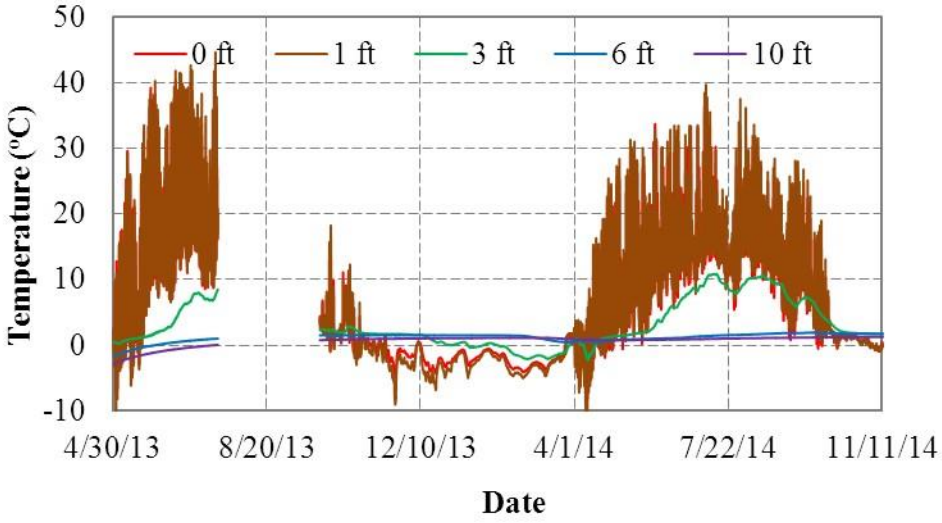

(c) top

Figure 7.11 Temperature variations in Section B

Similar to the temperature variation in Section A, due to the air temperature increase during the time period between April 30 and July 15, 2013, soil temperatures increased throughout the monitoring period at different depths and decreased during the time period between November and December 2013, as seen in Figure 7.11. Then, in March, soil temperature at 0 ft started to rise up with fluctuations till the end of June. The soil temperature at depths below 0 ft continuously decreased from January to April and then rose up till the end of June. At the slope surface, the temperature changes closely followed air temperature variation. Also, the temperature variations for the bottom, middle, and top of the section were consistent with one another due to the thickness uniformity of the coconut blanket, except for the temperatures at the middle with depths of 1 and 3 ft. At 1 ft below the slope surface in this section, especially for the temperatures at the top and bottom of this slope, the soil temperature changes closely followed the daily air temperature variation. Compared with the layer of wood chips, the coconut blanket (as expected) offered essentially no insulative benefit. Three ft below the slope surface of this section, soil temperature changes smoothly followed the long-term increase in air temperature—in a damped response compared with the soil at 1 ft depth.

Figure 7.12 shows temperature changes at the bottom, middle, and top of Section C (Tecco-mesh and coconut blanket) at different depths (0, 1, 3, 6, 10, and 20 ft). Temperature variations at different depths are presented in different colors. Due to thaw-related slope failures in this

section, the Tecco-mesh and coconut blanket were removed and replaced by crushed rock on June 17, 2013. The layer of crushed rock was of variable thickness due to the uneven surface of the damaged slope. The thickness of the rock blanket ranged from about 1 to 3 ft. Temperature sensors located at depths of 6 and 10 ft at the bottom of Section C stopped working after the June 17, 2013 repair work.

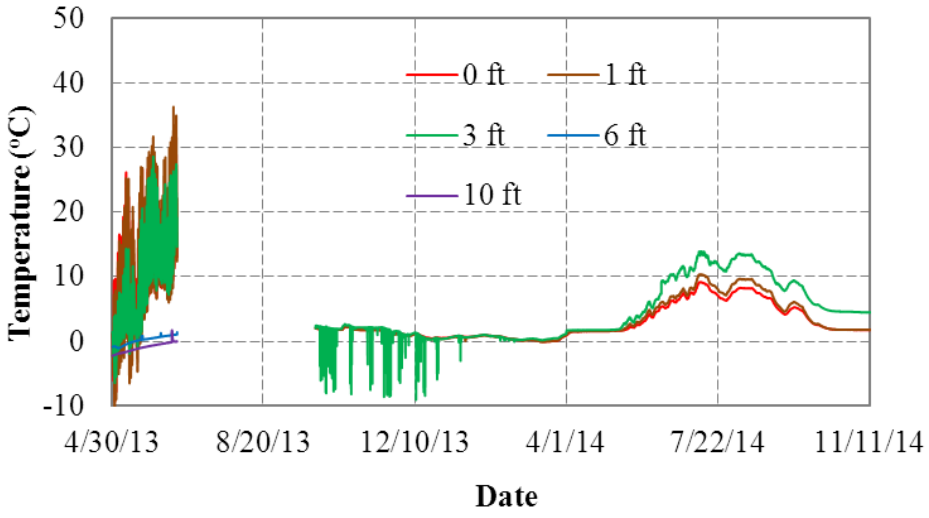

(a) Bottom

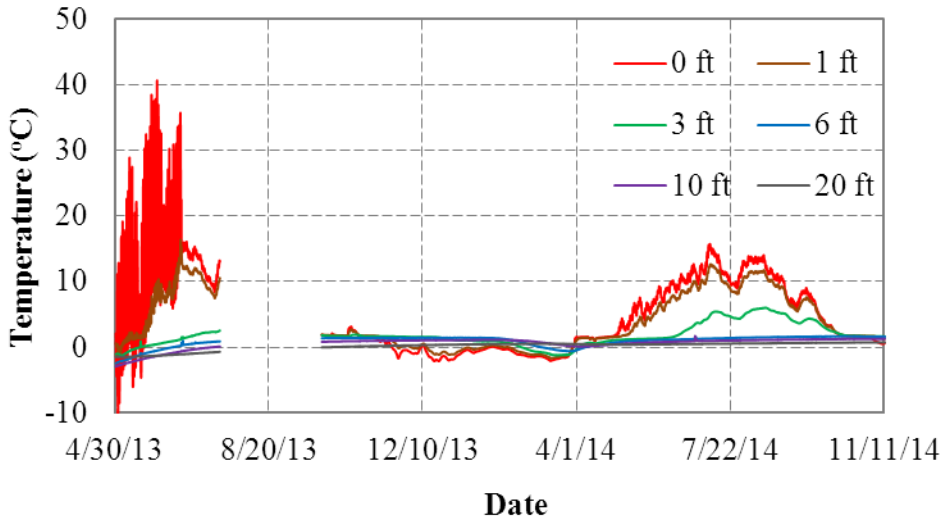

(b) Middle

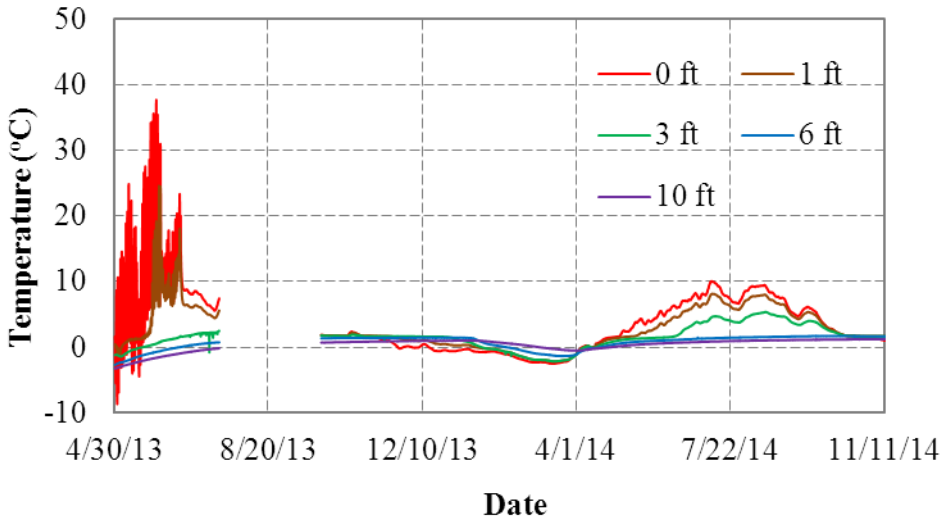

(c) Top

Figure 7.12 Temperature variations in Section C

Before the major repair work on June 17, 2013, temperature variations within Section C were generally similar to those of Sections A and B, as seen in Figure 7.12. At the slope surface and 1 ft below, temperatures followed the daily air temperature variation. Compared with the wood chip section (Section A), the coconut blanket together with the Tecco-mesh offered essentially no insulative benefit, as expected. After the replacement of the Tecco-mesh and coconut blanket with a rock blanket, temperature sensors at the original slope surface and originally 1 ft below indicated that a period of cooling occurred. No such period of cooling was seen in Sections A or B. Soil temperatures variations between October, 2013 and August 2014, which was after the repair work on June 17, 2013, were also similar to that in Sections A and B.

Figure 7.13 shows the temperature changes at the bottom, middle, and top of Section D (crushed rock) at different depths (0, 1, 3, 6, 10, and 20 ft). At the top of Section D, no temperature data were obtained from the sensor at a depth of 3 ft due to malfunctioning. Due to erosion in Section D, associated with repairs and placement of crushed rock in Section C, more crushed rock was placed in Section D.

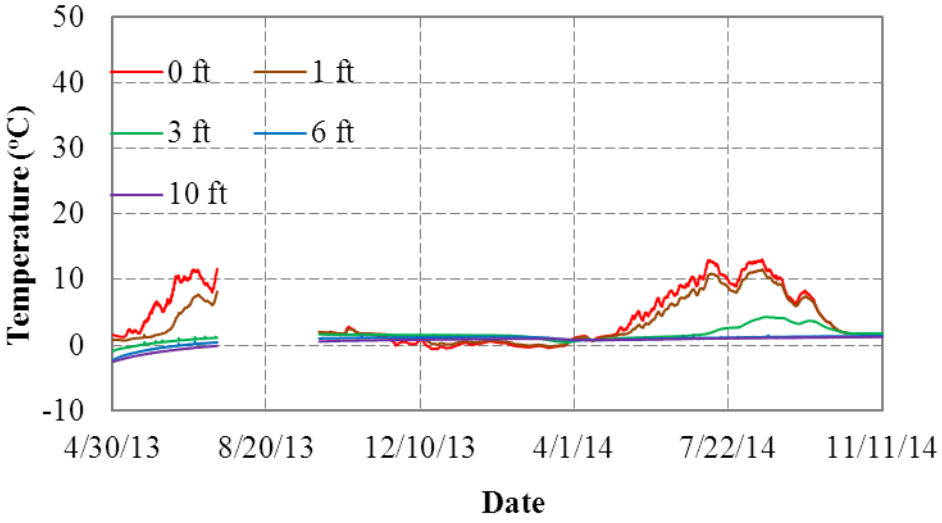

(a) Bottom

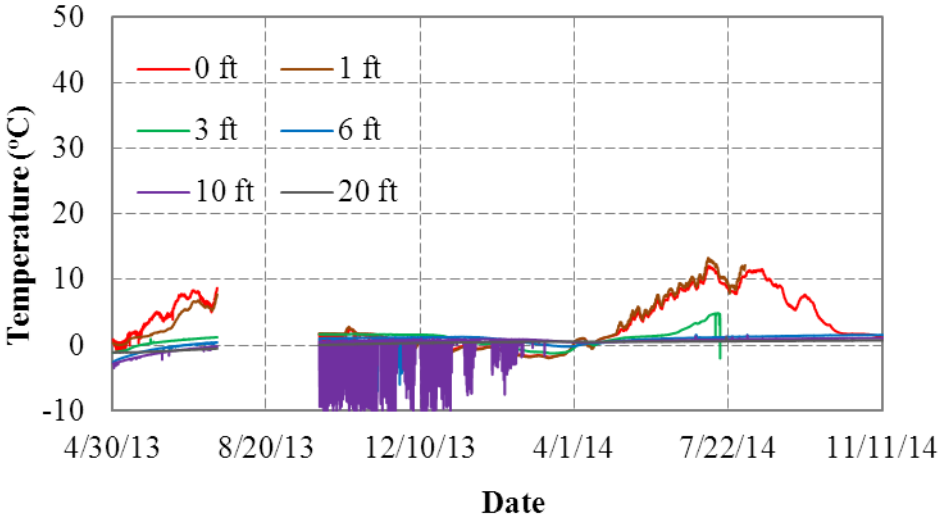

(b) Middle

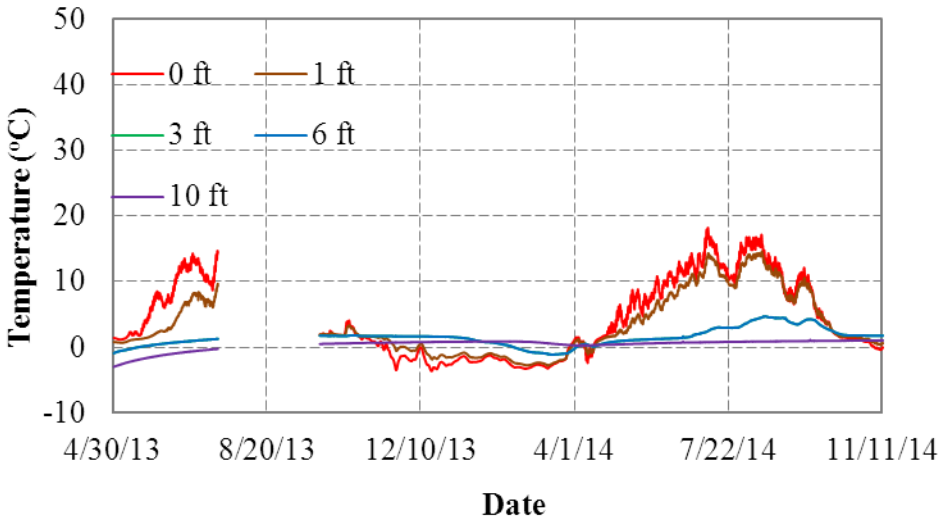

(c) Top

Figure 7.13 Temperature variations in Section D

As shown in Figure 7.13, soil temperature variations follow the same pattern as for Sections A through C except that the soil temperature response is damped by the overlying rock blanket. Due to the presence of the covered 1 ft of crushed rock, soil temperatures at 0 and 6 ft were higher and lower than that in Sections B and C in summer and winter, respectively.

Besides the temperature variations with time at individual slope locations, temperature contours at different times in degrees Celsius for four sections are presented in Figures 7.14 to 7.17. Each plot provides soil temperature contours for a specific date, interpreted from the temperature sensor data recorded on that date. Each plot provides a "map" of isothermal contours of soil temperatures at various depths from the bottom of the slope (left side of plot) to the top of the slope (right side of plot) for the indicated date. For Section A shown in Figure 7.14, the isotherms were approximately parallel to the slope surface right after construction on April 30, 2013. Also, the temperature gradient was almost evenly distributed with depth. However, after construction, the temperature varied dramatically within 1 to 2 ft below the slope surface. The maximum temperature variation occurred at the top of the section, possibly because, as was discussed previously, the wood chip thickness was greater at the bottom than at the top of the slope. The highest and lowest temperatures were both identified to be at the top of the section in summer and winter, respectively. In Section B, as shown in Figure 7.15, the temperature varied

dramatically within 3 to 4 ft of the slope surface. A comparison of Figures 7.14 and 7.15 strikingly illustrates that the single-layer coconut blanket provided essentially no thermal protection for the frozen cut slope soils compared with 1 ft of wood chips. The isothermal lines more or less parallel the slope face at the different times plotted. In Section C, as shown in Figure 7.16, isothermal lines were at an angle to the slope surface, which is different from the other sections. The bottom of the slope within Section C, the Tecco-mesh section, was warming much faster than at the top of the slope for reasons that are yet unknown. Unfortunately, due to construction of the Section C slope protection replacement on June 17, 2013, the temperature sensors at the bottom of the slope stopped working. After that date, temperature information for defining a 3-point isotherm was not available; hence, Figure 7.16e and 7.16f only present half of the isotherm lines. Soil temperatures for Section D are presented in Figure 7.17. Until late May, 2013, the bottom of the slope experienced more rapid warming than the upper portions of the slope. This accentuated warming at the bottom of the slope was similar to what occurred at Section C, but not as severe. Penetration of the thaw front within this section appears to have been somewhat slowed by the additional rock placed in Section D during the Section C repairs.

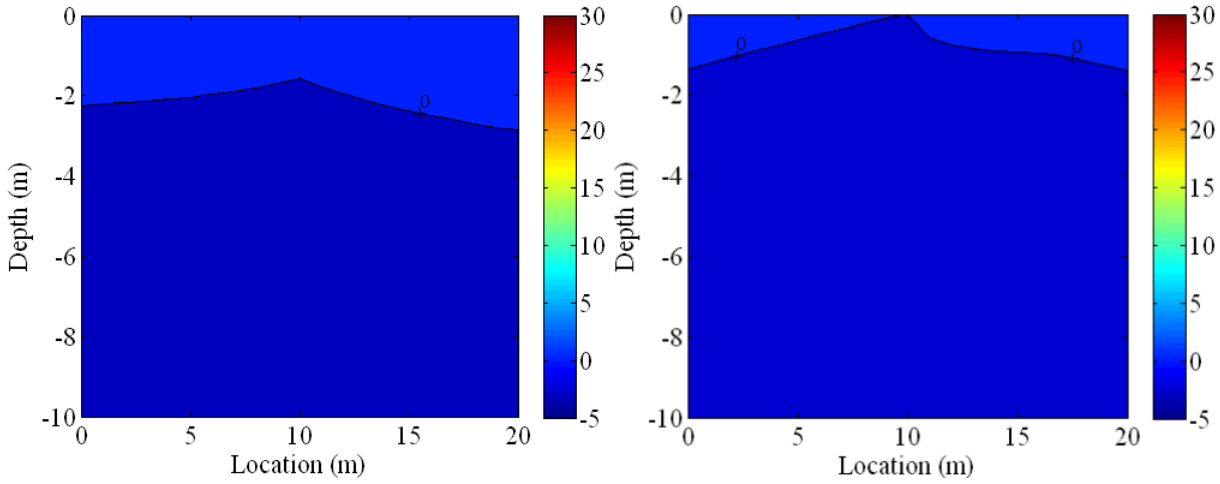

(a) At 7:00 p.m. on April 30, 2013

(b) At 7:00 p.m. on May 8, 2013

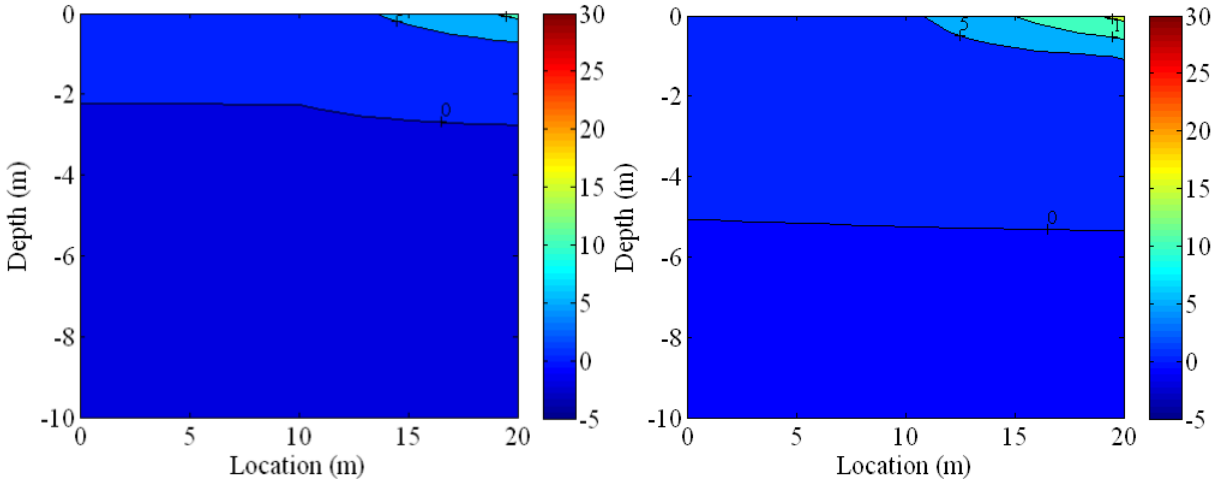

(c) At 7:00 p.m. on May 23, 2013

(d) At 7:00 p.m. on June 13, 2013

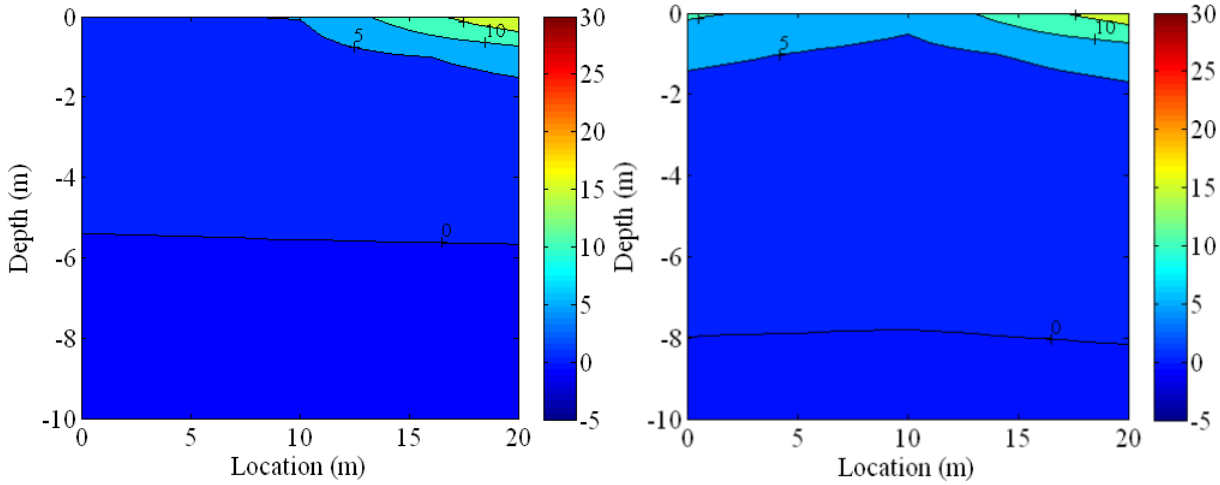

(e) At 7:00 p.m. on June 17, 2013

(f) At 7:00 p.m. on July 14, 2013

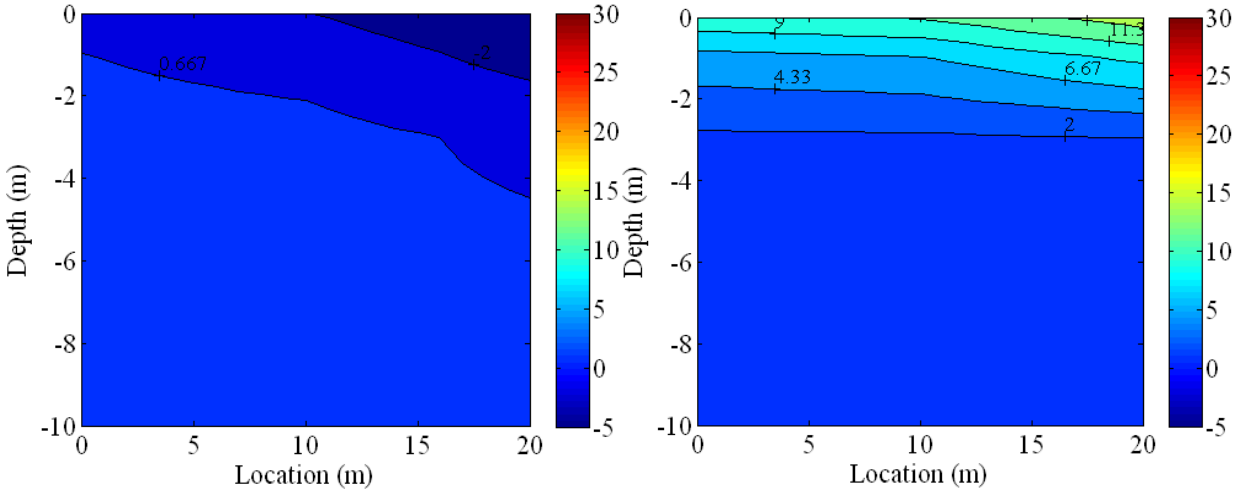

(g) At 7:00 p.m. on January 1, 2014

(h) At 7:00 p.m. on August 7, 2014

Figure 7.14 Temperature contours at different times in Section A

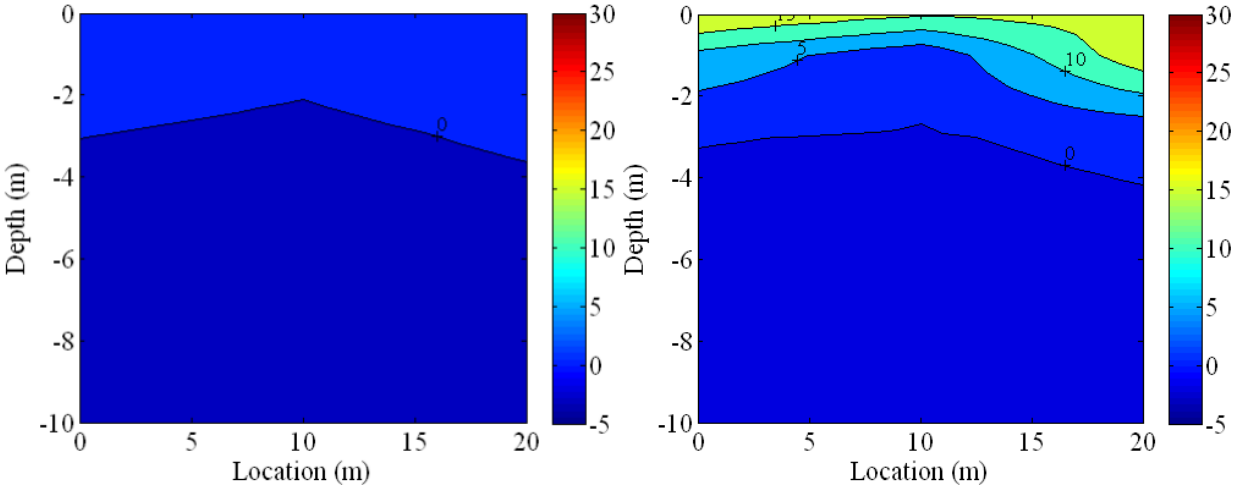

(a) At 7:00 p.m. on April 30, 2013

(b) At 7:00 p.m. on May 8, 2013

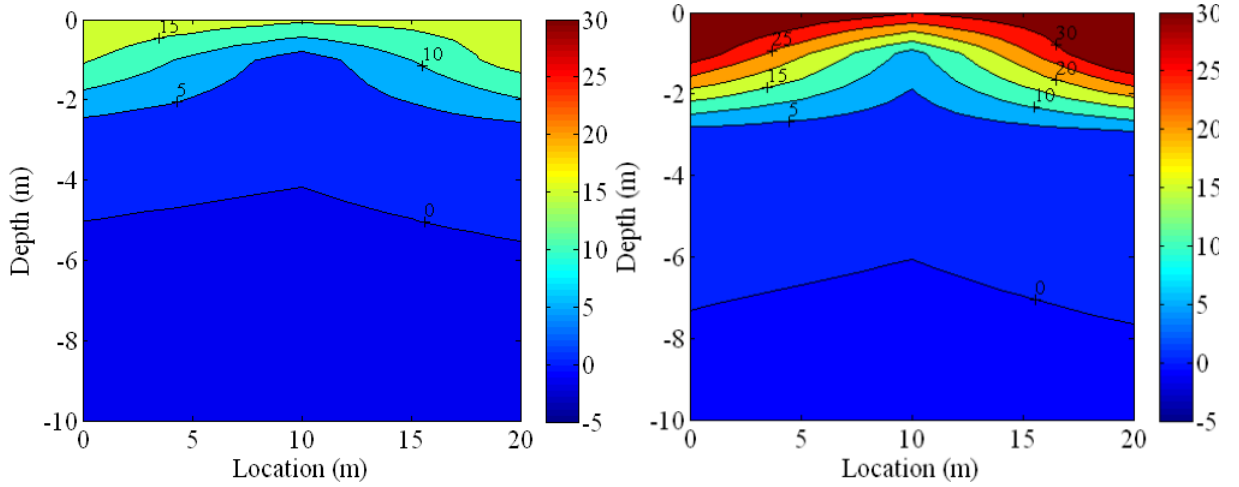

(c) At 7:00 p.m. on May 23, 2013

(d) At 7:00 p.m. on June 13, 2013

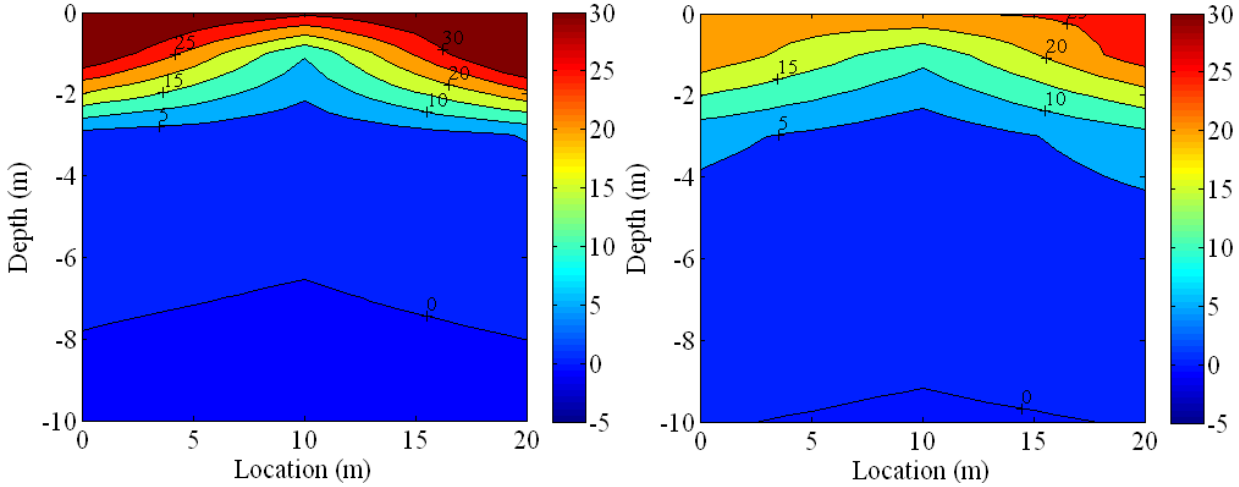

(e) At 7:00 p.m. on June 17, 2013

(f) At 7:00 p.m. on July 14, 2013

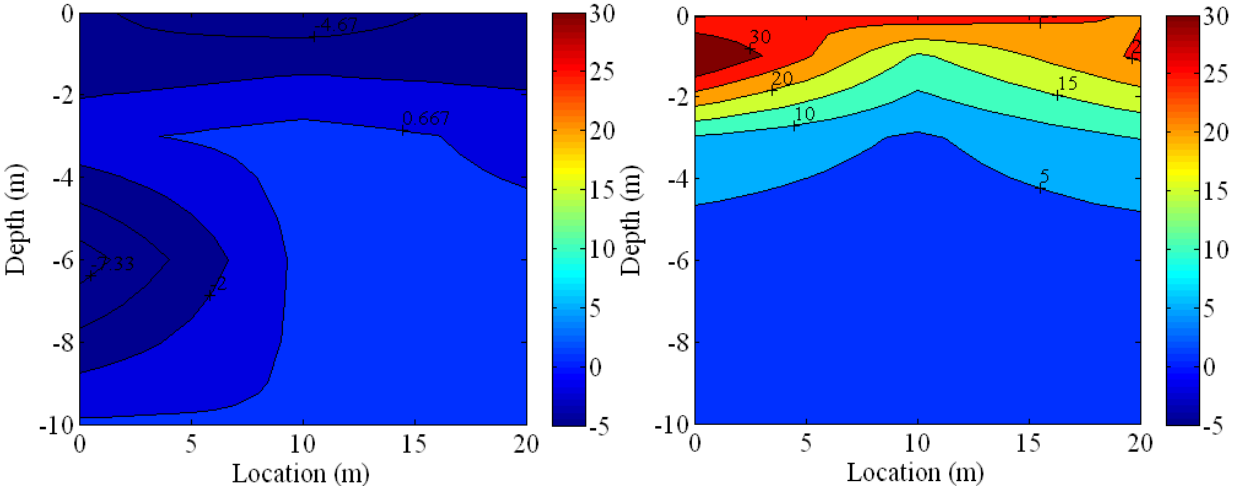

(g) At 7:00 p.m. on January 1, 2014 (h) At 7:00 p.m. on August 7, 2014

Figure 7.15 Temperature contours at different times in Section B

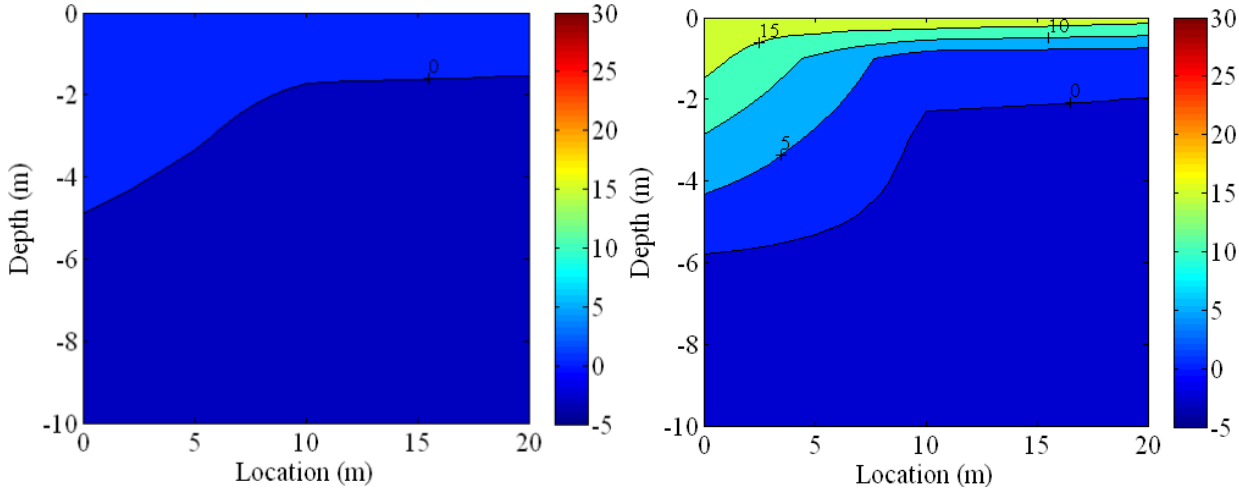

(a) At 7:00 p.m. on April 30, 2013 (b) At 7:00 p.m. on May 8, 2013

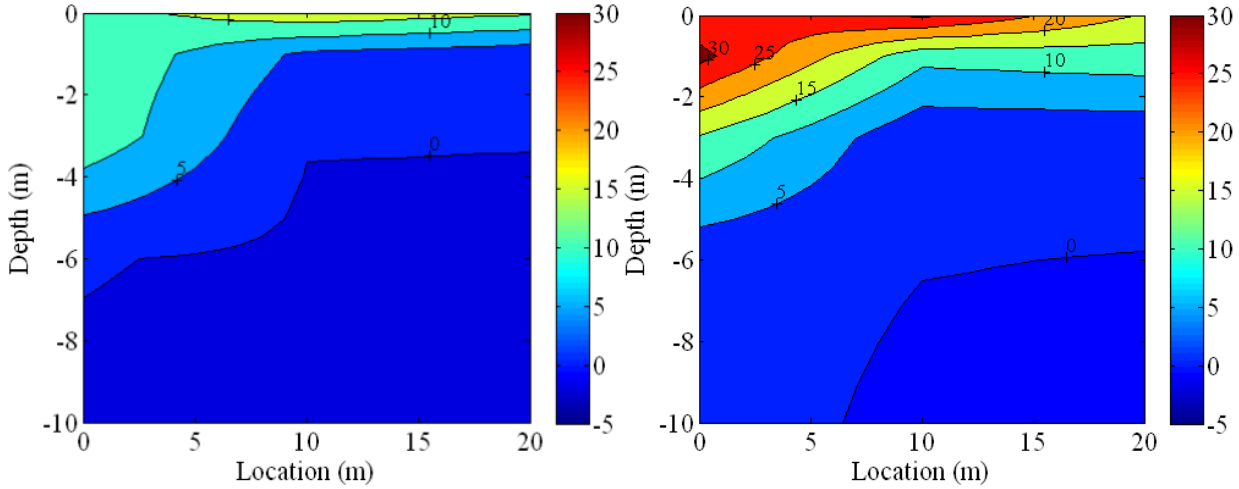

(c) At 7:00 p.m. on May 23, 2013 (d) At 7:00 p.m. on June 13, 2013

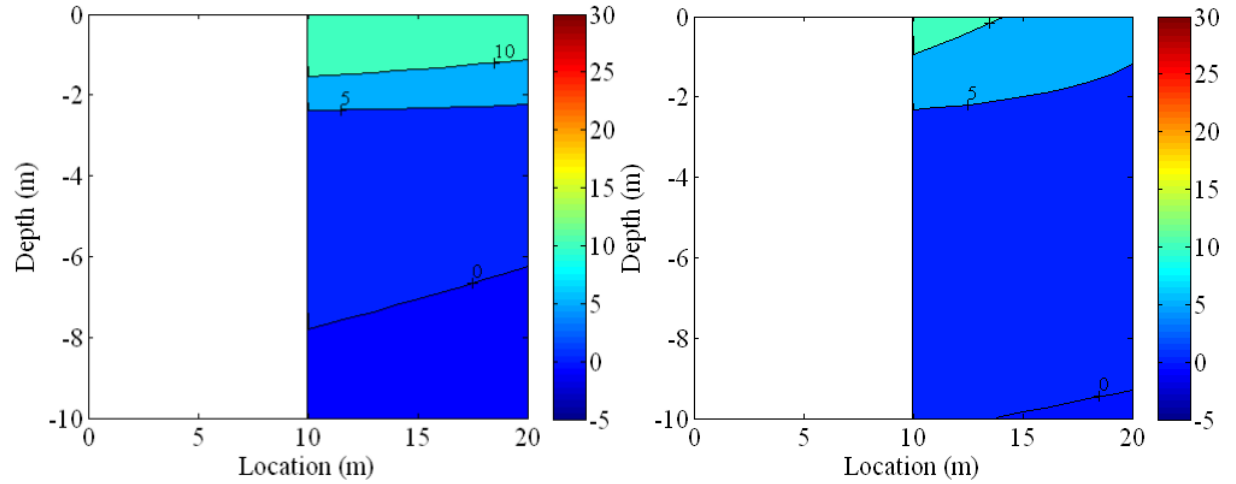

(e) At 7:00 p.m. on June 17, 2013

(f) At 7:00 p.m. on July 14, 2013

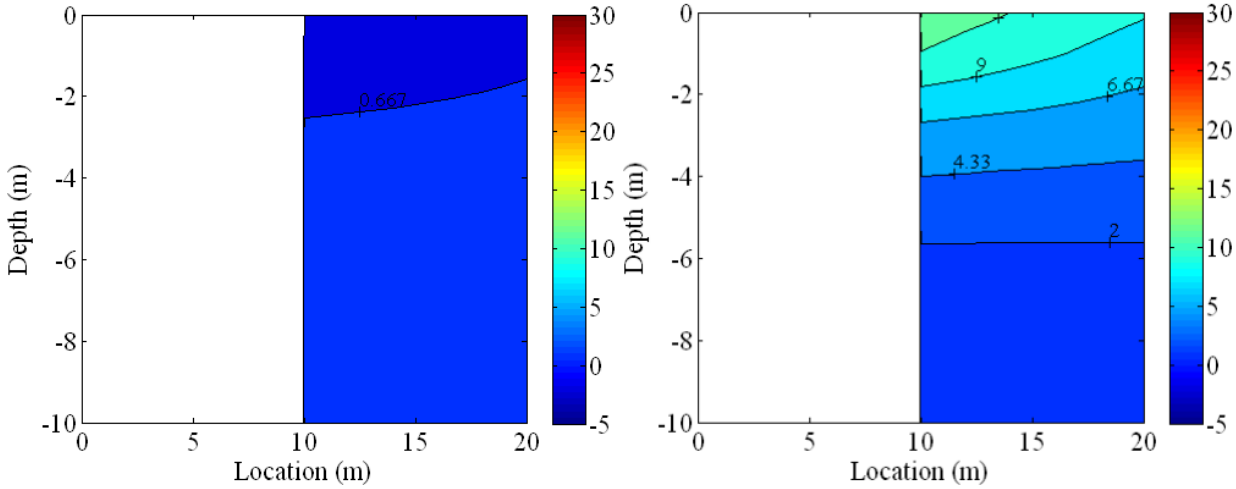

(g) At 7:00 p.m. on January 1, 2014

(h) At 7:00 p.m. on August 7, 2014

Figure 7.16 Temperature contours at different times in Section C

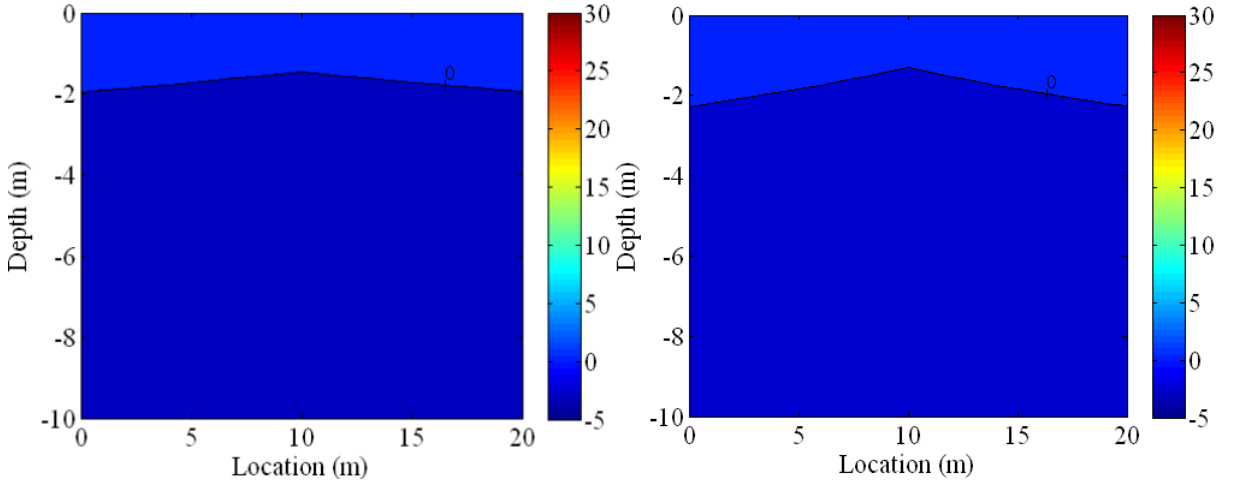

(a) At 7:00 p.m. on April 30, 2013

(b) At 7:00 p.m. on May 8, 2013

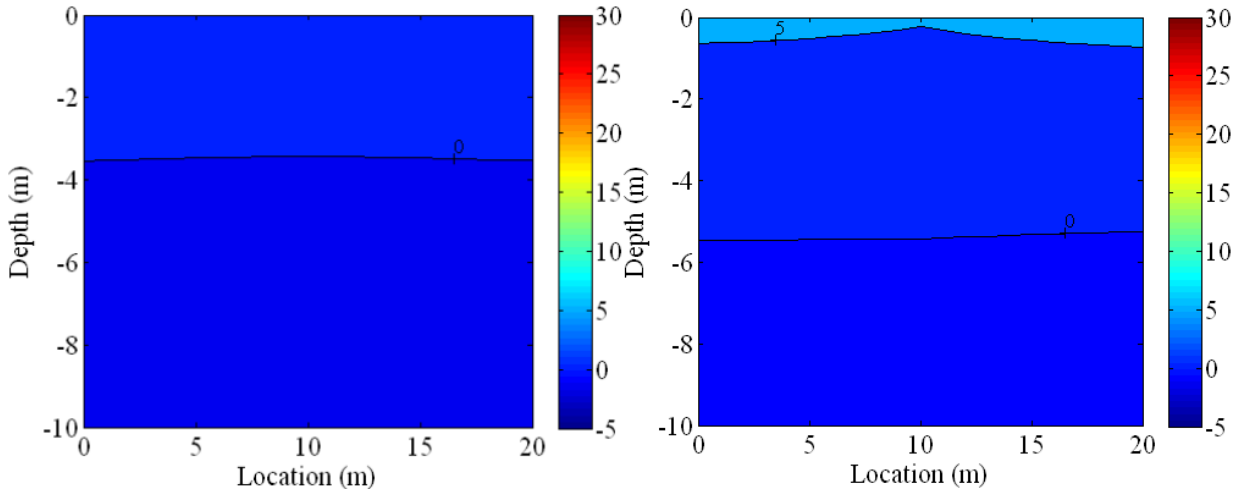

(c) At 7:00 p.m. on May 23, 2013

(d) At 7:00 p.m. on June 13, 2013

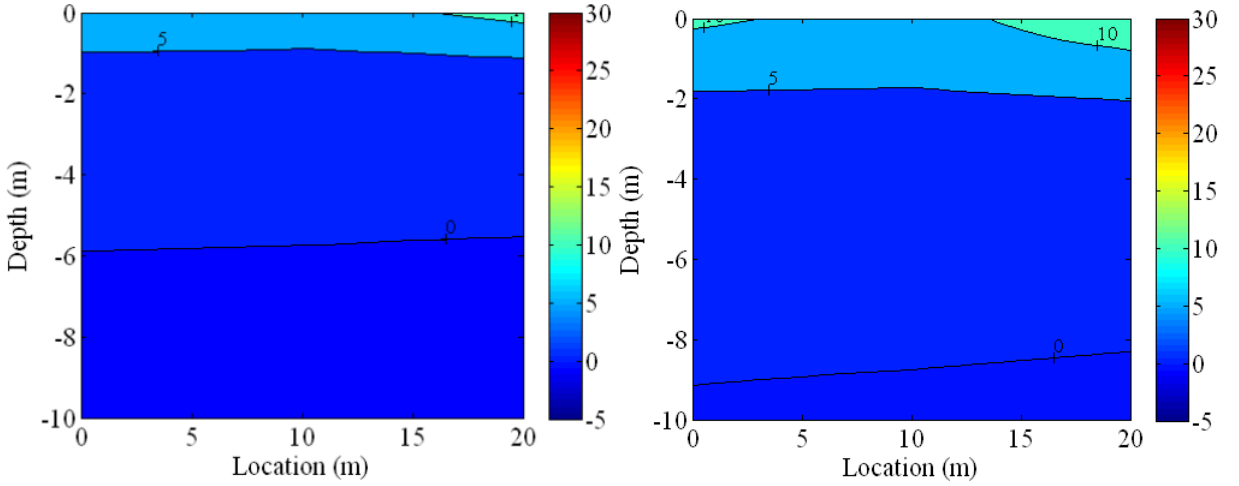

(e) At 7:00 p.m. on June 17, 2013

(f) At 7:00 p.m. on July 14, 2013

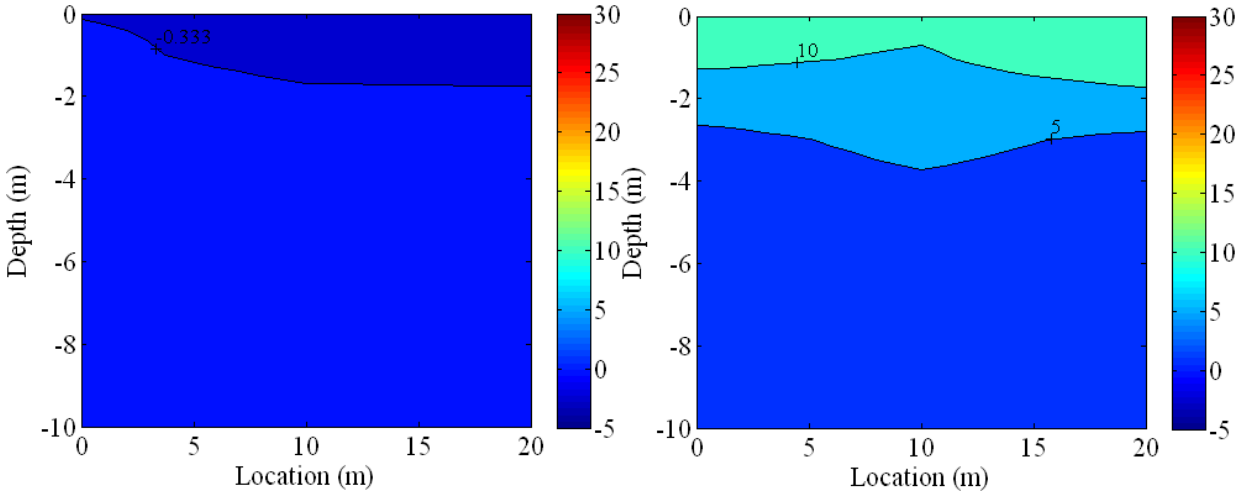

(g) At 7:00 p.m. on January 1, 2014

(h) At 7:00 p.m. on August 7, 2014

Figure 7.17 Temperature contours at different times in Section D

Figure 7.18 presents the temperatures reported by the temperature sensors installed at the middle height of all four sections at different times. On June 1, 2013, which was before the repair on June 17, 2013 as shown in Figure 7.18a, among the four sections, temperatures at Section A and B at depth of 3 ft, were the lowest and highest, respectively. In other words, 1 ft wood chips worked better than the coconut blanket in terms of insulate benefit. At Sections B and C, the same coconut blanket was used for slope protection. However, at depth of 3 ft, the temperature at Sections B was higher than that at Section C due to the presence of massive ground ice at Section C. On January 1, 2014, for four sections, soil below 1ft was not frozen according to Figure 7.18b. At depth of 1 ft, temperature at Section B was lowest. On July 1, 2014, at depth of 3 ft, similar to temperature distribution on June 1, 2013, temperature at Sections B was the highest. Due to the repair on June 17, 2013, temperature at Section D was the lowest since Sections D were covered with more crushed rock.

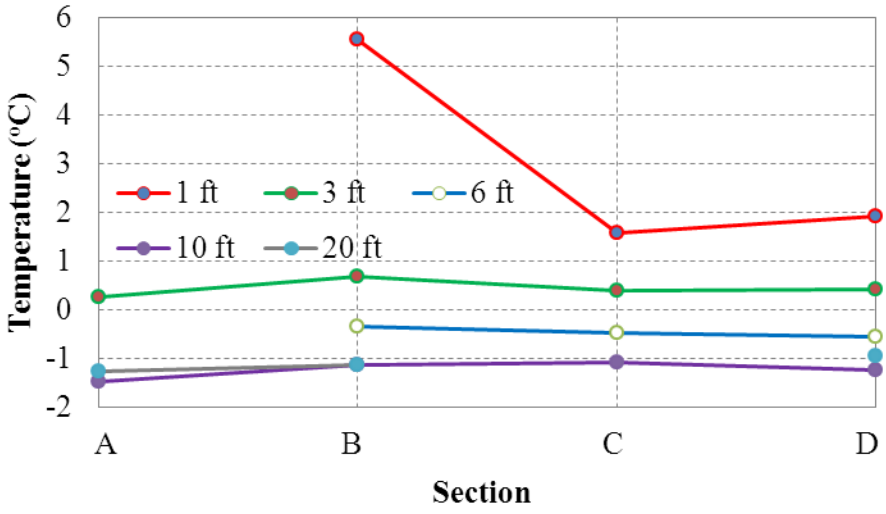

(a) At 7:00 p.m. on June 1, 2013

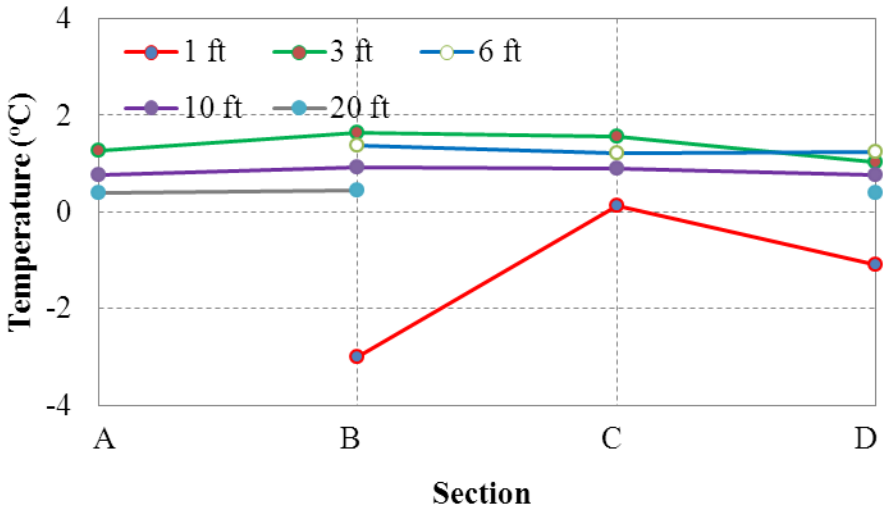

(b) At 7:00 p.m. on January 1, 2014

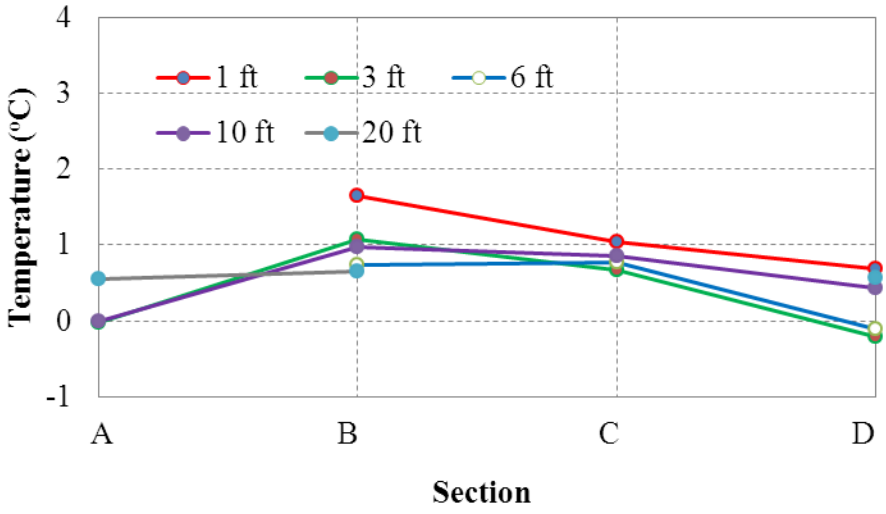

(b) At 7:00 p.m. on July 1, 2014

Figure 7.18 Temperature contours at different times in Section D

Moisture Changes in the Test Section

In this project, all volumetric moisture content sensors (TDR) were placed at the slope surface. Moisture content variations throughout the measurement period were recorded, and they are presented in Figures 7.19 to 7.22. Figure 7.19 shows volumetric moisture content variations reported by the TDR sensors at the slope surface in Section A (wood chips), located at the left side of the cut slope. Only one of the three sensors in Section A was functional after the

installation. Shortly after construction, the volumetric moisture content decreased slightly and then stabilized for about two weeks. This minor desiccation was probably associated with exposure of the slope face to air circulation during construction, before the wood chips were placed. Beginning in late May, 2013, volumetric moisture content gradually increased from approximately 10% to 40% in October because of high temperature in the summer, which resulted in melting of ice in the slope. In November, 2013, the soil volumetric moisture content in Section A decreased dramatically to approximately 10 % due to the air temperature drop and then stabilized till April, 2014. Then, the soil volumetric moisture content in Section A started to increase till June 2014. Subsequently, the soil volumetric moisture content in Section A continuously decreased with fluctuations due to decreasing air temperature. For Sections B and C, the volumetric moisture content continually increased from 20% to 50% on May 25, 2013, after which it was mostly stable or slightly decreased till November. Similar to Section A, the soil volumetric moisture content in Sections B and C decreased dramatically to approximately constant values due to the air temperature drop in November, 2013. The stabilized volumetric moisture content at the lower part of the cut slope was higher than at the upper part, likely due to drainage of water down the slope face. The soil volumetric moisture content in Section B, C, and D started to increase dramatically in April 2014 till the end of June, 2014 and then stabilized or continuously decreased again. For Section D (crushed rock), the volumetric moisture content stabilized at approximately 50% at the beginning of June, 2013 and mid-May, 2014 which was approximately one week later than in Sections B and C. Even though only one data point is available for Section A, it appears that the longer moisture stabilization times for Sections A and D may be supporting the temperature-based observation that wood chips and a rock blanket are thermally superior to the treatments used in Sections B and C. Similarly, it would appear that the wood chip treatment in Section A provides better thermal protection than the rock blanket in Section D during the mid-months of summers in 2013 and 2014.

Before leaving this subject, it is necessary to comment briefly on a very positive characteristic of certain rock blankets. The authors do realize and acknowledge that a rock blanket of sufficient thickness and permeability has the potential to significantly cool underlying soils during the winter season via convective heat transport. If properly designed, such a rock blanket can more than compensate for its lack of summertime insulation value by its considerable wintertime heat extraction.

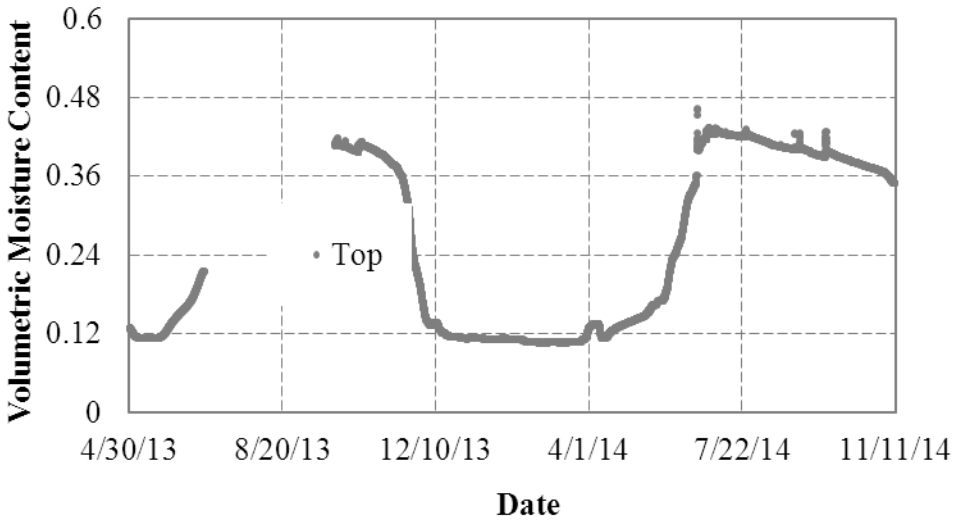

Figure 7.19 Volumetric moisture content variations in Section A

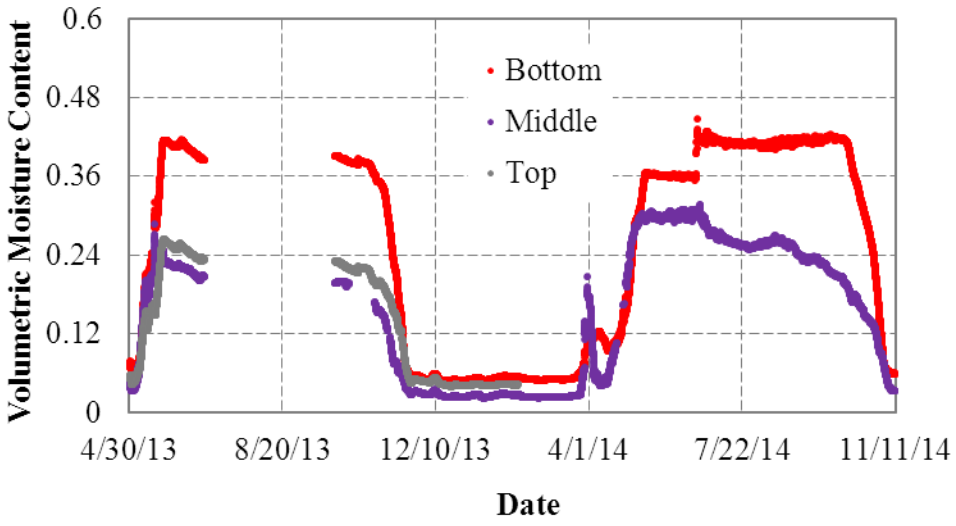

Figure 7.20 Volumetric moisture content variations in Section B

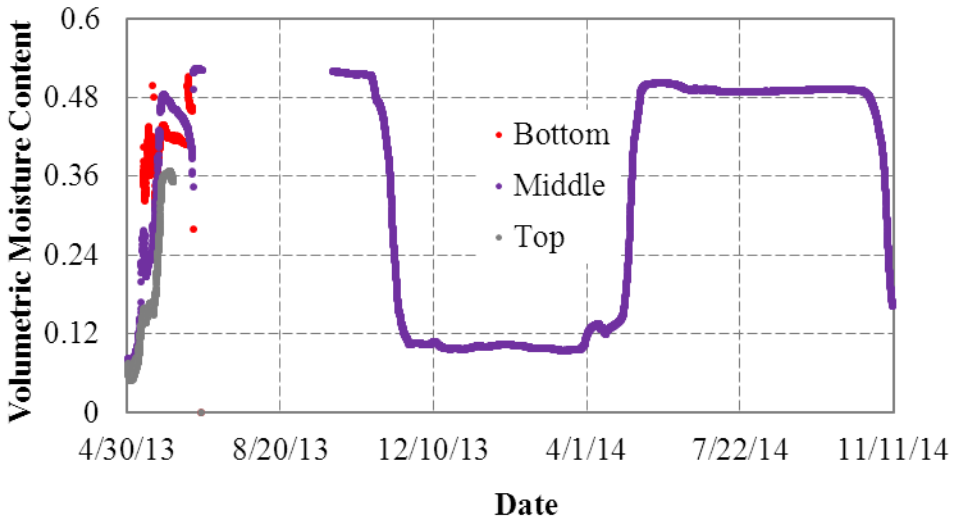

Figure 7.21 Volumetric moisture content variations in Section C

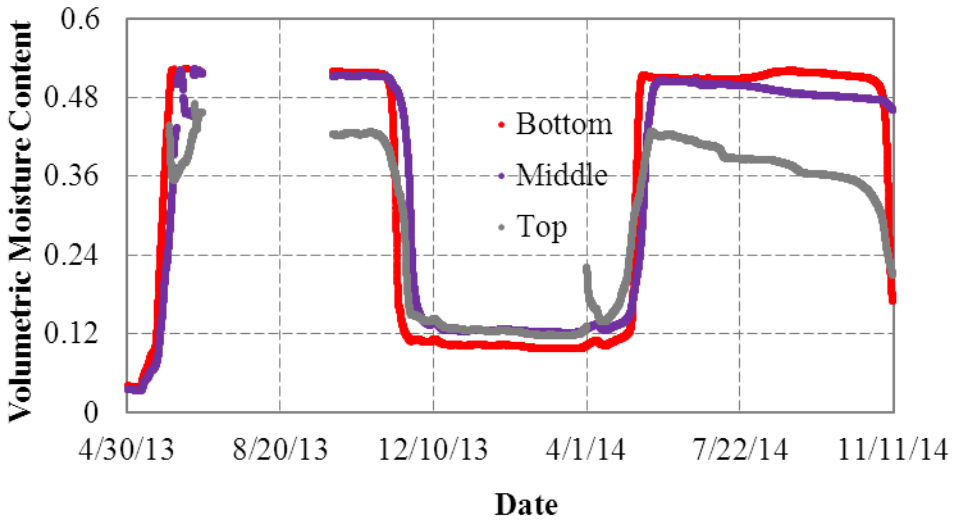

Figure 7.22 Volumetric moisture content variations in Section D

Photogrammetric Erosion Monitoring

Nowadays, rapid developments in digital camera technology and low-budget photogrammetric software products mean that standard consumer-grade cameras may be a viable option for photogrammetric measurements. To perform the erosion measurement using photogrammetric methods, a digital camera was required to obtain the photos. To reach a high level of accuracy, a digital single-lens reflex camera with a fixed focal length lens was needed. Before being used for

erosion measurement, the camera required calibration. For a single measurement, several images of the cut slope were captured for photogrammetric analysis. Then, a 3D point cloud, which indicated the 3D position of the slope surface, was generated. Based upon the movement of the slope surface, the erosion could be calculated. Principles of photogrammetry and detailed information on erosion measurement are presented in Appendix A.

On April 26, after slope construction on the Section A, the volume of this section above the reference *x-y* plane was measured using the photogrammetric method previously explained. The difference between the volume measured on April 26, 2013 and the volumes measured on subsequent dates indicates the cumulative volume gains or losses with time along the face of Section A. Volume losses were interpreted as a loss of material through surface erosion or thaw-settlement. Volume gains were interpreted as an increase in surface cover whether by vegetation of other materials.

A record of the cumulative surface volume changes for Section A between April 26 and September 27, 2013, is shown in Figure 7.23. In this figure, volume changes are indicated on various dates between April 26 and August 8, 2014: a volume *increase* relative to the slope face condition on April 26 is shown as a positive value; a volume *decrease* relative to April 26 is shown as a negative value. Figures 7.24 and 7.25 are photos of Section A on April 26 and April 30, 2013 respectively. Figure 7.23 indicates that the volume along the Section A slope face actually increased (varying between 8 and 12 m^3) during this period. Part of the increase is due to the additional wood chips applied over Section A after April 26. Another reason for the increase is the light snow cover on Section A from snowfall between April 26 and 30, 2013. After April 30, 2013, there were small fluctuations in the volume of material added to the surface of Section A. Observation of this section identified no significant erosion throughout the 2013 monitoring period, as indicated by the excellent condition of the slope on September 27, 2013 (see photo in Figure 7.26). However, based on two volume change measurement results in 2014 (May 20 and August 08 as shown in Figures 27 and 28), volume of Section A continuously decreased significantly as presented in Figure 23. There were two reasons for this is which is the melting of ground ice in the slope and the possible movements of the anchors in Section C, which were used as control points for survey purpose, due to frost heave in the slope during winter time.

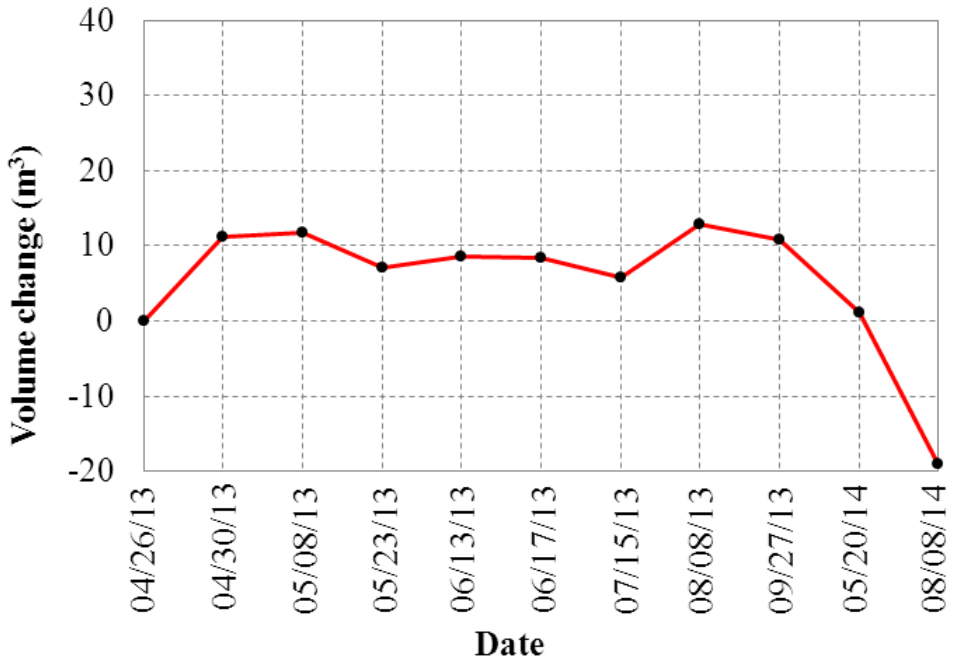

Figure 7.23 Surface volume change on Section A

Figure 7.24 Section A after construction on April 26, 2013

Figure 7.25 Section A with more wood chips on April 30, 2013

Figure 7.26 Section A with more wood chips on September 27, 2013

Figure 7.27 Section A with more wood chips on August 8, 2014

Similar to Section A, no erosion on Section B (the coconut blanket section) was observed, which is consistent with the photogrammetric erosion measurement results shown in Figure 7.28. Before June 17, 2013, the volume change on the surface of Section B was not significant. Figure 7.29 presents a picture of this section on June 17, 2013, prior to the rapid growth of grass on the slope surface. After June 17, 2013, significant grass growth on this section was observed. Figures 7.30 and 7.31 are photos of this section captured on July 15 and August 8, respectively. Figure 7.31 is a photo showing the surface of Section B on September 27, 2013. This fall-time photo shows that the grass has wilted. This wilting process was detected as surface volume loss during the fall season, as shown in Figure 7.32. For two volume change measurement results in 2014 as shown in Figure 7.28, volume of Section B continuously decreased significantly which is similar to Section A. Part of the reason for this may be attributed to the melting of ground ice in the slope The other two reasons is the grass grow in 2014, as shown in Figure 7.33, was not as good as that in 2013.

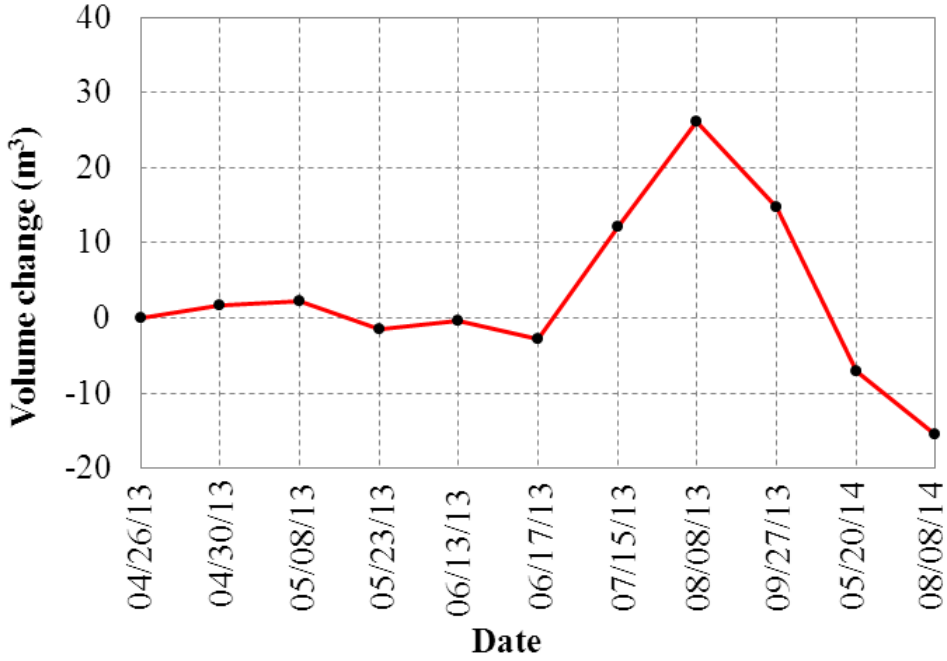

Figure 7.28 Surface volume change on Section B

Figure 7.29 Section B on June 17, 2013

Figure 7.30 Section B on July 15, 2013

Figure 7.31 Section B on August 8, 2013

Figure 7.32 Section B on September 27, 2013

Figure 7.33 Section B on August 8, 2014

As discussed previously, massive ground ice was found in Sections C and D. Erosion within these two sections was much greater than the erosion observed in Sections A and B. Figure 7.34 provides a very misleading record of total surface volume changes for Section C (Tecco-mesh and coconut blanket), because the photogrammetric process was only able to discern changes at the surface of the Tecco-mesh instead of at the underlying soil surface.

At the beginning of the photogrammetric record, April 26, measurements indicated a small surface volume increase due to the snow cover shown in Figure 7.35. During the period between about April 30 and June 13, 2013, a rather large volume of icy soil (and massive ice) materials, originally located beneath the Tecco-mesh slope cover, were lost to runoff and thaw-consolidation. Photogrammetric measurements, as indicated in Figure 7.34, keyed on the surface of the Tecco-mesh, and therefore provided no indication of the volume loss that was occurring under the Tecco-mesh. Figure 7.36 shows obvious signs of the actual condition of the cut slope face under the Tecco-mesh by June 13, 2013. Obviously, the deterioration process of the cut slope face under the Tecco-mesh was not detected by the photogrammetric process!

On June 17, the Tecco-mesh and coconut blanket on this section were removed and replaced by crushed rock as shown in Figure 7.37. This significant slope surface volume change (due to the added crushed rock) was captured by the subsequent set of photogrammetric measurements (indicated on the right-hand side of Figure 7.37). Figure 7.38 shows the appearance of Section C on September 27, 2013. Figure 7.34 indicates than an attenuation of thaw-related volume change was occurring in Section C prior to September 27, 2013. In 2014, slope surface volume continuously decreased till May 20, 2014 as shown in Figure 34. Figure 7.39 shows the appearance of Section C on May 20, 2014. However, after that, a volume increase change was captured on August 8, 2014. One reason for this volume increase was the grass grown as shown in Figure 7.40.

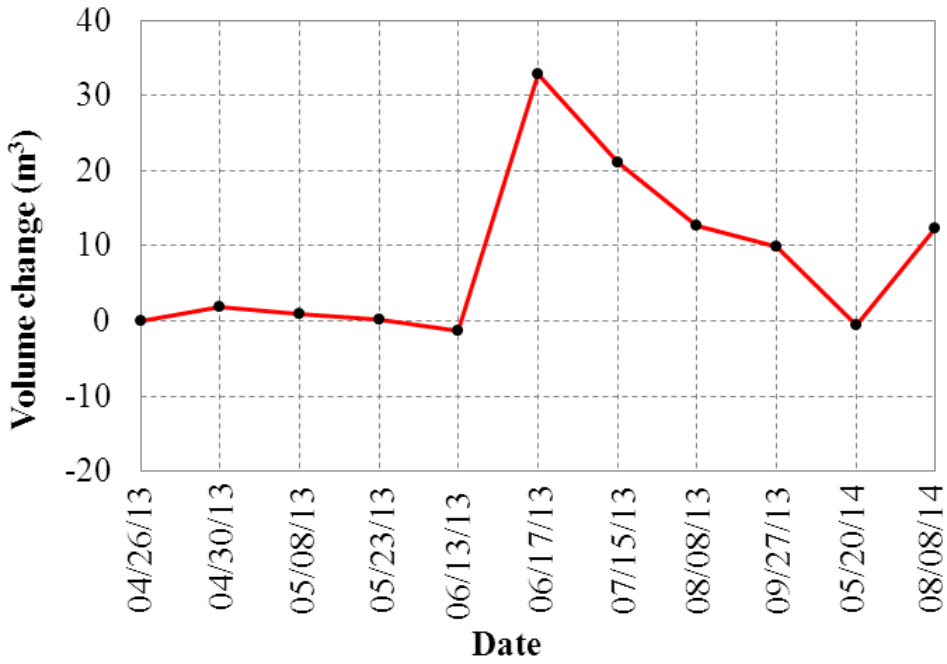

Figure 7.34 Surface volume change on Section C

Figure 7.35 Section C on April 30, 2013

Figure 7.36 Section C on June 13, 2013

Figure 7.37 Section C on June 17, 2013

Figure 7.38 Section C on September 27, 2013

Figure 7.39 Section C on May 20, 2014

Figure 7.40 Section C on August 8, 2014

Section D (originally constructed with a crushed rock blanket) serves as the control section for the Experimental Feature. Figure 7.41 indicates that a more or less continual loss of slope surface volume occurred through September 27, 2013. The initial small volume increase at the surface of Section D was because of the late April snowfall shown in the photo in Figure 7.42. Loss of surface volume (through erosion and/or thaw-consolidation) continued through June 13. Figure 7.43 shows the condition of the slope face on June 13, 2013. Then, on June 17, 2013, a volume of rock material was added to the surface of Section D during Section C repairs (see photo in Figure 7.44). The immediate surface volume increase due to this addition of material in Section D is plotted in Figure 7.41. After placement of additional crushed rock on June 17, 2012, the loss of surface volume continued through the end of this report's monitoring period, on September 27. The condition of the slope at that time is shown by the Figure 7.45 photo. Figure 7.41 indicates that the surface volume loss rate for Section D had not attenuated much prior to September 27, 2013. As shown in Figure 7.41, in 2014, surface volume of Section D increased. On May 20, 2014, no grass was shown at this section. However, grass grown was identified at Section D as show in Figure 7.42 on August 8, 2014.

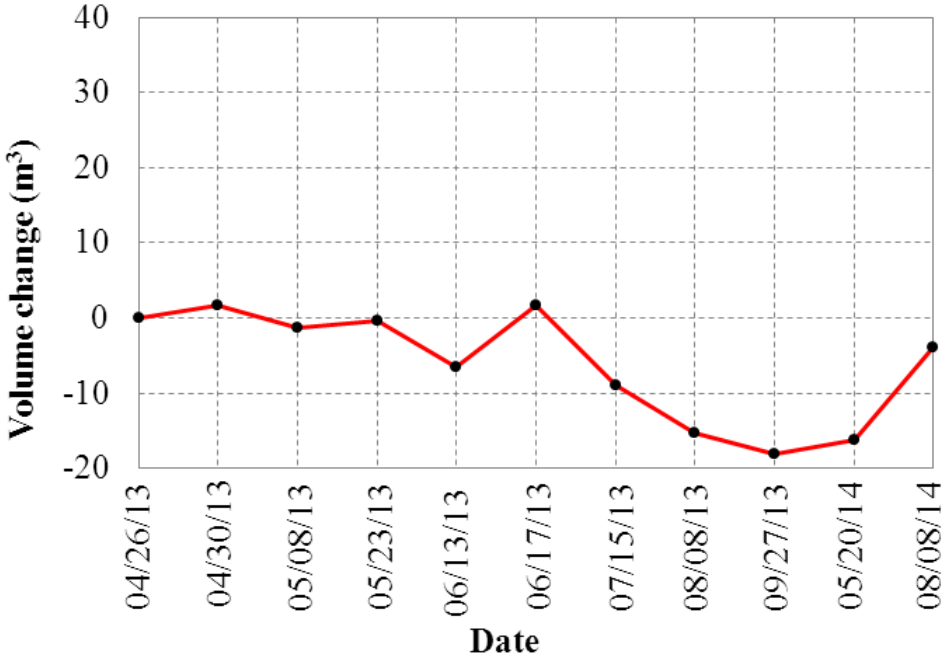

Figure 7.41 Surface volume change on Section D

Figure 7.42 Section D on April 30, 2013

Figure 7.43 Section D on June 13, 2013

Figure 7.44 Section D on June 17, 2013

Figure 7.45 Section D on September 27, 2013

Figure 7.46 Section D on May 20, 2014

Figure 7.47 Section D on August 8, 2014

CHAPTER 8. CONCLUSIONS AND RECOMMENDATIONS

This report focuses on the design, construction, and initial performance of an Experimental Feature located at Dalton Highway 9 Mile Hill. The Experimental Feature examines three methods for protecting a permafrost cut slope, exposed during a highway construction project, in an environmentally acceptable, permanent way. The Experimental Feature also incorporates a fourth slope-protection design—a control section, where the frozen cut slope surface is treated with the standard-design rock blanket for protecting permafrost cut slopes. The Experimental Feature project is introduced in Chapter 1. Chapter 2 reports on the review of pertinent literature, conducted during an early phase of this study. The design and construction of the four slope treatments is discussed in Chapters 3 and 4. Hydroseeding was performed for all test sections before applying any treatment for slope protection purpose. The four forms of slope treatment addressed in this report are as follows:

Section A, incorporating a wood chip slope treatment,

Section B, incorporating standard-type coconut mat slope treatment,

Section C, incorporating a mechanically robust slope surface treatment of Tecco-mesh underlain by coconut matting, and

Section D, the control section, incorporating a rock blanket treatment on the cut slope.

Conclusions Specific to the Experimental Feature

The following points summarize some of the research findings to date. Recommendations obtained from this research on methods of ice-rich cut slope protection are incorporated.

1. The performance of each slope protection method was heavily dependent on the ice content in areas of the slope where that particular protection method was used. In Sections B and C, the same coconut blanket was used to cover the slope surface. However, about one and a half months after the construction, Section C failed due to thermal erosion. No such erosion was found at Section B. The drastic difference in performance is considered mainly due to the presence of the massive ground ice in Section C. The construction process exposed large areas where the presence of massive ice was obvious, and of course, the exposed ice was immediately subjected to air and solar warming. Even though the coconut blanket and Tecco-mesh were soon placed on

the thawing surface, these layers provided little thermal protection. It is assumed that air spaces that quickly developed between the Tecco-mesh and the soil surface retained pockets of still air warmed by solar heating of the overlying coconut blanket (a sort of "hot house" effect), thus adding more heat to the thawing soils. Another source of added heat is thought to have been the long steel anchor shafts that had been installed in the frozen soils. These shafts would have been excellent heat conductors.

2. The strong, anchored Tecco-mesh survived intact during the soil thawing process that occurred beneath it. Just prior to removal, the Tecco-mesh was simply providing a strong tent covering for the degrading soil surface and, at some spots, was suspended several ft above that surface. The Tecco-mesh did not protect the ice-rich slope that contained massive ice inclusions. Once the ice-rich permafrost in the slope thawed, a large quantity of the fully saturated silty soil behaved like mud and flowed out from under the very robust and intact tent of strongly suspended Tecco-mesh. The Tecco-mesh itself did not fail, but it did nothing to hold the saturated silty soil in place. **It is stressed here that there were absolutely no problems with the Tecco-mesh material itself. This use of Tecco-mesh was simply an experimental application for which it was not suited.**

3. In Section D, crushed rock was used to protect the slope. Due to massive ground ice detected during construction, obvious thermal erosion was also found in this section, even though 1 ft of crushed rock was used to cover it. However, temperatures in this section were generally lower than those recorded in Section C. Also, erosion in Section D was less than in Section C and was not problematic—even though Section D also contained considerable massive ice. The crushed rock treatment worked much better than the Section C treatment.

4. Wood chips were used to protect Section A. No significant erosion was identified in this section until the end of September. The temperature in this section was lower than in Sections B and C, which indicates that wood chips insulate better than the coconut blanket.

5. Photogrammetry offered a cost-effective way to monitor the changing topography of the ice-rich cut slope. To apply this photogrammetric method for such a purpose, stable

control points were required to build the coordinate system. By comparing the exact locations of the slope surface at different times within a given period, the total volume of the erosion or surface accumulation during that period could be measured. Results from this study were consistent with previous research-related observations, indicating that the measurement results were reliable.

6. It is recommended that long-term performance monitoring at the Experimental Feature site continues as long as the sensors and recording devices at the site remain functional.

Some Generalized Thoughts and Conclusions Pertinent to the Experimental Feature

As of this reporting, it is appropriate to offer some *informed conjecture* regarding the Experimental Feature based on observations of the test sections themselves as well as on the research team's many years of combined permafrost-related experience. In considering various methods for protecting permafrost cut slopes, it appears that it is essential at any specific location to identify and consider the *morphology* of the soil's frozen moisture content, in addition to simply quantifying the moisture content of the frozen soil. More specifically, the question to ask is whether the frozen moisture in the soil is uniformly dispersed throughout the soil or whether it is segregated in massive ice features (a much worse case). A standard drilling program in Alaska geared to highway route exploration will likely not provide enough information, prior to construction, to make this determination for a specific cut slope.

The case without massive ice — For example, freshly exposed cut slope soils known to have an average volumetric frozen moisture content of, say, 40% or higher might be treated in an environmentally acceptable way by using a combination of standard slope-protection matting and the rapid establishment of a dense grass cover—*if* the frozen moisture is evenly distributed throughout the soil. Given this "desirable" frozen soil type, such treatments need not necessarily prevent the permafrost from thawing. The treatment function is to retard the thaw process by virtue of shading and evapotranspiration offered by the surface vegetation while equipping the surface with armor against external sources of erosion (spring runoff, etc.). The result is that the cut slope generally remains stable, while clean water is slowly released to the ditch during the thaw-consolidation process. However, even if the frozen soils exposed in the cut slope are the "desirable" form of permafrost (having uniform ice distribution), unresolved design issues

remain. At some high level of frozen moisture content, the previously described slope protection method will not work. At some yet unknown high frozen-moisture content—and considering the local air/soil temperature regime—the soil will not thaw-consolidate in a stable manner during the thaw process. Such problems may be countered by some combination of lowering the slope angle and/or increasing the strength of the stabilization matting and density of vegetative covering, but such variables have not been systematically studied in Alaska.

The case with massive ice — Exposure of massive ice in a new cut slope poses a real problem! To date, including consideration of the Experimental Feature of this report, there are four ways of contending with this problem:

1. Reroute the road to avoid cutting into massive ice—often economically or geographically impossible
2. Remove the massive ice—expensive, many unknowns, almost never attempted
3. Keep the massive ice frozen—except perhaps in some of the coldest areas of Alaska, requires installation of an expensive passive refrigeration system or an active system with perpetual power supply
4. Cover the slope with a thick blanket of free-draining material—the subject Experimental Feature now contains three such installations including Section A (wood chip blanket per original design), Section C (crushed rock blanket repair expedient), and Section D (the control section w/crushed rock blanket per original design)

At this time, the blanket (Option 4) appears to provide a reasonably practical form of slope treatment where massive ice is involved. Such a blanket, composed of individual pieces of aggregate, wood chips, etc., has several desirable characteristics. The blanket material is easily placed against the cut slope face and may be relatively inexpensive for some projects. More important, the loose blanket cover will settle and stay in close contact with the slope face as it undergoes significant change in shape during the time that the massive ice feature is thawing.

In both of the above cases, it is assumed that the thawing process finally stops. Eventually, the combined thickness of slope protection material (including vegetative covering) and the

accumulating under-layer of thawed material becomes great enough that a practical level of thermal equilibrium is reached and the mature slope becomes reasonably thaw-stable.

REFERENCES

APSC (Alyeska Pipeline Service Company). (1974). Report on Thermal Erosion Test Sites, Hess Creek, Alaska (Phase I – July-August, 1973). *Report Number TE-005*.

APSC (Alyeska Pipeline Service Company). (1975). Hess Creek Thermal Erosion Site – 1974 Evaluation. *Report Number TE-006*.

Berg, R. and Smith, M. (1976). Observations along the Pipeline Haul Road between Livengood and the Yukon River. *U.S. Army CRREL Special Report* 76-11. Oct. 1976.

Mageau, D.W. and Rooney, J.W. (1984). Thermal Erosion of Cut Slopes in Ice-rich Soil. FHWA-AK-RD-85-02 Final Report. Alaska Department of Transportation and Public Facilities. http://www.dot.state.ak.us/stwddes/research/assets/pdf/fhwa_ak_rd_85_02.pdf

McHattie, R.L. and Vinson, T.S. (2008). Managing ice-rich permafrost exposed during construction. *Proceedings of the 9th International Conference on Permafrost*. University of Alaska Fairbanks, Fairbanks, Alaska, USA, pp. 1167–1172.

Naviq Consulting Inc. and AMEC Earth & Environmental. (2007). Monograph on the Norman Wells Pipeline Geotechnical Design and Performance – 2006 Update. Geological Survey of Canada Open File 5702. Natural Resources Canada, Ottawa, Ontario, 214 pp.

Tecco slope stabilization system product manual, 2010.

Vinson, T.S. and McHattie, R.L. (2009). Documenting Best Management Practices for Cutslopes in Ice-rich Permafrost. FHWA-AK-RD-09-01 Final Report, Alaska Department of Transportation and Public Facilities Research Development, and Technology Transfer Library: http://www.dot.state.ak.us/stwddes/research/assets/pdf/fhwa_ak_rd_09_01.pdf

APPENDICES

Appendix A. Photogrammetric Method for Erosion Monitoring

A Nikon D7000 (pixel resolution: 4928 × 3264) with a fixed focal length lens (AF-S NIKKOR 20 mm f/2.8D), shown in Figure A.1, was used for erosion measurement.

Figure A.1 Camera and lens

Photogrammetry principles are illustrated in Figure A.2, using the ideal pinhole camera model. When a photograph of an object is taken, a two-dimensional (2D) image is obtained and the depth of the object is lost. For the same object (Figure A.2a), 2D images taken from different positions differ due to the varying perspectives. These differences can be used to calculate the orientation of the camera for each image. Using a combination of images and known camera orientations, one can reconstruct the three-dimensional (3D) geometry of the object. In Figure A.2a, the perspective center (center of an ideal pinhole camera lens) of the left camera (S_1) is set as the origin of an arbitrary coordinate system. For the camera on the right (S_2), the three coordinates of the perspective center (Xs, Ys, Zs) and directional angles (κ, ω, φ) are unknown.

Usually the distance between any two points can be used as a scale, which reduces the unknowns to five. In Figure A.2b, five equations can be generated by identifying five pairs of corresponding points on the two images, and the second camera orientation can be solved. Since there are numerous pairs (far more than five) of corresponding points on the two images, the redundancy in information can be used to perform an optimization analysis to accurately determine the camera orientation so that the errors in measurement are minimized. In addition,

multiple images can be taken from different orientations and, with sufficient overlap, can provide more redundant equations to improve the accuracy of the camera orientation determination. Once camera orientations are determined, a straight optical ray can be mathematically projected from the object (point) on the photograph through the perspective center of each camera, as shown in Figure A.2b (collinearity). The intersection of these rays for cameras at different orientations (triangulation) can then be used to determine the 3D coordinates of the point. As a noncontact 3D measurement technique, photogrammetry has proven highly accurate.

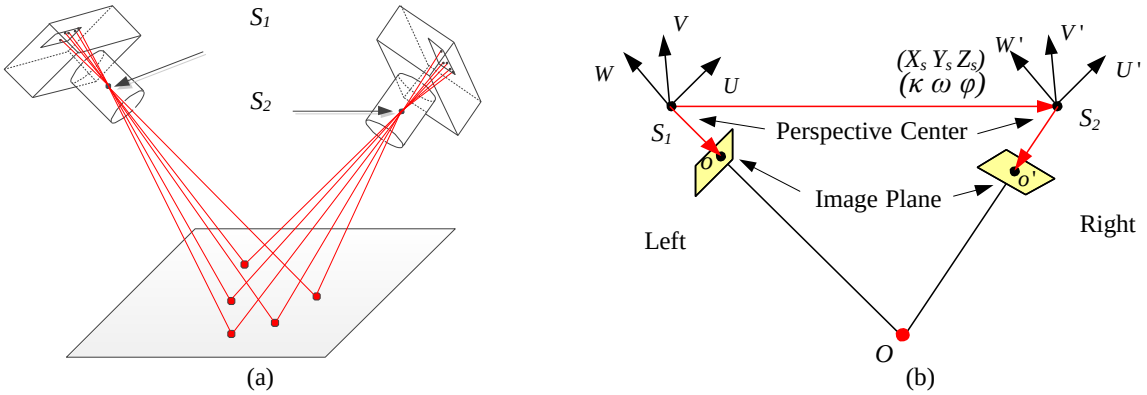

Figure A.2 Principle of photogrammetry

For high-accuracy photogrammetric measurements, camera calibration is required. For the subject research, camera calibration was performed by capturing a group of images for a point grid from different orientations. After calibration, the image sensor format size (23.9974 × 15.8961 mm), principal point (x = 12.0249 mm, y = 8.0434 mm), and focal length (f = 20.9611 mm) as well as some other distortion parameters were determined, as tabulated in Table A.1. As can be seen in Table A.1, the actual focal length of the 20 mm fixed focal length lens is 20.9611 mm when the camera is treated as an ideal pinhole camera model. After slope construction, several images of the slope were captured. For such images, a small aperture size (f-stop number > F10) was used to ensure a longer depth of field for better image clarity. Also, image quality could be improved using the highest possible shutter speed permitted by the ambient or artificial light conditions, and further improved using a tripod-mounted camera.

Table A.1 Camera calibration parameters

f (mm)	20.9611
M (pixel)	4928
N (pixel)	3264
F_x *(mm)*	23.9974
F_y *(mm)*	15.8961
P_x *(mm)*	12.0249
P_y *(mm)*	8.0434
K_1 (10^{-4})	2.594
K_2 (10^{-7})	-4.081
P_1 (10^{-6})	-3.411
P_2 (10^{-6})	2.612

Figure A.3 is a typical picture of the ice-rich slope captured for erosion measurement. After obtaining photos along the slope, the images were processed to obtain orientations of camera stations by marking and referencing the targets in different images.

Figure A.3 Typical image captured for erosion monitoring

A coordinate system was defined as shown in Figure A.4. The origin was set to be at the lower left corner and the *x* and *y* axes were set to be parallel to the road and slope directions. For the precise measurements required in this study, stable reference points along the slope were necessary. These stable points were required as the basis for building a coordinate system from which relative movements of the surrounding slope face could be calculated. The long, grouted soil anchors installed in Section C, as part of the Tecco-mesh system, were considered reasonably stable, and were therefore used as the required reference points. The 3D coordinates for each of the reference points were photogrammetrically determined at a defined scale. For all subsequent photogrammetric measurements of slope face topography, the 3D coordinates of the reference points were set at the initially determined values. As the study progressed, changes in slope face topography could be determined at any time by obtaining a new set of photos and performing the necessary photogrammetric computations based on the initial 3D coordinates of the stable reference points.

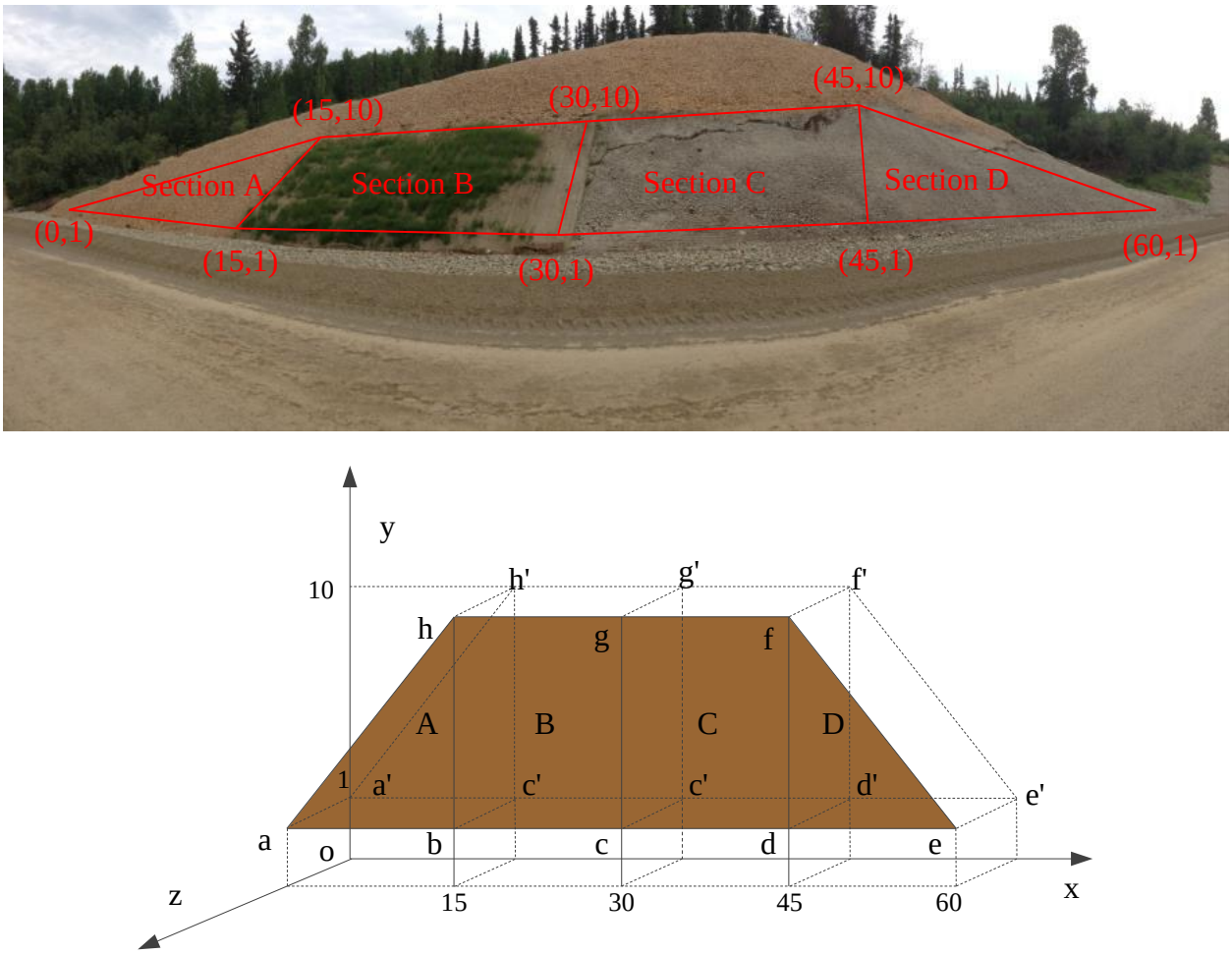

Figure A.4 Coordinate system for erosion measurement

As a result of photogrammetric analysis, point clouds representing the surface topography of the slope at specific times, can be generated as shown in Figure A.5 (the same point cloud view at different angles). Stations representing camera locations for the various images are illustrated in that figure. Typically, around 25 images were required to reconstruct the entire slope. Each point in the point cloud is defined by its *x*, *y*, and *z* coordinate. Taken together, the points represent a topographic surface above an *x*-*y* reference plane. Conceptually, given two such surfaces (each representing the topography of the cut slope surface at a different time), the volumetric difference, with respect to the reference plane, between the two surfaces represents the volume changes along the slope surface. And volume changes along the slope surface represent material actually lost through erosion or thaw consolidation. This process is further explained below.

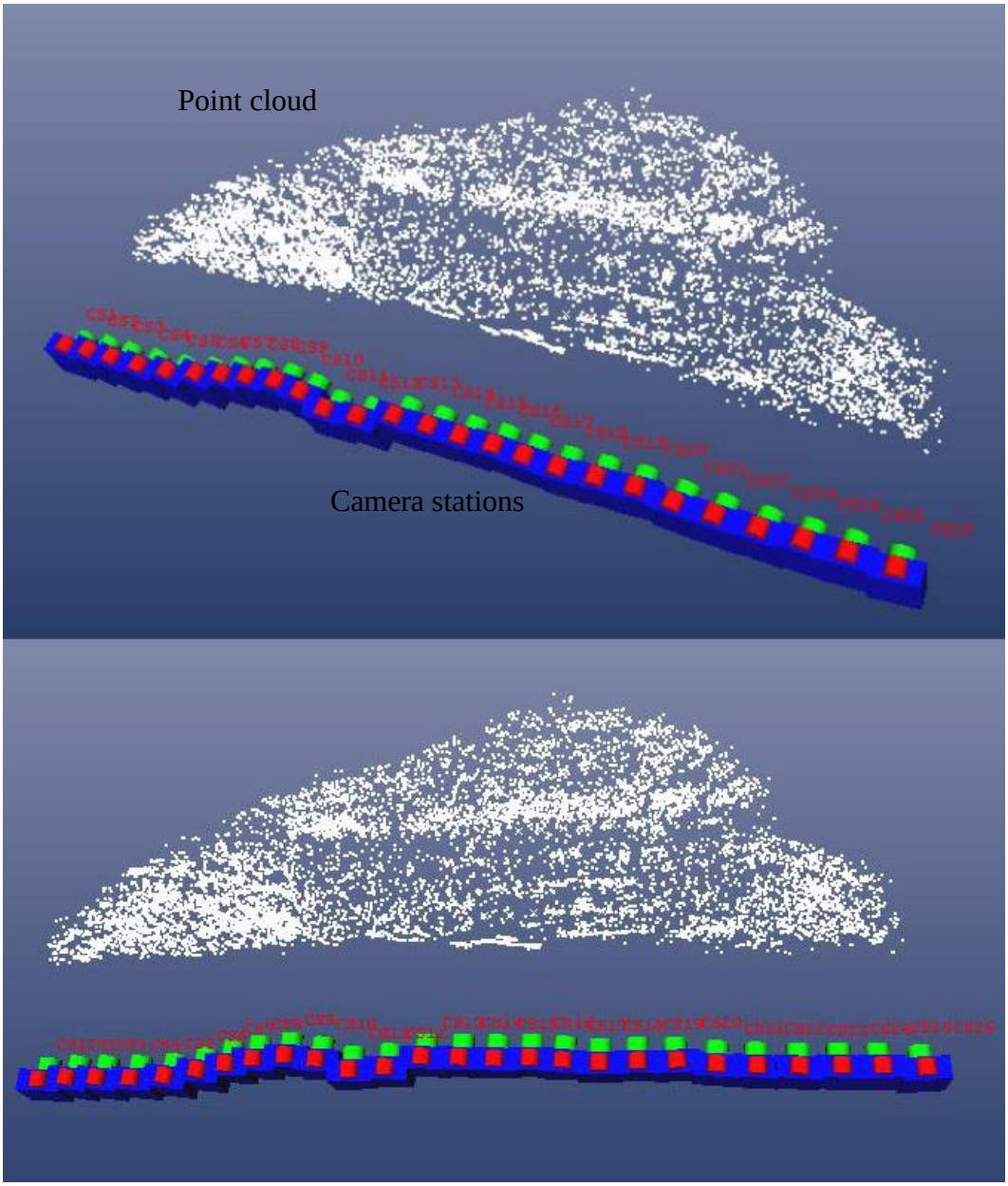

Figure A.5 Camera stations at different view angles

Figure A.6 shows a typical point cloud generated from one set of photos. Using the points lying within each of the four sections indicated in Figure A.4, a triangular mesh was generated for each section using MatLab function "DelaunayTri." Triangular meshes for Sections A, B, C, and D are shown in Figures A.7 to A.10. After mesh generation, the volume between each triangular mesh cell and its projected surface on the *x*-*y* reference plane can be calculated. The difference between this volume and the volume calculated for the same mesh cell later represents the loss or

gain of soil material bounded by that mesh cell. The specific method used for calculating each mesh volume is explained in the following paragraph and illustrated in Figure A.11.

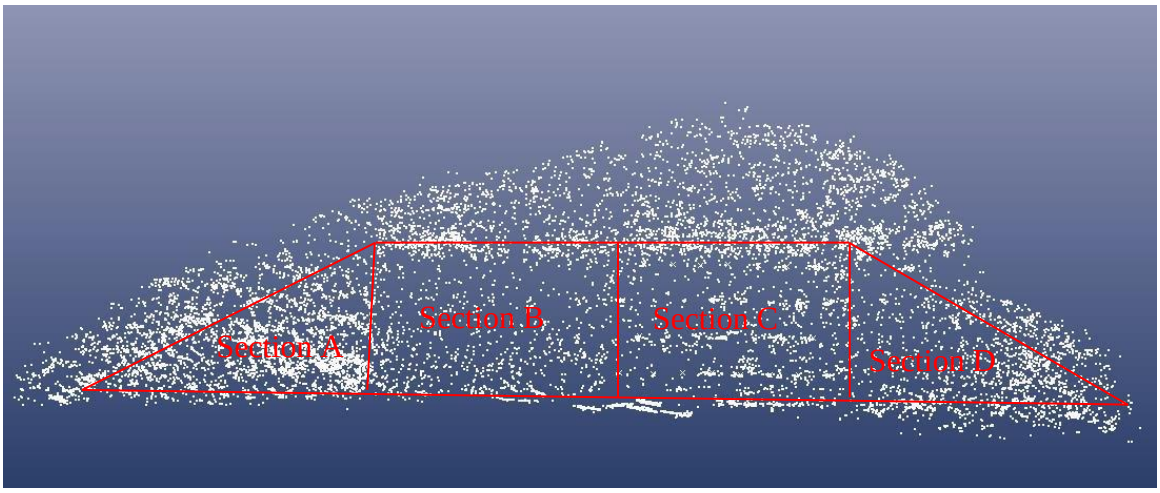

Figure A.6 Point cloud for erosion monitoring

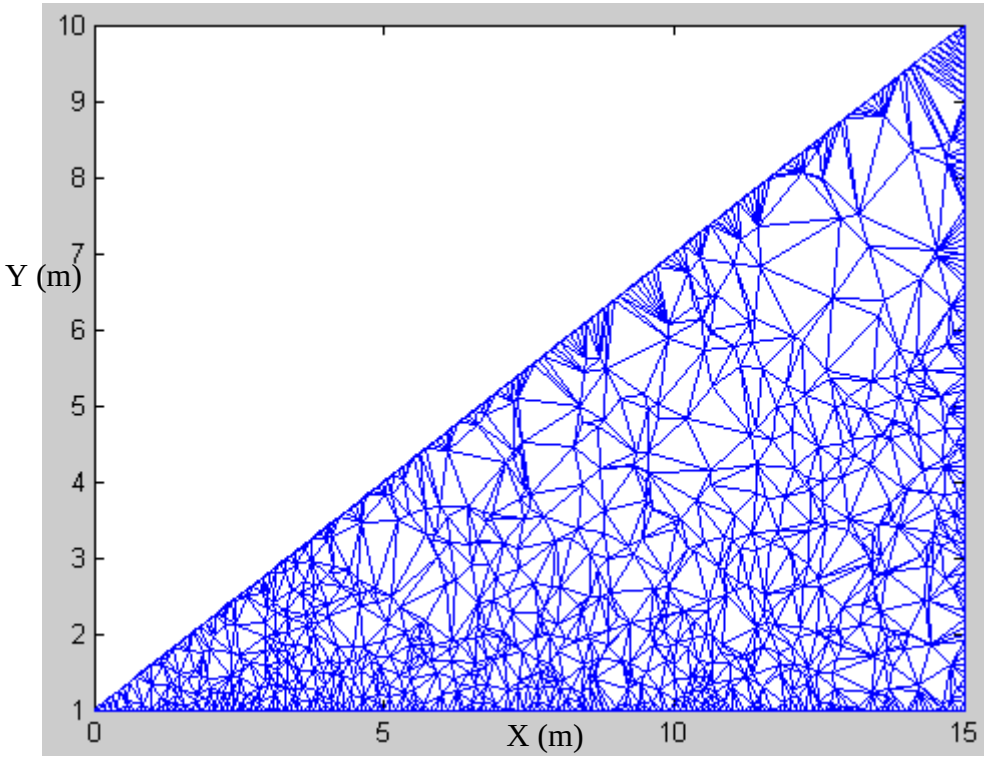

Figure A.7 Mesh generated for Section A for volume calculation

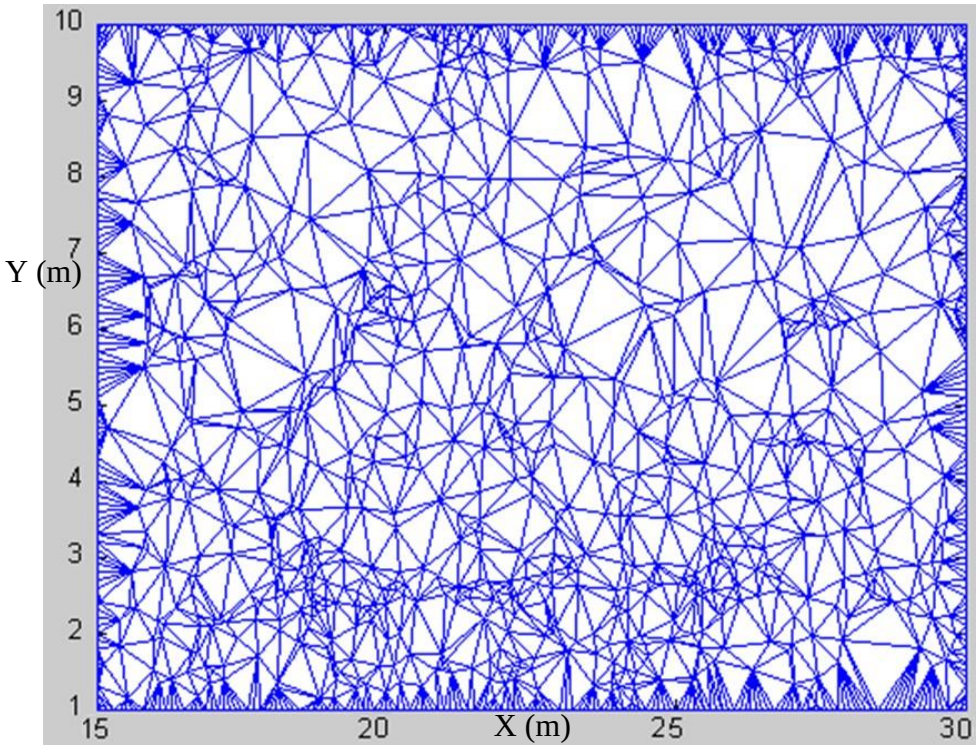

Figure A.8 Mesh generated for Section B

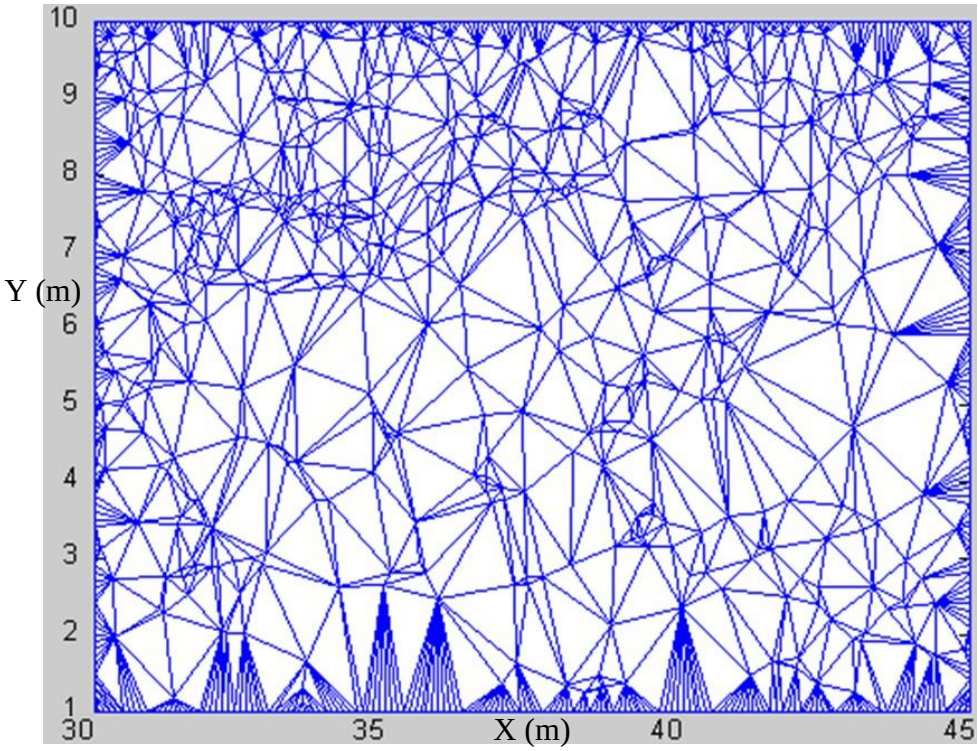

Figure A.9 Mesh generated for Section C

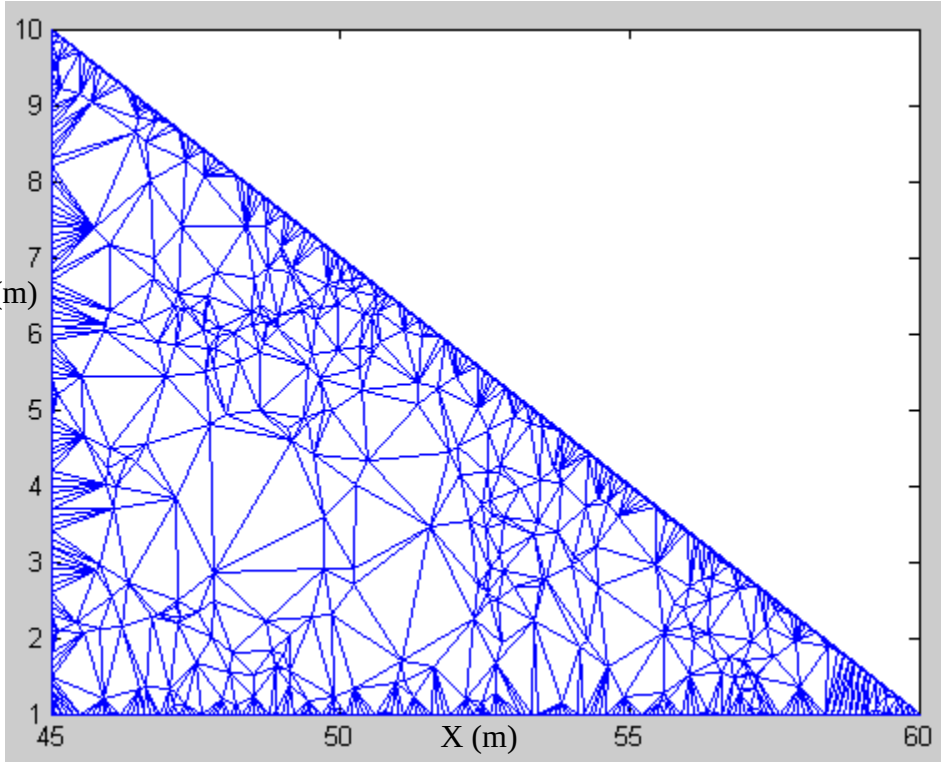

Figure A.10 Mesh generated for Section D

As an example of calculating a mesh cell volume, we begin with the mesh cell triangle ABC shown in Figure A.11. A new triangle A'B'C' is formed by projecting points A, B, and C onto a plane parallel to the *x-y* reference plane and which passes through point C (point C being the closest of the A, B, and C points to the *x-y* reference plane). A", B", and C" are the projections for A, B, and C onto the *x-y* reference plane. The volume between the A, B, C triangle area and its projection onto the *x-y* reference plane is equal to the summation of volumes for triangular prism ABCA"B"C", tetrahedrons AA'B'C', and BB'AC. The total volume for each test section (using a single set of photos) can be calculated by summarizing volumes for all triangular cells within that test section. A new total volume for all triangular cells in the test section can be determined later based on a new set of photos, and the difference between the two volumes equals the loss or gain of material at the slope face for the period between photo sets.

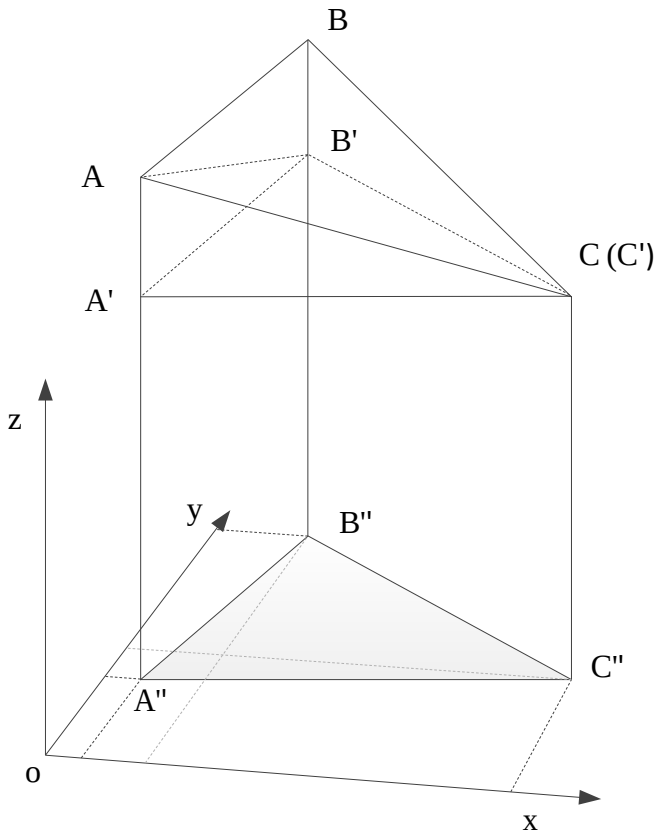

Figure A.11 Volume calculation for a single mesh cell

Appendix B. Alaska DOT&PF Construction Observations and Comments

(presented in a construction diary/timeline format)

Wednesday, April 17 to Tuesday, April 23

Drill subcontractor works on drilling the holes for the temperature sensors as well as the anchor bolts for Test Section C.

Friday, April 19

After concerns were voiced from Great Northwest's superintendent, it was decided to cover the back slope with concrete insulating blankets in an effort to keep the hillside frozen until the four treatments of slope protection were in place.

Wednesday, April 24

Anchor bolts were all installed in Test Section C today.

Thursday, April 25

1. Hand seeding of Test Sections B and C performed early in morning, while staging for other work on slope.
2. Most of day one was spent installing the treatment for Section C (Erosion Control Matting plus Tecco-mesh). After Great Northwest (referred to as GNI from here on) had the erosion control matting in place, they proceeded to use their CAT 330B L excavator to hoist the rolls of Tecco-mesh to the top of the test section. Crew members secured the top of each roll onto the slope and then proceeded to use the excavator bucket to help control the unrolling of the rest of the roll down the slope. The spike plates were put in place today, but wire rope was not installed.
3. After this section was mostly in place, most of GNI's crew went back to other activities, but three laborers were left behind to clamp Tecco-mesh overlaps together, and then began work on pinning down erosion control matting for Section B.
4. Borrow B slope protection Material placed on Test Section D. Approximately 212.45 tons per scale tickets.

Friday, April 26

1. Laborers continue with installation of erosion control matting on Test Section B. Progress is slow due to difficulty installing circle top wire pins. Two laborers securing rolls at a rate of approximately ½ a roll per hour.
2. First round of 4 side dumps loaded with woodchips arrive at approximately 10:15 a.m. Excavator starts placing wood chips along top "half" of slope, above test sections, starting at right end, working from Section D toward Section A. A CAT 966F loader was used to place woodchips on most of Test Section A. A Morooka MST-2200VD tracked end dump was used to transfer wood chips up to the top surface of cut slope where excavator was used to place them on back slope.
3. Two rolls of erosion control (*matting*) remain to be pinned at end of work shift.

Saturday, April 27

Two laborers on site to pin remaining two rolls of erosion control matting, taking about 3 hours.

Tuesday, April 30

Two laborers spend approximately three hours tightening down spike plates and tensioning wire rope on Test Section C. Installation of slope treatments complete.

Summary of Problems and Thoughts Provided by ADOT&PF Construction Personnel:

1. The drilling equipment being used by the subcontractor for drilling the holes for the anchor bolts was rather old. A newer piece of equipment with driers on the air compressor might have prevented some of the problems we observed.
2. The drilling equipment also used a certain proprietary drill steel, which was not readily available locally (in Alaska). In fact, replacement parts had to be acquired from Germany, which delayed progress by a couple days.
3. It seems to us like the anchor bolts for Section C of the experiment (Tecco-mesh and Erosion Control Mat) might have acted as heat conductors once we got into the warmer months of summer, heating up the frozen back slope enough that frozen areas of the slope melted.

4. The 1.5:1 slope that the experiment was installed on was at times difficult for the workers to work on; part of their effort is spent just on staying upright without falling down the slope.
5. The circle-top wire pins were not strong enough to be hammered into the slope by themselves. GNI laborers tried hammering pilot holes with nails, and then ended up settling on using some cordless drills with drill bits to pre-drill the hole for the pins. Using the drills occasionally resulted in matting getting tangle around the drill bit. Different hardware for securing the matting to the slope would be worth researching for a future application like this.